Dissertation
submitted to the

Combined Faculty of Natural Sciences and Mathematics
of the Ruperto Carola University Heidelberg, Germany

for the degree of
Doctor of Natural Sciences

Presented by

Rodrigo Antonio Gama Brambila, M.Sc.
Born in: Mexico City, Mexico

Oral examination: May 4th, 2022

Biological Assessment and Tests of Activity of Two Novel Proteolysis Targeting Chimeras (PROTACs)

Referees:

PD Dr. Xinlai Cheng
Prof. Dr. Stefan Wölfl

To my mother and sisters:
Beatriz, María and Gabriela

Acknowledgements

It is now, writing these lines, when the realization that my PhD comes to an end, truly sinks in. And I cannot help but remembering all the way through, and all the people who have been by my side, both physically and at the distance. All the people who were there in the good and bad times, who always had time and support for me, even in days when all I had was a bunch of complains I needed to speak out. Thank you all, also, for being there to listen to my countless jokes and help me build up the good memories. During these years, I truly made friends, hopefully, for a lifetime.

First, I would like to thank Dr. Xinlai Cheng for having trusted me with his first ever PhD position. He is an example of persistence, goal-oriented work, and an impressive capacity to remain equanimous and calm even when individuals from his working environment lose their temper or patience.

To Prof. Dr. Stefan Wölfl for having always been supportive and helpful anytime within his capabilities. Not only did he give me the opportunity to do my master thesis in his lab, making it the beginning of this story, but also did he agree on supporting my doctoral work in every way he could.

To Prof. Dr. Ulrike Müller, for having agreed on being part of my Thesis Advisory Committee, from whom I knew nothing but kindness, support, and constructive, valuable observations and suggestions for this work.

To Prof. Dr. Gert Fricker who completed my thesis evaluation committee. Even though we interacted at the end of my PhD only, your professionalism and commitment came at a time when it was most needed and helped me feel a good deal of support.

To the Heidelberg Biosciences International Graduate School (HBIGS), for having accepted my application and supported my doctoral studies. Thank you for all the very useful curricular activities, which really helped shaping the course of the research. Specially I would like to remark my acknowledgements to Martina Galvan, who always was incredibly kind to me, was on the watch of my progress, and never hesitated to spend some time to listen to me, and to Dr. Lutz, who gave always made some time to support me, when everything looked blurry and uncertain.

To the entire AG Wölfl for having made a truly exceptionally friendly, relaxed and cooperative environment. Not only was it a great professional experience to have worked with you, while it lasted, but also did it make up a good deal of memories to take along the way. To Saskia Schmitteckert, without her, the second half of my PhD would have been a true ordeal. To Dr. Suzan Can, for all the friendly talk and the hours of practice and German language. To Dr. Ali Ghanem, who was my first contact and guide to the group and the city. To Dr. Jannick Theobald and Dr. Fadi Almouhanna not only for all the technical and scientific advice, but also countless hours of fun and laughter in and out of the lab. To Dr. Jee Young Kim, for she told me some of the most comforting words anyone has ever told me with regards of my academic track, though our time together in the group was very short. To Anastasiia Zuieva, Biljana Blagojević, and Marija Banićević (even though she belongs to a different group), we more or

less started our PhDs at the same time, and thus, we stood for each other, shared a lot of talks, time, fun and support whenever needed. To Dr. Shahrouz Ghafoory for all the kindness and appreciation he always showed to me, and his eagerness to have more out-of-the-lab bonding activities. Last, but not least, all the Azubis who were working in the group for shorter or longer time, specially to Paraschiva Ghiata, Raúl Lara Bajandas, and Alina Sperl, with whom I had the pleasure to work the closest with.
To Dr. Mohamed Abu el Maaty and Dr. Yasamin Dabiri, for they made the word "friend" fall way too short. Not only were they in the good and bad times, as well, but also did they become the strongest support I had over these years, and they gave me freedom to rely on them as no one else did. I have nothing but infinite gratitude and love for them both.

I would like to thank very specially all the students I had the chance to supervise during these years. I hope they had the chance to learn from me as much as I learnt from them and from working with them, and this last line is not about just academic knowledge. From them all, I would like to emphasize my gratefulness to Jan Wieland, Pauline Hansen, and Olmo Medina Martínez. Their hard work, long hours and weekends are a fundamental part of this work. I do not have enough words to thank them.

From all the people I had the chance to meet in what later in my PhD became my working place, the Buchmann Institute for Molecular Life Sciences of the Goethe University Frankfurt, I would like to thank most specially Haotian Wang and Diana Grewe. I truly do not know what I would have done without them, and at a more personal level, also Haotian for the pop-corn/therapy Fridays, Mariana Tellechea and Javier García Pardo. A true friend does not just listen to you, they also tell you what you probably do not want, yet need to hear to move on in the right direction.

A very special acknowledgment to Gabriel J. Martín. I am honoured and grateful beyond words that you call me your friend. A truly unique person… One who is capable of showing love to his friends as I had never seen before. Through all his work, he had helped me numerous times even before he knew of my existence. It was his words what stopped me from quitting at the beginning of my PhD. Words, that I carried along all the way until the end.

To my family: mum, sisters, and niece, for the absolutely unconditional love, acceptance, and support. For being available for me at all times (despite being, literally, at the other side of the world) for anything I might have needed. Also, to Jorge Gama, without his support I would literally not be here and have had the chance to do a PhD.

To Nicole Hassepaß. From all the people I met in Germany, it is unarguably her the one I owe the most to and am most grateful to. Not only was she an exceptionally good boss, but also did she do everything, to the best of her capabilities, to help me out in the most difficult times I had in Germany. Without her help, I probably could not have stayed in the country to achieve my goals. On top of that, she offered a most sincere friendship. I cannot write enough to express my gratefulness. Despite all the hardships, I hope she never changes (at all) as a boss. When I daydream about the ideal job, there is a boss like she in it.

Last, but not least, the paragraph I fear the most. I am honoured with so many friends, that I am afraid I would leave out some of them, yet, just leaving it on "my friends" feels hollow.

Mischa Bender was not only a most loyal friend, but also became the source of my entire lab-free social network. Even if he left Heidelberg too soon, we never lost touch and a bit of him was in every friend he helped me make. Daniel Guimarães, inspite of having a remarkably tight social agenda, he always found a way to have time for me. He was the one and only who stood forward to make me company when I felt the loneliest. There are some little details that become enormous in the right circumstances. Ruth Moreno, Isbo Núñez, Vero Ayala, Mariana and Fernanda Dávila, Alex Zimmermann, Olivia Téllez, Paloma Ramos and Edith Garfias, Karla Sánchez. Despite the years, despite the distance, none of them ever left me. They all stayed in touch and were there for me when the times and chances to meet again arose.

To all members of the Heideldrag family. Not only you make the words “chosen family” be true, but also did you help me fill that gap I had had in Heidelberg along all these years. Even if at the very end of my PhD, you do represent “that” bit I was missing, people I can connect with in a unique way, people around I can be fully myself with, and express myself with limitless freedom. In no time you let me in and embraced me as one of you. Thank you all for all the support, acceptance, learning, trust, and, most valuably, all the care.

Ricardo Vieira, a brother more than a friend (and roommate and Covid19-lockdown 24/7 companion), thank you so much for everything. To Federica Fioretino and Chiara di Ponzio, whom I owe the start out of what later became a bit more than a hobby, as well as countless hours of conversation unrestricted mutual support. Thank you for all the recommendations. Lizbeth Ramírez, Yazmín Brito and Sadat Hasan, we started the Germany adventure together, and stuck together all the way along. Thanks for being some of the greatest and most loyal friends I have ever made. And Alberto Medina. From all, you have been the one and most, who has unconditionally ever been there for me. The one who never gave up on me, despite everything. You are one of the most solid columns of my life, thank you forever.

Nahum, Cristian, Yael, Agni and Gabriel. Some of the friends I made last, but also the fiercest. You all are living proof that distance is nothing when the bond is true. Thank you for being my connection to that bit of Mexico I just can no longer enjoy and be part of. Your sincere and loyal friendship make me feel like I do have a space there.

PUBLICATIONS

Dabiri, Y., Gama-Brambila, R. A., Taskova, K., Herold, K., Reuter, S., Adjaye, J., Utikal, J., Mrowka, R., Wang, J., Andrade-Navarro, M.A., Cheng, X. (2019). Imidazopyridines as Potent KDM5 Demethylase Inhibitors Promoting Reprogramming Efficiency of Human iPSCs. iScience, 12, 168-181. doi:10.1016/j.isci.2019.01.012

Cheng, X., Haeberle, S., Shytaj, I. L., Gama-Brambila, R. A., Theobald, J., Ghafoory, S., Wolker, J., Basu, U., Schmidt, C., Timm, A., Taskova, K., Bauer, A.S., Hoheisel, J., Tsopoulidis, N., Fackler, O.T., Savarino, A., Andrade-Navarro, M.A., Ott, I., Luisc, M., Hadaschik, E.N., Wolfl, S. (2020). NHC-gold compounds mediate immune suppression through induction of AHR-TGFbeta1 signalling in vitro and in scurfy mice. Commununication Biololgy, 3, 10. doi:10.1038/s42003-019-0716-

Gama-Brambila, R. A., Chen, J., Dabiri, Y., Tascher, G., Němec, V., Münch, C., Song, G., Knapp, S., Cheng, X. (2021). A Chemical Toolbox for Labeling and Degrading Engineered Cas Proteins. Journal of the American Chemical Society Au, 1(6), 777-785. doi:10.1021/jacsau.1c00007
G-B R.A., C. J., and Z.J. are equal contributors in this publication.

Gama-Brambila, R. A., Chen, J., Zhou, J., Tascher, G., Munch, C., & Cheng, X. (2021). A PROTAC targets splicing factor 3B1. Cell Chemical Biology. doi:10.1016/j.chembiol.2021.04.018
G-B R.A. and C. J., contributed equally in this publication.

Zhou, j., Dabiri, Y., Gama-Brambila, R.A., Ghafoory, Altinbay, M., Mehrabi, A., Golriz, M., Blagojevic, B., Reuter, R., Han, K., Seidel, A., Dikic, I., Wölfl, S., Cheng, X. (2021). pVHL-mediated SMAD3 degradation suppresses TGF-β signalling. Cell Biology. doi: 1083/jcb.202012097
Z.J. and D.Y. contributed equally in this work.

Table of contents

LIST OF FIGURES I

LIST OF TABLES II

LIST OF ABBREVIATIONS III

SUMMARY VI

ZUSAMMENFASSUNG VII

1. INTRODUCTION 1

1.1. Protein Degradation 1

1.2. Ubiquitin-Proteasome System 2

1.3. Targeted Protein Degradation Strategies 5

1.4. PROTACs 14

1.4.1. Chronology of PROTACs 15

1.4.2. Aspects to Consider During PROTAC Design 31

1.5. Development and Biological Testing of Two New PROTACs. Objectives of this Doctoral Work 34

1.5.1. Cas Proteins: A new target of PROTACs 35

1.5.2. SF3B1: another target of PROTACs 36

2. AIMS OF THE PROJECT AND HYPOTHESIS 37

3. RESULTS 38

3.1. Part I: PROTAC-FCPF 39

3.1.1. The activity of PROTAC-FCPF in cells 39

3.1.2. PROTAC-FCPF inhibits the activity of $Cas9^{FCPF}$ through degradation 41

3.1.3. The mechanism of PROTAC-FCPF 45

3.1.4. PROTAC-FCPF activity in other Cas proteins 49

3.2. Part II: PROTAC-O4I2 50

3.2.1. O4I2 activity in RNA synthesis 50

3.2.2. PROTAC-O4I2 protein-degrading activity in human cancer cells 51

3.2.3. The mechanism of PROTAC-O4I2 53

3.2.4. Cytotoxicity of PROTAC-O4I2 58

4. DISCUSSION AND FUTURE PERSPECTIVES 60

5. CONCLUSIONS 65

6. MATERIALS AND METHODS 67

6.1. Materials 67

6.2. Cell culture 75

6.2.1. Cell lines maintenance 75

6.2.2. Cell seeding for assays 76
6.2.3. Transfection 76
6.3. Techniques and Assays 77
6.3.1. MTT Cell Viability Assay 77
6.3.2. FITC-FCPF Staining 77
6.3.3. In vitro Ubiquitination Assay (for Cas proteins) 78
6.3.4. T7 Endonuclease I Assay 78
6.3.5. Luciferase Assay 80
6.3.6. Detection of Newly Synthesized RNA 80
6.3.7. FLAG-tagged Protein Purification and Determination of Denaturation Temperature 81
6.3.8. Fluorescence-Based Thermal Shift Assay 81
6.3.9. Alternative Splicing Assay 82
6.3.10. Apoptosis Assay 83
6.3.11. Immunoprecipitation and Ubiquitination (for SF3B1) 84
6.3.12. FRET assay 85
6.3.13. SDS PAGE and Western Blot 85
6.3.14. FACS 87
7. REFERENCES 88

LIST OF FIGURES

Figure 1: schematic representation of the Ubiquitin-Proteasome System. _____3

Figure 2: schematic representation of the Anchor Away Technology. _____7

Figure 3: 26S proteasome mechanism induced by the deGradFP System. _____8

Figure 4: 26S proteasome-mediated protein degradation mechanism induced by the dTAG system. 9

Figure 5: Schematic representation of the proteasomal degradation mechanism induced by HaloTag and HyT13. _____10

Figure 6: schematic representation of the proteolytic mechanism driven by the AiD system. _____12

Figure 7: Schematic representation of the PROTAC-mediated protein degradation. _____15

Figure 8: Timeline of PROTAC development. _____30

Figure 9: Chemical structure of PROTAC-FCPF _____36

Figure 10: Chemical Structure of PROTAC-O4I2. _____37

Figure 11: Proof of concept. The FCPF sequence can be targeted in live HeLa cells. _____40

Figure 12: The protein-degrading activity of PROTAC-FCPF in $HeLa^{Cas9\text{-}FCPF}$ cells. _____42

Figure 13: The protein degradation mechanism of PROTAC-FCPF is based on the UPS._____47

Figure 14: The Activity of PROTAC-FCPF in other proteins tagged with the FCPF sequence. _____49

Figure 15: in vitro activity of O4I2 with SF3B1._____50

Figure 16: Effects of PROTAC-O4I2 in cancer cells. _____52

Figure 17: Elucidating the action mechanism of PROTAC-O4I2. _____55

Figure 18: Antiproliferative effects of PROTAC-O4I2 in cancer cells._____59

LIST OF TABLES

Table 1: plastic ware and disposable supplies _____67

Table 2: chemicals and reagents_____68

Table 3: Cell culture media, supplements and reagents _____69

Table 4: list of Antibodies _____70

Table 5: list of Oligonucleotides _____70

Table 6: list of Recombinant DNA_____71

Table 7: list of sgRNA _____71

Table 8: list of Cell Lines _____71

Table 9: list of Kits_____71

Table 10: list of Buffers and Solutions _____72

Table 11: list of Machines and Devices_____74

Table 12: list of Softwares_____74

LIST OF ABBREVIATIONS

AA	Anchor-Away
AAVS1	Adeno-Associated Virus Integration Site 1
ABC	ATP-Binding Cassette
ACRII4	Anti-CRISPR protein
AD	Actinomycin D
AID	Auxin-Inducible Degron System
AMPK	AMP-activated Protein Kinase
ALK	Anaplastic Lymphoma Kinase
APS	Ammonium Persulfate
ATP	Adenosine Triphosphate
BET	Bromodomain And Extraterminal domain
BSA	Bovine Serum Albumin
CACYBP	Calcyclin Binding Protein
DCAF13	DUBB1 and CUL4 Associated Factor 13
$Cas9^{WT}$	Cas9 Wild Type
$Cas9^{FCPF}$	Phenylalanine-Cysteine-Proline-Phenylalanine Cas9 mutant
$Cas12^{FCPF}$	Phenylalanine-Cysteine-Proline-Phenylalanine Cas12 mutant
$Cas13^{FCPF}$	Phenylalanine-Cysteine-Proline-Phenylalanine Cas13 mutant
cDNA	complementary Desoxyribonucleic acid
CHIP	C-Terminus HSP70-Interacting Protein
cIAP	Cellular Inhibitor of Apoptosis
CMV	Cyromegalovirus
CRISPR	Clustered Regularly Interspaced Short Palindromic Repeats
CRBN	Cereblon
CRBN KD	Cereblon Knock Down
CRBN KO	Cereblon Knock Out
crRNA	CRISPER Ribonucleinc Acid
dCas9	Nuclease-dead Cas9
DDB1	DNA Damage-Binding Protein 1
DNA	Deoxyribonucleic Acid
DNAJB1	DnaJ Heat Shock Protein Family (Hsp40) Member B1
DMEM	Dulbecco's Modified Eagle Medium
DMSO	Dimethyl Sulfoxide
DSB	Double-strand breaks
dsDNA	Double-stranded Desoxyribonucleic acid
DPBS	Dulbecco's Phosphate-Buffered Saline
dTAG	Degradation TAG System
DUB	Deubiquitinating Enzymes
EDTA	Ethylenediamine Tetraacetic Acid
E1	Ubiquitin Activating Enzyme
E2	Ubiquitin Conjugating Enzyme
E3	E3 ligase
EGF	Epidermal Growth Factor

EGFR	Epidermal Growth Factor Receptor
EGTA	Ethylene glycol-bis(β-aminoethyl ther)-N,N,N‘,N‘-tetraacetic Acid
ELC	Enhanced Chemoluminescence
ELISA	Enzyme-Linked Immunosorbent Assay
EtOH	Ethanol
EYFP	Enhanced Yellow Fluorescent Protein
FACS	Fluorescence-Activated Cell Sorting
FCS	Fetal Calf Serum
FCPF	Phenylalanine-Cysteine-Proline-Phenylalanine Sequence
FGFR	Fibroblast Growth Factor Receptor
FITC	Fluorescein isothiocyanate
FKBP12	FK506-binding protein 12
FLAG	Octapeptide (tag) DYKDDDDK
FRAP	FKBP12-Rapamycin Associated Protein
FRET	Fluorescence Resonance Energy Transfer
GAPDH	Glyceraldehyde 3-Phosphate Hydrogenase
GFP	Green Fluorescent Protein
GLB 5x	5-fold concentrate Gel Loading Buffer
GSK-3(α,β)	Glycogen Kinase 3 (α or β)
HA	Human Influenza Hemagglutinin Tag
HCC	Hepatocellular Carcinoma
HCV	Hepatitis C virus
hiPSC	Human induced Pluripotent Stem Cells
HMT	Histone Methyl Transferase
HPK1	Hematopoietic Progenitor Kinase 1
HyT	Hydrophobic Tagging
IAA	Indole-3-Acetic Acid
ICC	Immunocytochenmistry
i-PrOH	Isopropanol
IRAK4	Interleukin-1 Receptor-Associated Kinase 4
KCTD17	Potassium Channel Tetramerization Domain containing 17
Keap1	Kelch-like ECH-associated Protein-1
L2DTL	Drosophila Lethal (2) Denticleless
MAPK	Mitogen-activated protein kinase
MAPKAPK3	MAPK-Activated Protein Kinase 3
MDM2	Mouse Double Minute 2 Homologue
MeOH	Methanol
mRNA	Messenger Ribonucleic Acid
MTT	(3-(4,5-dimethylthiazol-2-yl)-2,5-diphenyltetrazolium (Assay)
NEAA	Non-Essential Amino acids
NS3	Non-Strusctural Protein 3
O4I2	Oct4 Inducing Compound 2
Oct4	Octamer Binding transcription factor 4
PCC	Protein-Catalyzed Capture agent
PCR	Polymerase Chain Reaction
PDE4	Phosphodiesterase-4

PD-L1	Programmed Cell Death-ligand 1 protein
PEG	Polyethylene glycol
PHOTACs	Photochemically Targeting Chimeras
PI	Propidium Iodide
PMSF	Phenylmethylsulfonyl Fluoride
POI	Protein of Interest
PSA	Polar Surface Are
PROTAC	Proteolysis Targeting Chimera
PROTAC-FCPF	Phenylalanine-Cysteine-Proline-Phenylalanine-targeting PROTAC
P/S	Penicillin/Streptomycin
PTBP2	Polypyrimidine Tract Binding Protein 2
PVDF	Polyvinylidene Fluoride
RBP	RNA-Binding Protein
RFP	Red Fluorescent Protein
RIPK2	Receptor Interacting Serine/Threonine Kinase 2
RNAse	Ribonuclease
RNF41	Ring Finger Protein 41
RNF154	Ring Finger Protein 152
RNF165	Ring Finger Protein 165
RNF 181	Ring Finger Protein 181
RNAi	Interference Ribonucleic Acid
RPMI 1640	Roswell Park Memorial Institute medium for cell culture
RT PCR	Real Time Polymerase Chain Reaction
ROCKi	Rho-associated Kinase inhibitor
SCF	SKP-Cullin-F-Box RING E3 ligase complex
SF3B1	Splicing Factor 3B Subunit 1
SF3B2	Splicing Factor 3B Subunit 2
SF3B2	Splicing Factor 3B Subunit 3
SLC	Solute Carriers
SDS	Sodium Dodecyl Sulfate
SDS PAGE	Sodium Dodecyl Sulfate-Polyacrylamide Gel Electrophoresis
sgRNA	Single Guide Ribonucleic Acid
siRNA	Small Interfering Ribonucleic Acid
SirReal	Sirtuin Rearranging Ligands
SNIPER	Specific and Non-specific cIAP-dependent Protein Erasers
snRNA	Small Nuclear RNA
SpyCas9	Cas9 from Streptococcus pyrogenes
ssRNA	Single-stranded Ribonucleic Acid
TBS-T	Tris-Buffered Saline-Tween 20
TEMED	Tetramethyl Ethylene Diamine
TGFβ	Transforming Growth Factor
TGFβR	Transforming Growth Factor Receptor
TKI	Tyrosine Kinase Inhibitors
Tris	Tris-(hydroxymethyl)-amino methane
RNA	Total Ribonucleic Acid
UB	Ubiquitin

UPS	Ubiquitin Proteasome System
VEGFR-2	Vascular Epidermal Growth Factor Receptor 2
VHL	Von Hippel-Lindau
WB	Western Blot
YFP	Yellow Fluorescent Protein

SUMMARY

In the last 20 years the Proteolysis Targeting Chimera (PROTAC) technology has revolutionized the field of drug discovery. PORTACs are heterobifunctional molecules consisting of a chemical ligand, named in this context warhead, and an E3 ligase recruiter united by a linker. These molecules bring the Ubiquitin Proteasome System machinery into the proximity of a protein of interest through for temporal and reversible degradation without the need of genetic manipulation. In comparison to classical chemical inhibitors, PROTACs provide a new approach to repress the activity of a pathogenic protein, which is independent of its catalytic or enzymatic activity. Because of lack of chemical binders, just a small fraction of the proteome has been reported to be targeted by PROTACs.

To increase the number of proteins prone to be targeted by PROTACs, two strategies are followed in this work, exemplified by two new PROTACs. First, the incorporation of a perfluoroaromatic moiety within the structure of the degrader, which can target the sulfhydryl motif in the cysteine residue of the sequence Phe-Cys-Pro-Phe in a nucleophilic aromatic substitution reaction. This tetrapeptide was inserted into the C-terminus of Cas9 ($Cas9^{FCPF}$), while the perfluoroaromatic moiety was tether to Lenalidomide, a broadly used ligand and recruiter of the E3 ligase cereblon. The resulting PROTAC-FCPF successfully degraded $Cas9^{FCPF}$ in a time- and concentration-dependent manner, with a Ubiquitin Proteasome System (UPS)-driven proved mechanism with a half-degradation concentration (DC_{50}) of around 150 nM over 24 hours treatment. PROTAC-FCPF was also effective against genetically engineered related proteins $dCas9^{FCPF}$, $Cas12^{FCPF}$, and $Cas13^{FCPF}$, all modified to have the Phe-Cys-Pro-Phe sequence inserted in their C-termini.
The second strategy was High-Throughput Screening, out of which the compound O4I2 was identified to chemically induce the expression of the Yamanaka factor Oct4 and, thus, supported the induction of somatic cell reprogramming and maintenance of human induced Pluripotent Stem cells. In a proteomics analysis of cells treated with O4I2, it was observed that the Splicing Factor 3 Subunit 1 (SF3B1) was the main hit, a protein that has been associated to several tumors. To target it, O4I2 was bound to another cereblon recruiter, Thalidomide. The resulting PROTAC-O4I2 successfully degraded SF3B1 in a time- and concentration-dependent manner, driven by the UPS with a DC_{50} of 244 nM over 24 hours of treatmenrt. Furthermore, the degrader spared other proteins that were also hits during the proteomics analysis, and successfully degraded the mutant $SF3B1^{K700E}$, present in 55% of patients with myelodysplastic syndromes.

ZUSAMMENFASSUNG

In den letzten 20 Jahren hat die Proteolysis Targeting Chimera (PROTAC)-Technologie die Wirkstoffforschung revolutioniert. PORTACs sind heterobifunktionelle Moleküle, die aus einem chemischen Liganden, in diesem Zusammenhang Gefechtskopf genannt, und einem durch einen Linker verbundenen E3-Ligase-Recruiter bestehen. Diese Moleküle bringen die Maschinerie des Ubiquitin-Proteasom-Systems in die Nähe eines interessierenden Proteins für einen zeitlichen und reversiblen Abbau ohne die Notwendigkeit einer genetischen Manipulation. Im Vergleich zu klassischen chemischen Inhibitoren bieten PROTACs einen neuen Ansatz zur Unterdrückung der Aktivität eines pathogenen Proteins, der unabhängig von seiner katalytischen oder enzymatischen Aktivität ist. Aufgrund des Mangels an chemischen Bindemitteln wurde berichtet, dass nur ein kleiner Bruchteil des Proteoms von PROTACs angegriffen wird.

Um die Größe von Proteinen zu erhöhen, die anfällig für das Targeting von PROTACs sind, werden in dieser Arbeit zwei Strategien verfolgt, um zwei neue PROTACs zu produzieren. Erstens der Einbau einer perfluoraromatischen Einheit innerhalb der Struktur des Abbauvermittlers, die in einer nukleophilen aromatischen Substitutionsreaktion auf das Sulfhydryl-Motiv des Cysteinrests der Sequenz Phe-Cys-Pro-Phe abzielen kann. Dieses Tetrapeptid wurde in den C-Terminus von Cas9 (Cas9FCPF) eingefügt, während die perfluoraromatische Einheit an Lenalidomid gebunden war, einem weit verbreiteten Liganden und Rekrutierer der E3-Ligase Cereblon. Das resultierende PROTAC-FCPF baute Cas9FCPF erfolgreich zeit- und konzentrationsabhängig ab, mit einem vom Ubiquitin Proteasom System (UPS) gesteuerten Mechanismus mit einer halben Abbaukonzentration (DC_{50}) von etwa 150 nM über 24 Stunden Behandlung. PROTAC-FCPF war auch gegen gentechnisch veränderte verwandte Proteine dCas9FCPF, Cas12FCPF und Cas13FCPF wirksam, die alle so modifiziert waren, dass sie an ihren C-Termini die Phe-Cys-Pro-Phe-Sequenz inseriert hatten.

Für die zweite Strategie wurde eine neue Verbindung O4I2 genutzt, die in einem High-Throughput-Screening auf Faktoren, die die Expression des Yamanaka-Faktors Oct4 chemisch induzieren können gefunden wird. O4I2 verbessert die Expression von Oct4 und kann die Reprogrammierung somatischer Zellen und die Erhaltung von humanen induzierten pluripotenten Stammzellen unterstützen. In einer Proteomikanalyse von mit O4I2 behandelten Zellen wurde beobachtet, dass die Splicing Factor 3 Subunit 1 (SF3B1) der Haupttreffer war, ein Protein, das mit mehreren Tumoren in Verbindung gebracht wurde. Um die Targetspezifität zu zeigen wurde O4I2 an Thalidomid als Rekrutierer für die Ubiquitinligase cereblon gebunden. Das resultierende PROTAC-O4I2 baute SF3B1 zeit- und konzentrationsabhängig erfolgreich ab, vermittelt über UPS mit einer DC_{50} von 244 nM über 24 Stunden Behandlung. Darüber hinaus verschonte der neue O4I2-Talidomid

Abbauvermittler andere Proteine, die als weitere Treffer in der Proteomik-Analyse gefunden wurden, baute jedoch sehr erfolgreich die Mutante SF3B1K700E ab, die bei 55% der Patienten mit myelodysplastischen Syndromen vorhanden ist.

1. INTRODUCTION

1.1. Protein Degradation

Homeostasis is a very complex system of mechanisms that is crucial for cellular and systemic survival and adequate function. It involves the regulation of activity or concentration of all components that constitute cells, tissues, organs, and systems of living beings. Such substances range from water, ions, carbohydrates to protein complexes, to mention a few. At a higher level, protein complexes constitute signalling pathways that rule gene expression and, therefore, function. Often, these signalling pathways are naturally regulated by potentiation of inhibition of the activity of a protein within the pathway, by means of ions, hormones, growth factors, cytokines and the intra- or extracellular concentration of metabolites (Churcher, 2018).

Proteins have multiple functions within cells and systems, mainly mechanical support/structural, scaffolding, communicating between the inside and outside of the cell and/or the nucleus, ion channels, transporting, and enzymatic. A few examples of each are next mentioned:

- Mechanical support: α-and β-tubulins, β-actin, vinculin, etc.
- Scaffolding: Kinase Suppressor of Ras-1 (Goettel et al., 2011), BCL10, AKAPs, etc. (Neklesa, et al., 2017).
- Communicating: Aryl Hydrocarbon Receptor Nuclear Transporter (Veldhoen & Duarte, 2010), G protein-coupled receptors, etc.
- Io channels: Na^+/K^+ ATPases, Ca^{2+} channels, proton pumps, etc.
- Transport: albumin, hemoglobin, aquaporins, etc.
- Enzymes: kinases, phosphatases, isomerases, hydrolases, aromatases, etc.

Multidomain proteins make the system even more complex, for different domains within the same protein may have different functions in the same protein, affecting simultaneously different pathways. Last, in higher organisms, proteins can be intracellular or extracellular. Thus, protein homeostasis is a very complex meshwork of different mechanisms.
The activity of some proteins can be inhibited by the presence or absence of other chemical entities. Some enzymes require cofactors or coenzymes to be functional, while others require phosphorylation or dephosphorylation of certain amino acid residues to be active or inactive.
The other major way to regulate proteins is degrading them. This set of mechanisms is very tightly regulated, since, as mentioned before, some proteins may have more than one function, and degrading them implies the loss of more than one function, some of which may be essential for cell survival (He, Khan, et al., 2020).
Thus, extra- and intracellular proteins are degraded through different mechanisms. Extracellular protein and most of transmembrane protein degradation occurs in the lysosomes. Upon endocytosis, the extracellular or transmembrane protein are captured in vacuoles, which are transported to lysosomes that contain acidic proteases such as cathepsins B, D, and H. In most of cells, this process is promoted when insulin or essential amino acids concentrations drop, and by glucagon in hepatocytes (Lecker, et al., 2006). This process is

observed also in transmembrane receptors that enter the cell upon activation of their corresponding ligands or their complexation with antibodies (Ocana & Pandiella, 2020).

Calpains are Ca^{2+} proteases that cleave proteins at cysteine residues. Its activity is correlated to an increase of calcium ions, which can be an immediate consequence of cell damage, and therefore, are related to injury and necrosis. An example of cysteine proteases are caspases, that act at aspartate residues and are essential for cell destruction during apoptosis (Lecker et al., 2006).

Intracellular proteins are degraded mostly once they become malfunctioning or when their concentration becomes saturating. Malfunction of proteins may be derived from physical damage such as denaturation by high temperatures, chemical damage such as that caused by free radicals, altered amino acid sequence consequence of missense, nonsense or shift mutations, misfolding during translation or incorrect post translational modifications (Lecker et al., 2006). Certain conditions, such as hypoxia or lack of other nutrients may lead to an increase of protein expression. The increased synthetic rate can overwhelm the capacity the endoplasmic reticulum to properly fold proteins leading to aggregation of misfolded proteins, triggering endoplasmic reticulum stress (Hetz & Papa, 2018). As this happens, misfolded proteins are re-located to the cytosol to be degraded by the Ubiquitin Proteasome System (UPS). Not only is this the major mechanism of intracellular protein degradation, but also is it the core of this doctoral thesis. Hence, this mechanism will be described in a separate section.

1.2. Ubiquitin-Proteasome System

Proteasomal degradation is a very complex mechanism, that is based on tagging proteins to be degraded with ubiquitin, a 76 amino-acid long protein with a weight of 8.5 kDa. Its C-terminus has a critical glycine residue that is crucial for the conjugation to its substrates. The sequence has multiple lysine residues, that function as binding links for ubiquitin chains. Ubiquitin is expressed as a fusion of several ubiquitin units, or else in a fusion with ribosomal protein subunits. This precursor can be cleaved into functional monomers for protein tagging (Lecker et al., 2006).

The process begins when Ubiquitin Activating Enzyme (E1), a 110 kDa protein, binds to and consumes ATP to produce a highly reactive acyl adenylated form of Ubiquitin at its C-terminus, that is later bound to a cysteine residue of E1 through a thioester bond with the sulfhydryl moiety (Lecker et al., 2006; Ocana & Pandiella, 2020).

Next, ubiquitin is transferred to one of the 40 known Ubiquitin Conjugating Enzymes (E2), through another thioester bond with the sulfhydryl moiety of a cysteine residue in E2. It is important to mention that E2, unlike E1, is a more numerous family of proteins, making it the beginning of the high specificity of the UPS (Lecker et al., 2006; Ocana & Pandiella, 2020).

The last step of the tagging procedure involves an E3 ligase, which brings the E2-ubiquitin complex into proximity of the target protein, except members of the Homologous to E6-AP carboxy-terminus (HETC) domain subfamily, that generate an intermediate thioester bond with ubiquitin, before it is last linked to a lysine residue of the target protein (Buckley & Crews, 2014; Ocana & Pandiella, 2020).

The process described is repeated to bind further units of ubiquitin to either the N-terminus or one of the 7 lysine residues within the sequence of ubiquitin. A chain of 4 ubiquitin units

at Lys^{48} suffices to tag a protein for proteasomal degradation. Nevertheless, there are other possible residues for ubiquitination (K^{6}, K^{11}, K^{27}, K^{29}, K^{33}, K^{48}, K^{63} and M^{1}). Yet, ubiquitination at different sites may result in several biological effects other than proteasomal degradation. Before the tagged protein starts being degraded, ubiquitin is removed by deubiquitinating enzymes (DUBs) and recycled to tag other proteins (Buckley & Crews, 2014; Churcher, 2018). The process is represented in Figure 1.

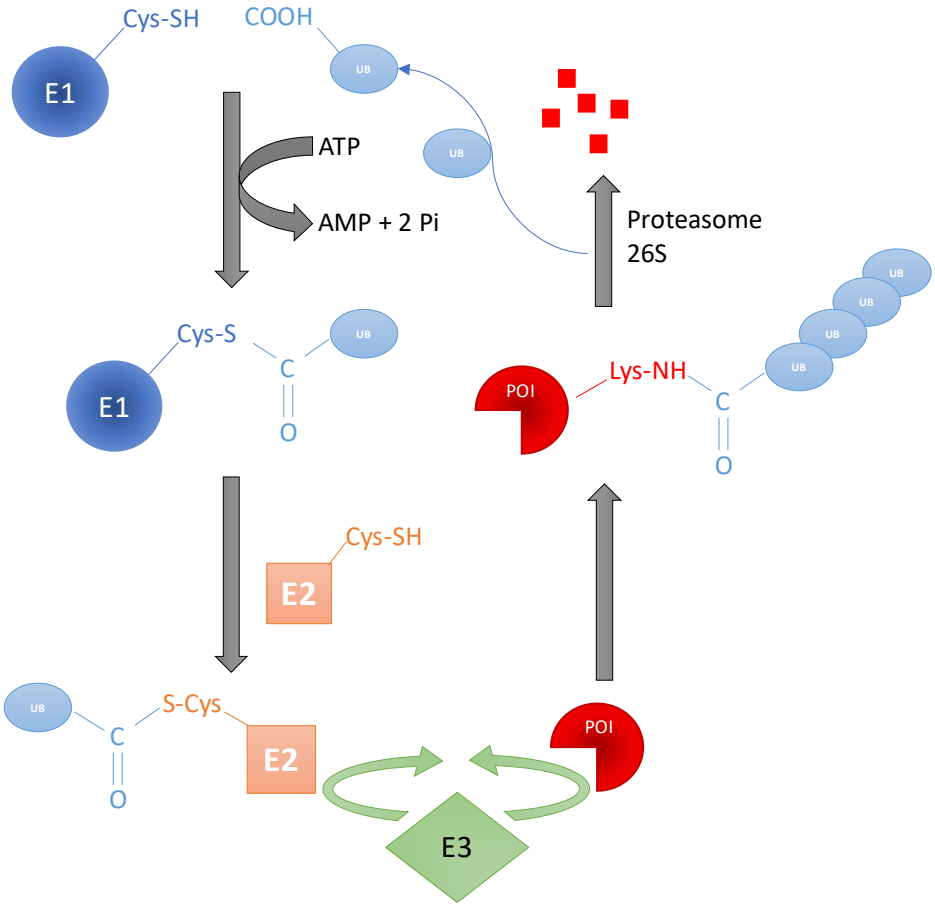

Figure 1: schematic representation of the Ubiquitin-Proteasome System.

This system is responsible for the degradation of intracellular proteins. E1: Ubiquitin-Activating Enzyme, E2: Ubiquitin-Conjugating Enzyme, E3: E3 ligase; POI: Protein of Interest, and UB: Ubiquitin units. E1 uses ATP to activate and bind to one Ubiquitin unit, which is then transferred to a E2 enzyme. Last an E3 ligase brings a Protein of Interest into proximity of the Ubiquitin-E2 complex for a last transfer or the Ubiquitin. This process is repeated until the Protein of Interest carries a Polyubiquitin tag, which leads to proteolysis by the 26S proteasome. Before, degradation, ubiquitin is detached from the Protein of Interest and recycled.

This family of proteins is estimated to have over 600 members which, in combination with the 40 E3 proteins, make a very specific system. This family divided into two major groups: first Homologous to E6-AP carboxy-terminus (HETC) domains, and secondly, the majority of E3 ligases, RING finger domains. HETC domain proteins are monomeric units, whose C-terminus, with 350 amino acids, binds to activated ubiquitin donated by E2 and allows transfer to the target protein. In the other hand RING domain proteins can be monomeric or part of large complexes. Neither of them has catalytic activity but are scaffold to bring the E2-Ub complex into proximity of the target protein. The most common of these proteins are the

Cullin-RING ligases, which possess a rigid and elongated subunit. On end interacts with the E2-Ub complex, while the opposite end interacts with the target protein (Lecker et al., 2006). The specificity of this system increases further, given that not all E3 ligases are ubiquitously expressed in all tissues. ASB9, a SOCS box E3 ligase can only be found in pancreas and in testis, while FBXl16 is mostly expressed in the cerebral cortex (Ocana & Pandiella, 2020).
Some E3 ligases are directly related to certain disease, because of their tissue specificity.
Ring Finer Protein 41 RNF41 is an E3 ligase that has been found to have a lower expression in Cellular Hepatocarcinoma (HCC), limiting the degradation of Calcyclin-Binding Protein (CACYBP), a factor necessary for a normal apoptosis cycle (Lian et al., 2019).
There are other E3 ligases related to Hepatocellular carcinoma, for example: the DDB1 and CUL4 associated factor 13 (DCAF13), which is also observed in other forms of cancer such as breast cancer (J. Cao et al., 2017), the human ortholog of Drosophila lethal (2) denticleless (L2DTL or simply DTL) (Pan et al., 2006), Potassium Channel Tetramerization Domain containing 17 (KCTD17) about which there is also proven evidence of having E3 ligase activity (Duan et al., 2019; Pinkas et al., 2017), RN181, also known as HSPC238, is a ring finger protein known to have E3 ligase activity for autoubiquitination, and was found to be down-regulated in HCC cells, and is also known to be a tumor suppressor in gastric cancer (S. Wang et al., 2011; S. Wang et al., 2019).
There are other reported E3 ligases to be specific of some other cancer tissues, for example Ring Finger Protein 152 (RNF152) was found to supress colorectal cancer cell proliferation (Cui et al., 2018), Ring Finger Protein 165 (RNF165) is associated to metastatic prostate cancer (Xu & Sun, 2015), similarly the Ring Finger Protein 181 (RNF181) interacts with CARD11 and limits the proliferation of diffuse large B cell lymphoma cells (Pedersen, et al., 2015), and the Ubiquitin-like Protein containing PHD and Ring Finger Domains 1 (UHRF1) is related to colorectal and gastric cancers (Niinuma et al., 2019; H. Zhang, et al., 2018).
PEX10, KBTBD4, PATZ1, RABGEF1, AREL1, LONRF2, FBXL16, ZBTB45, KCNB1, RNF2208, KCTD16, KCTD4, DPF1, MKRN3, and RHOBTB1 have all remarkable expression levels in neural tissue, specifically at the temporal lobe, but are absent in other organs. The gastrointestinal tract, prostate and pancreas have all high levels of K8T8, but it is barely expressed in neurons and blood cells. RBX1, ZFAND5, WSB1, ANAPC11, SOCS3, KRT8, RNF181, LGALS3BP, BIRC3, and IVNS1ABP are all found mostly, but for instance K8T8 and RNF181 not exclusively, in hematopoietic cells (He, Khan, et al., 2020).

The 26S proteasome is a remarkably large complex of proteases found in all cells, located in the cytoplasm and the nucleus. The 26S fraction has around 60 subunits, making it considerably larger than any other extracellular protease. This fraction is constituted by a central 20S barrel or cylinder with 19S subunits at its extremes, that operate as regulators or gates in and out of the barrel. The 20S cylinder has 2 outer α-rings and 2 β-rings with proteolytic sites facing in lumen of the structure. The α-rings are the external particles of the structure, making pores through which the targeted protein enters, and the resulting amino acids leave (Lecker et al., 2006).
The 19S fractions at either side of the 20S particle have 18 subunits with 6 ATPases at the bases, which are also bound to the outermost rings of the 20S cylinder. The outer surface of the 19S particles have several subunits that bind to polyubiquitin and are adjacent to DUBs that cleave the polyubiquitin chain away and disassemble it, for ubiquitin to be recycled and used for further tagging of other proteins. The ATPases at the base bind to the target protein, linearize it and relocate it into the 20S barrel. This step is crucial, for the internal diameter of

the cylinder is not wide enough for globular proteins. Once inside, the sequence of the protein to be degraded is cleaved by the six proteolytic sites into 3- to 25-amino acid-long peptides. Longer peptides are further cleaved into short peptides that finally leave the proteasome. These peptides are immediately cleaved into single amino acids by all the cytosolic endo- and aminopeptidases (Lecker et al., 2006).

1.3. Targeted Protein Degradation Strategies

Historically, an important fraction of pharmacological treatment of diseases has consisted in occupancy-driven approaches, that imply the use of small molecules that fit in and interact with active sites of proteins, thus inhibiting them or activating them, to produce a biochemical or physiological response (Pettersson & Crews, 2019). Nevertheless, over the years the disadvantages of this approach have become clear and consistent. First, the use of small molecules as agonists has very often limited specificity and the small molecule may interact with other proteins besides the protein of interest (POI). It can also be that the small molecules have relatively good selectivity for a POI, but does not have tissue specificity, therefore the drug may have activity in tissues where it is not required, or else, the concentration of the drug in the tissue of interest is lower, due to its systemic distribution and accumulation in other tissues, being the clearest example of this problem most of the chemotherapeutic agents that intervene in the cell cycle, such as cyclophosphamide, etoposide, cis-platinum, etc., despite the higher activity they exhibit against highly proliferative cells, healthy cells are often not spared (Maeda & Khatami, 2018) . Thus, it would be required to increase the dose to reach the necessary levels of the drug, yet this would result in an increase of the risk of toxicity. Second, the occupancy-driven pharmacological approach relies on constant interaction of the POI with its agonist, in this case, drug (Pettersson & Crews, 2019). This impacts on the dosing frequency needed to maintain the systemic concentrations of the drug to be active, with the disadvantage that this also increases the exposure time of other tissues where the drug is not required, leading to increased risk of toxicity, as well. Third, competition with other molecules for the active site is another factor to increase the needed dose, with the consequences previously described. Fourth, prolonged exposures to a drug or misuse of it, typically in chronical or infectious diseases respectively, often lead to resistance development, meaning that the standard dose stops being functional and must be increased, or the drug may simply not be effective anymore, creating the need of newer generations of such drugs. Fifth, and probably most important, this approach is limited to the existence of an active site, where the drug can bind to. Such active sites are mostly exclusive to enzymes (kinases), meaning that 80 to 85% of the proteome is left out, and with it, many therapeutic opportunities (Bondeson & Crews, 2017; Neklesa et al., 2017)

In the past decades, alternative approaches have been researched on. One of the most recent and unquestionably most successful in cancer treatment was the use of monoclonal antibodies that target POI with very high specificity and have, thus, revolutionized cancer treatment, by reducing remarkably toxicity and side effects. Yet, monoclonal antibodies have major disadvantages. Clinically, being very large proteins, they are uncapable of crossing the cell membrane, being therefore limited to trans membrane and surface proteins only. Also, clinically, monoclonal antibodies have the disadvantage of being restricted to intravenous

infusion. Industrially and commercially, monoclonal antibodies development, process and, as a finish product, come with a very high cost (Neklesa et al., 2017).

Another strategy has been the use of antisense oligonucleotides, such as interference RNA (RNAi) and small interfering RNA (siRNA). Nevertheless, these nucleotides have proved more useful in research than in therapeutics. When unmodified, Antisense Oligonucleotides are unstable in serum, but when modified they accumulate in the kidneys, and when prepared in nanoparticles the accumulation happens in the liver (Lai & Crews, 2017). Thus, the resulting half-life time is considerably short, which compromises their efficacy, mostly in proteins with long lifetimes and low turnover rate. This shortened life may also make it difficult to distribute and deliver to cells. Shortly, they exhibit poor pharmacokinetic profiles (Churcher, 2018). Despite these poor characteristics, Antisense oligonucleotides have good pharmacodynamic properties because of their catalytic nature, resulting, ironically, in durable effects. The Transthyretin mRNA targeting siRNA Patisiran is being trialed at 0.3 mg/kg every 3 to 4 weeks, not only because of its catalytic nature, but also because of high intracellular retention (Neklesa et al., 2017). Currently there are 9 nucleic acid-based drugs in the USA, but not all are approved, for instance, in Europe (Stein & Castanotto, 2017; Yamakawa, et al., 2019).

Another technology that attracted a lot of attention was the innovative Clustered Regularly Interspaced Short Palindromic Repeat (CRISPR)-Cas9 system that allows very powerful gene editing. However, its clinical applicability quickly became questioned and controversial, for off-target mutations have been reported (Fu et al., 2013), and probably more problematic in the context of clinical protein regulation, the resulting gene editions are irreversible, which immediately discards this strategy for proteins that have more than one function and are essential for cell survival and function.

The solution came when it was first reported that protein degradation can be controlled and targeted and several approached to do so have been developed.
Degrading a POI pool can be a very effective solution to suppress its activity, primarily, because the effect is reversible, making it easy to research on and easier to control. It would also give the opportunity to study the cellular adaptive responses consequence of the absence of the depleted protein (Prozzillo et al., 2020).
Some of the most common strategies are next mentioned and described:

- Anchor Away (AA)

  This technique is not a protein degradation strategy, but it is based in the relocalization of proteins, away from their site of action, and it is mostly effective against nuclear proteins. The mTOR inhibitor rapamycin bridges between the FK506 binding Protein (FKBP12) and FKBP12-rapamycin associated protein (FRAP). Then, at one side of it, FKBP12 is fused to an anchor protein. An Example is Rpl13A, a ribosomal protein that is relocated to the nucleus in the process of building up ribosomes, and then definitely moved out towards the nucleus. At the other side, FRAP is fused to a POI. Thus, when mammalian cells expressing these fusion proteins are treated with rapamycin, an anchor protein-FKBP12-rapamycin-FRAP-POI complex is formed, and

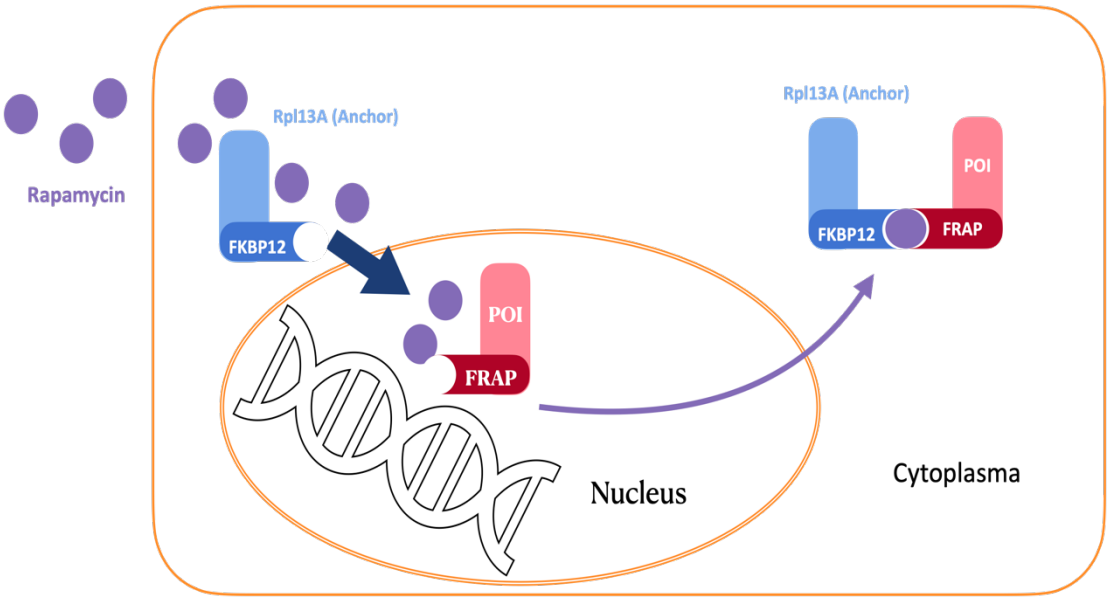

Figure 2: schematic representation of the Anchor Away Technology.

FKBP12: FK506 binding Protein, FRAP: FKBP12-rapamycin associated protein, POI: Protein of Interest. The mTOR inhibitor rapamycin bridges between the engineered Protein of Interest, fused to FRAP, and a ribosomal protein (e.g., Rpl13A) that is also engineered and fused to FKBP12. After the complexation and when the ribosomal protein leaves the nucleus, the entire complex is relocated, taking the Protein of Interest out of its site of action, thus, depleting its activity without compromising its integrity.

re-located to the nucleus all together and, therefore, away from its site of action, thus depleting its activity without compromising the protein integrity. The process is reversible upon rapamycin withdrawal (Prozzillo et al., 2020). This approach is clearly applicable in research only, due to the need of fused proteins. The process is represented in Figure 2.

- deGradFP

In contrast with AA, this technique is a protein degradation approach, and relies on the 26S proteasome mechanism described earlier in this text. A POI is fused to a fluorescent protein, most commonly Green Fluorescent Protein (GFP). Then, the Skp-Cullin-F-box (SFC)-containing E3 chimeric complex is attached to an anti-GFP nanobody (VhhGFP4) to recognize and bind to the POI. It is important to mention, that in the SFC complex, the F-box is engineered to an inducible form (NSlmb). It is also important to notice that other fluorescent proteins have been used, such was Yellow Fluorescent Protein (YFP), Enhanced Yellow Fluorescent Protein (EYFP), and Red Fluorescent Protein (RFP).

The use of a fluorescent protein is very advantageous, practically. It is used as a tag to the POI, but it also functions as a reporter that can be easily measured. It has been reported that the fluorescence signal starts decreasing after 30 minutes only. There have been reports of proteins from different cellular compartments (cytosol, nucleus, and membrane) being comparably targeted and successfully degraded.

A disadvantage of this system is that fluorescent proteins are large and may affect the tridimensional conformation of the POI, resulting in GFP being hidden, and thus, inaccessible to the nanobody. Another, effectively similar limitation, is when the POI is present in large complexes, which can easily hinder the fluorescent protein tag. It

also has been reported that the GFP tag is not recognized by the nanobody, unless attached to another protein or peptide, which may lead to size limitations.
Last, but not less important, this system has also been proved to be adaptable. The nanobodies can be bound to different E3 ligases to target specific proteins, or else to target proteins from specific cellular compartments (Prozzillo et al., 2020).
The mechanism is schematized in Figure 3 next presented.

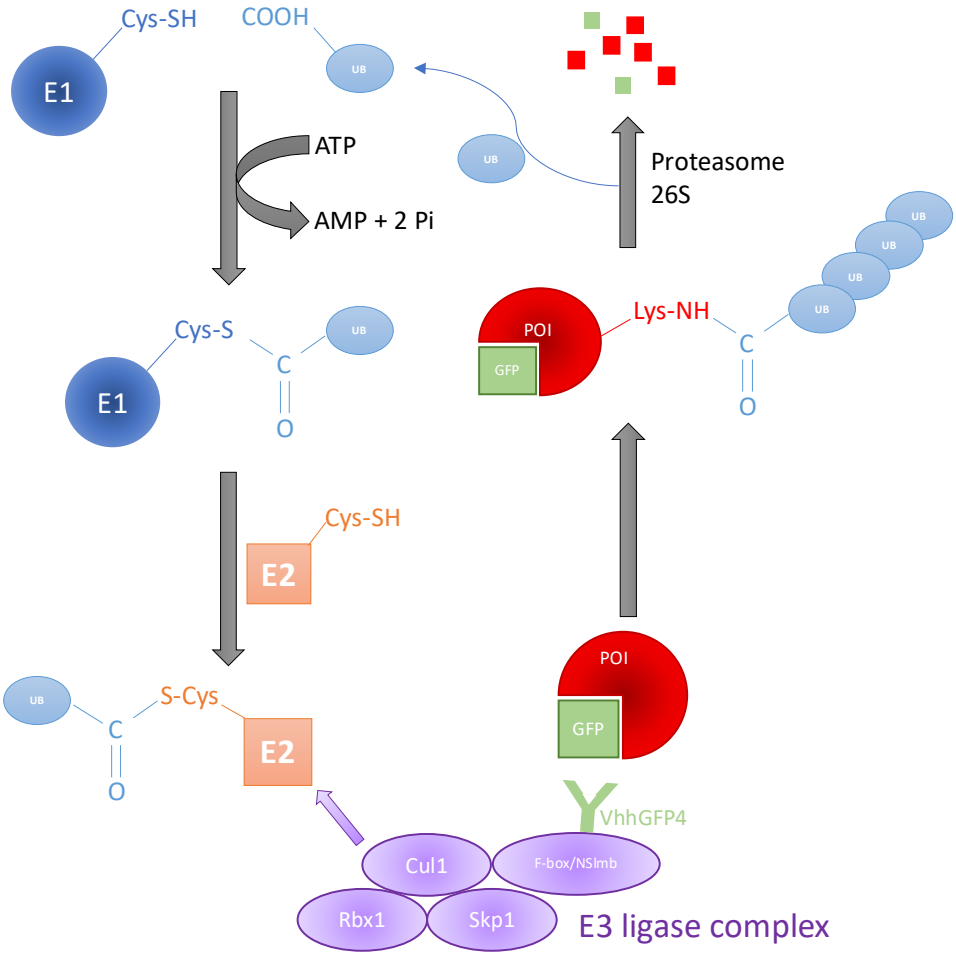

Figure 3: 26S proteasome mechanism induced by the deGradFP System.

E1: Ubiquitin-Activating Enzyme, E2: Ubiquitin-Conjugating Enzyme, E3: E3 ligase; POI: Protein of Interest, and UB: Ubiquitin units. The F-box of the SFC complex is engineered to the inducible form NSImb. Then the complex is bound to the GFP nanobody VhhGFP4, while the Protein of Interest is fused to GFP. The E3-Nanobody fusion protein then recognized the GFP-fused Protein of interest as it simultaneously recruits the UPS, leading the 26S proteasomal degradation of the Protein of Interest. This is not only a techique to degrade proteins with very high specificity, but it also is a tool to detect and quantify the loss of the Protein of Interest.

- Degradation TAG (dTAG) System

The dTAG is another targeted protein degradation strategy that also relies on gene editing to produce a protein chimera, using a destabilized mutant allele of FKBP12 ($FKBP12^{F36V}$) within the transcription frame of a POI, by means of CRISPR/Cas9-mediated locus-specific knock in. The resulting fused protein binds to a

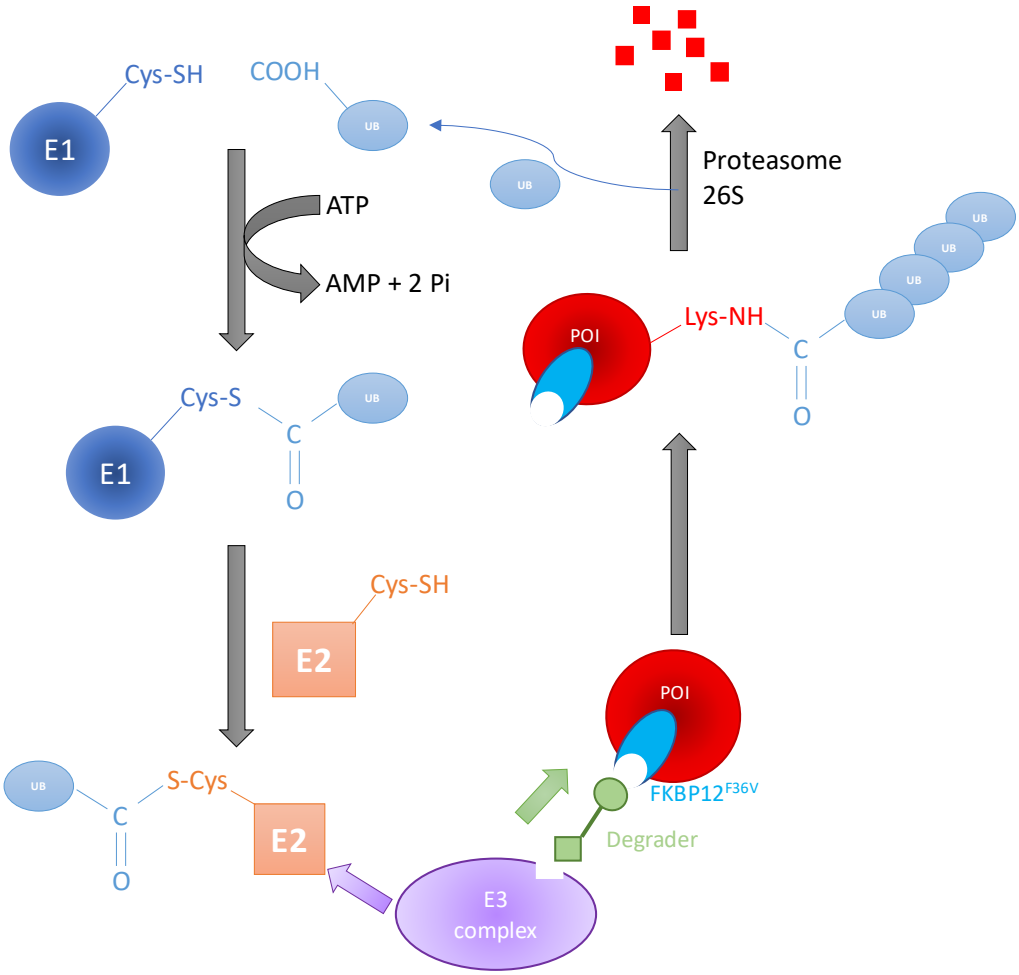

Figure 4: 26S proteasome-mediated protein degradation mechanism induced by the dTAG system.

E1: Ubiquitin-Activating Enzyme, E2: Ubiquitin-Conjugating Enzyme, E3: E3 ligase; POI: Protein of Interest, UB: Ubiquitin units, $FKBP12^{F36V}$: destabilized mutant allele of FKBP12. The Protein of Interest is engineered and fused to $FKBP12^{F36V}$ that can be targeted with a degrader (e.g. dTAG13) which, being a heterobifunctional molecule also has at the other side of the molecule a moiety to recruit an E3 complex, resulting in highly specific proteasomal degradation.

heterobifunctional molecule (dTAG13) that stabilizes and binds to $FKBP12^{F36V}$ in one end of the molecule, and from the other end binds to cereblon (CRBN), the recognition unit of the DDB1-Rbx1-CRL4-N8-CRBN E3 ligase complex. Thus, the $FKBP12^{F36V}$-POI fusion protein is brought to the proximity of the E3 ligase complex to be polyubiquitinated, and consequentially degraded by the 26S proteasome. This strategy has been successfully employed to degrade several proteins, with varying degradation rates in different intracellular compartments.

The system has also been adapted by using $dTAG^{V}$-1 a ligand that binds to the CUL2-Rbx1-EloC-EloB-von Hippel-Lindau (VHL) E3 ligase complex instead. This degrader, $dTAG^{V}$-1, showed a superior pharmacokinetic and pharmacodynamic profile, compared to that of dTAG-13, with a longer half-life time, making it, thus, possible to obtain longer exposure times to the degrader, and consequentially increasing the protein degradation rate (Nabet et al., 2018; Prozzillo et al., 2020).

The advantages of this technology in research are the very high specificity of protein degradation, given that it is founded on genetically engineered fusion proteins, and that the protein degradation is acute and easy to control, for it will stop shortly after

withdrawal of the degrader. This is also its main disadvantage clinically, the need of irreversible gene editing.
A general mechanism is showed schematically in Figure 4. Note that E3 complex is used instead of either of the specific cases mentioned before. Also “degrader” is used interchangeably for dTAG-13 and dTAG^{V}-1.
26S proteasome-mediated protein degradation mechanism induced by the dTAG system

- Hydrophobic Tagging (HyT)

This system is also another strategy based on the 26S proteasomal degradation system and on the presence of a fused tag. In this case, the purpose is to tag the POI with a

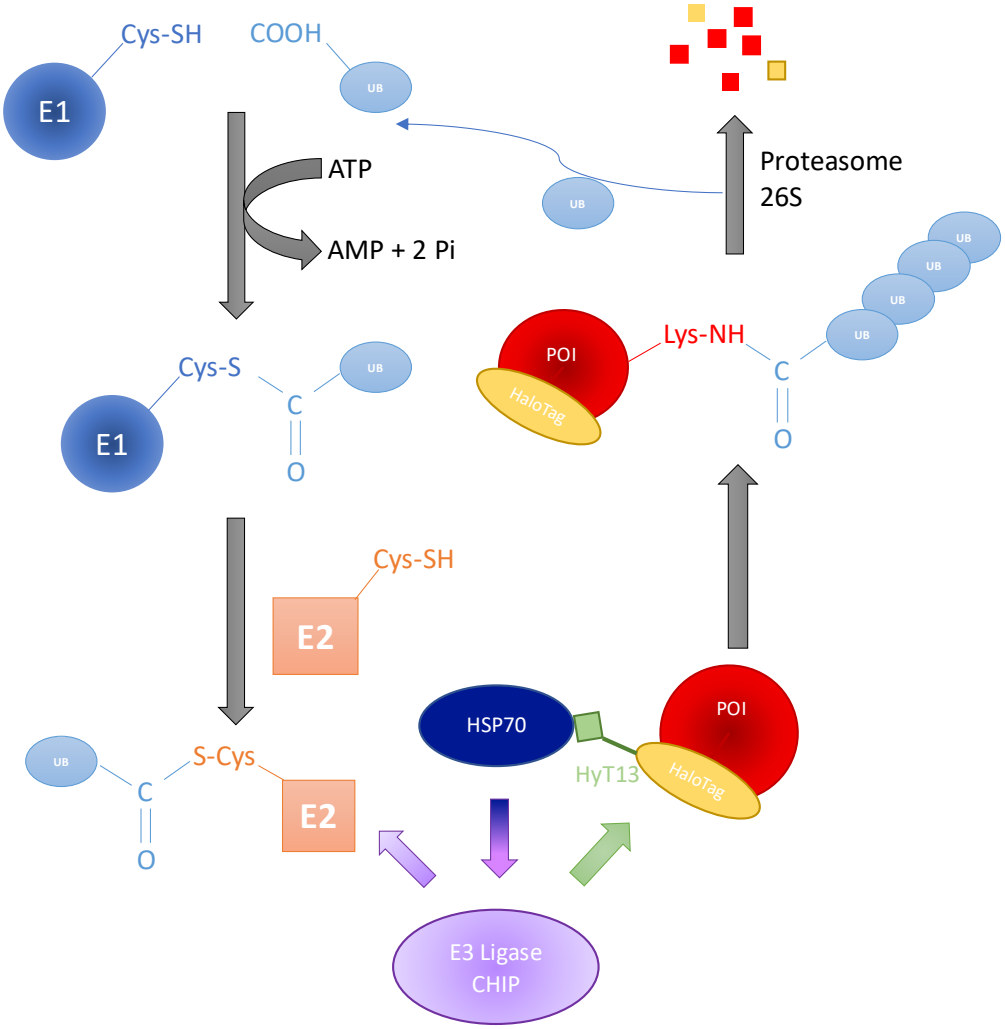

Figure 5: Schematic representation of the proteasomal degradation mechanism induced by HaloTag and HyT13.

E1: Ubiquitin-Activating Enzyme, E2: Ubiquitin-Conjugating Enzyme, E3: E3 ligase; POI: Protein of Interest, UB: Ubiquitin units, HSP70: molecular chaperon Heat Shock Protein 70, CHIP: C-terminus of HSP70 Interacting Protein E3 ligase, HaloTag: bacterial dehalogenase, HyT13: covalent adamantly-containing-linker. A Protein of Interest is fused to a bacterial dehalogenase. Then, cells expressing this engineered Protein of Interest are treated with a linker that binds covalently to the HaloTag, from one end. At the other end, the linker has an adamantly moiety that increases the hydrophobicity of the surface, mimicking a misfolded protein, resulting in the activation of the misfolded protein response, where HSP70 binds to the hydrophobic surface, at the same time that it recruits the CHIP E3 ligase, to ultimately trigger the UPS-mediated degradation of, in this case, the HaloTagged Protein of Interest.

hydrophobic moiety, that mimics the state of a misfolded protein, that would expose its normally buried hydrophobic amino acid side chains. When proteins are misfolded, the molecular chaperon BiP binds to the protein to help it fold properly (Neklesa et al., 2011). If the cell is unable to fold the protein correctly, the molecular chaperons HSP70 and HSP90 recruit the E3 ligase C-terminus of HSP70 Interacting Protein (CHIP) to polyubiquitinate misfolded proteins, labelling them for proteasomal degradation. The POI is fused to a bacterial dehalogenase (HaloTag), once ectopically expressed, the cells can be treated with a linker (HyT13 being the most common) that can bind covalently to the HaloTag in one end, and in the other has adamantyl acetamide moiety to increase the hydrophobicity of the complex's surface (Lai & Crews, 2017; Neklesa et al., 2011; Roth, et al., 2019).
This system initially used GFP and luciferase as a proof of concept. Later other proteins were successfully degraded with it, including cytosolic and transmembrane proteins.
As the other strategies described so far, the protein specificity is high, but clinically the main disadvantage remains being the need of fusion proteins.
Figure 5 next shows a schematic representation of this mechanism.

- Small Molecule Assisted Shutoff Tag Degron (SMASH)

  This protein degradation system is significantly different to any of the previously described, although it is also based on fused POIs. Even though the exact proteolytic mechanism is not yet fully understood, the Non-Structural Protein 3 (NS3), expressed in the Hepatitis C virus (HCV), is fused to its cofactor NS4 through its protease domain to produce a complex with degron properties. This degron is then further fused to either the C- or N-terminus of a POI through the cleavage site of NS3. The degron has the capacity to detach itself from the POI, making it a self-removable tag. The detachment can be controlled treating with protease inhibitors, e.g. asunaprevir, which binds to the active site of NS3, preventing it from detaching from the POI, thus, ultimately causing its degradation (Roth et al., 2019).
  The activity of this system was observed in a range from very low nano molar to low micro molar range, with no detectable side effects (Roth et al., 2019).
  A main advantage of this system is that only newly synthesized proteins with the fused degron will be affected, leaving the pre-existent proteins untouched, making it easier to study the degradation kinetics (Roth et al., 2019).
  Once more, the need of fusion proteins makes this approach clinically unapplicable.

- Auxin-Inducible Degron System (AiD)

  This strategy is also based on 26S proteasomal degradation of POIs, but it has a very singular characteristic: the use of phytohormones to recruit the ubiquitination machinery to tag proteins for degradation. In plants, when the levels of phytohormones of the auxin family, like indole-3-acetic acid (IAA), increase, the expression of auxin-responsive genes is allowed by degrading the proteins that otherwise repress them. These hormones, namely AUX/IAA Transcriptional Repressor Proteins, are degraded by the eukaryote-widely conserved SKP-Cullin-F-Box (SCF)-RING E3 ligase complex, along with the Transport Inhibitor Response 1 (TIR1) (Roth et al., 2019).

Given the fact that the SFC complex is present in all eukaryotes, it has been applied in cells of different species, including humans. To do so, the POI must be fused to the IAA17 degron (AID tag or AX3) and TIR1 must be overexpressed in the cell study system. Upon treatment with IAA, the phytohormone makes a complex with the AID-tagged POI and the SCF-TIR E3 ligase leading to very fast protein degradation (Prozzillo et al., 2020). IAA is not thought to have significant side effects in mammalian cells, for it is mostly present in plants. However, it has also been observed that its oxidation mediated by peroxidases yields a product that shows toxicity. This should be considered, because this degradation system requires relatively large amounts of IAA (Roth et al., 2019).

Initially, this system was developed from TIR1 derived from Arabidopsis thaliana (atTRI), but it was observed to be denatured at cell-culture temperature. Hence, TIR1 derived from Oryza sativa (osTIR1) was used, because it remains stable at higher temperatures (Roth et al., 2019).

Figure 6 shows a scheme of the mechanism previously described.

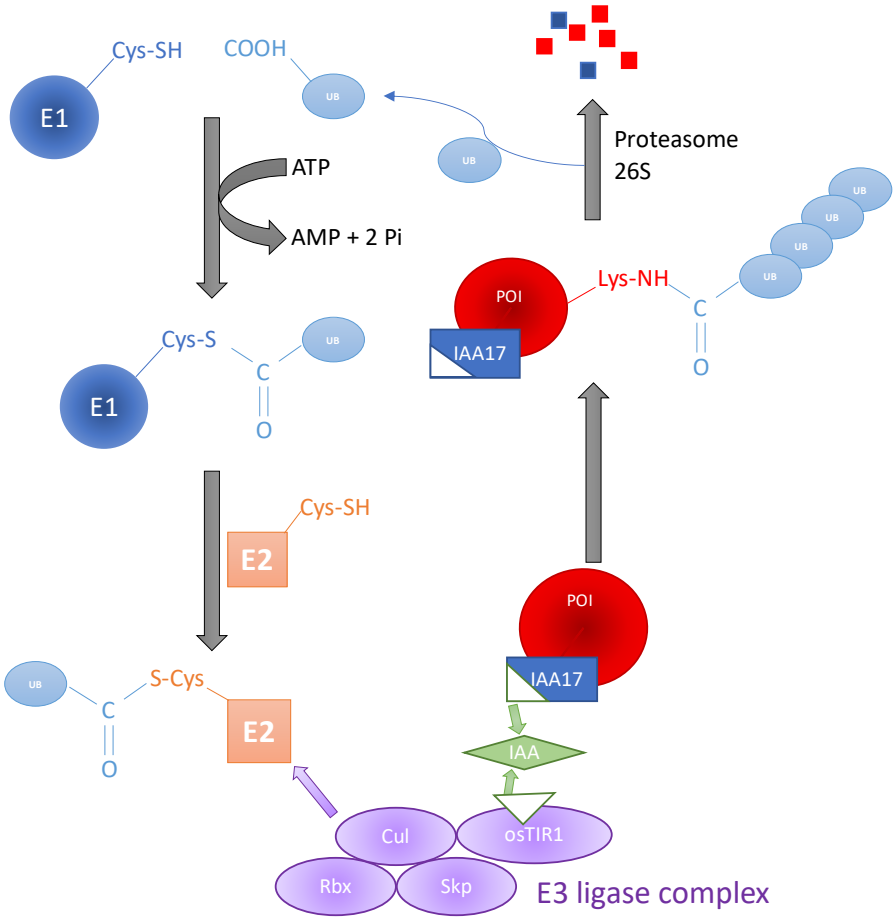

Figure 6: schematic representation of the proteolytic mechanism driven by the AiD system.

E1: Ubiquitin-Activating Enzyme, E2: Ubiquitin-Conjugating Enzyme, E3: E3 ligase; POI: Protein of Interest, UB: Ubiquitin units, Cul, Rbx, Skp, and osTIR1 are all components of this TIR1 E3 ligase complex derived from Oryza sativa, IAA: indole-3-acetic acid, IAA17: AID tag or AX3 degron. A Protein of Interest is fused to a degron from an AUX/IAA Transcriptional Repressor Protein. In parallel, the TIR1 E3 ligase from Oryza sativa must be overexpressed in the study system (e.g., human cells), to form a complex with the eukaryote-widely expressed SFC complex. In the presence of a phytohormone, e.g., IAA, the UPS is recruited through the SCF-osTIR1 E3 ligase complex for the proteasomal degradation of the IAA17-Protein of Interest chimera.

- TRIM away

  Tripartite Motif (TRIM) proteins have various roles within cells, being the response to viral infections one of the most important. These proteins have a RING-box domain that confers them the E3 ligase activity and a C-terminal PRYSPRY domain, among other domains, that is thought to confer them specificity to different targets. TRIM21 is an intracellular protein that binds with high affinity to the F_c region of IgGs. After viruses are recognized and labelled with antibodies, they are endocytosed, to be then recognized by TRIM21 through the antibodies bound to them, and thus, polyubiquitinated for proteasomal degradation (Roth et al., 2019). The resulting peptides are further used for antigen presentation as part of the Major Histocompatibility Complex I response (Lecker et al., 2006).

  Thus, the TRIM away consists in the internalization of antibodies specific to a POI either by microinjection or electroporation, with or without TRIM21 overexpression. This method has been reported to lead to POI degradation within minutes with very high specificity, given the fact that it is antibody based. This strategy was successful in degrading all proteins that are accessible from the cytosol but, due to the large size of antibodies, it failed to degrade nuclear proteins. The effect was also observed to linger for three to four days, although the efficacy time varied with the amount of TRIM21 within the cell and the amount of POI (Roth et al., 2019).
  Unarguably the two main disadvantages of this strategy are the intrinsic high cost derived from the need of using selective immunoglobulins and the technical difficulty implied in internalizing them into cells (Roth et al., 2019). Combined, these two factors also make the technique clinically inapplicable.

These strategies are just some examples of targeted protein degradation techniques and there are certainly several more strategies, although not all of them are covered in this work. Next, one of the most promising technologies in the field will be more thoroughly described, as it is the core of this doctoral thesis. This technology has developed very quickly in 20 years, due to its versatility, adaptability, effectiveness, low toxicity, high selectivity and reversibility, characteristics that not only give rise to many possibilities for cell biology research, but also open a door for a clinically applicable targeted-protein-degradation technology.

This technology, as most of the previously described, is based on the polyubiquitin tagging system that leads to 26S proteasomal degradation. The difference, as next described, is that it relies purely on chemistry –in the context of classical pharmacology— and requires no genetic modification or editing.

1.4. PROTACs

The immediate alternative to overcome the disadvantages common to most the strategies described before, is eliminating the need of genetic modifications implied in fusion proteins. To achieve that, the feasibility to tag a protein for degradation must be accomplished externally, it is to say, chemically.
The first example of this is the targeted degradation of the Estrogen Receptor α (ERα), a nuclear hormone receptor with various effects on different physiological systems of both male and female (Lai & Crews, 2017). It also is a known oncoprotein associated to breast cancer, that can be targeted for proteasomal degradation by Fulvestrant, approved by the FDA in 2002. Selective Estrogen Receptor Downregulators (SERDs) have been proved to produce conformational changes in ERα, making it expose its hydrophobic motifs. Consequently chaperons may tag if for degradation (Bondeson & Crews, 2017). Upon binding to a chaperon, unfolded proteins are subjected to post-translational modifications, including ubiquitination, as part of the Unfolded Protein Response (UPR) to ultimately be degraded by the proteasome (Hetz & Papa, 2018; Lai & Crews, 2017).

The foundational technology of this doctoral work is the PROteolysis TArgeteing Chimeras (PROTACs), broadly defined in scientific literature as heterobifunctional molecules that consist of a small molecule, commonly named warhead, that can interact or bind to a POI, while the opposite end of the PROTAC has a small molecule capable of recruiting an E3 ligase, bringing it into the proximity of the POI, and thus force its polyubiquitination to be degraded by the 26S proteasome, being these two components united by a linker of variable composition and length (Bondeson & Crews, 2017; Pettersson & Crews, 2019).
Figure 7 displays the mechanism behind PROTAC-mediated POI degradation.
A different definition is difficult to assign, for PROTAC is a technology that has been developing for over 20 years, and many different combinations of warheads, linkers and recruiters have been used to target equally varied proteins. During these years, also several sub-technologies have emerged. Also, during these two decades, several aspects of the technology have been refined in the quest of producing more effective, faster, and more selective protein degraders.
Many of these modifications of the system went as far as producing sub-technologies, all based in the same principle of PROTACs, but add different details. Some PROTACs are fully assembled within the cells, whereas some others are activated upon exposure to light. Some (most) of PROTACs rely on non-covalent, classical electrostatic interactions between the proteins and the small molecules involves, while a few PROTACs based on covalent bonds have been developed.

Because of all these reasons, instead of trying to aim for a more specific definition, a chronology of PROTAC development is next described, followed by a description of the sub-technologies that have resulted of variations to this targeted protein degradation system, as well as all the technical aspects that have been studied and found to be important for PROTAC activity and, therefore, are very necessary to keep into account for the design of new PROTACs.

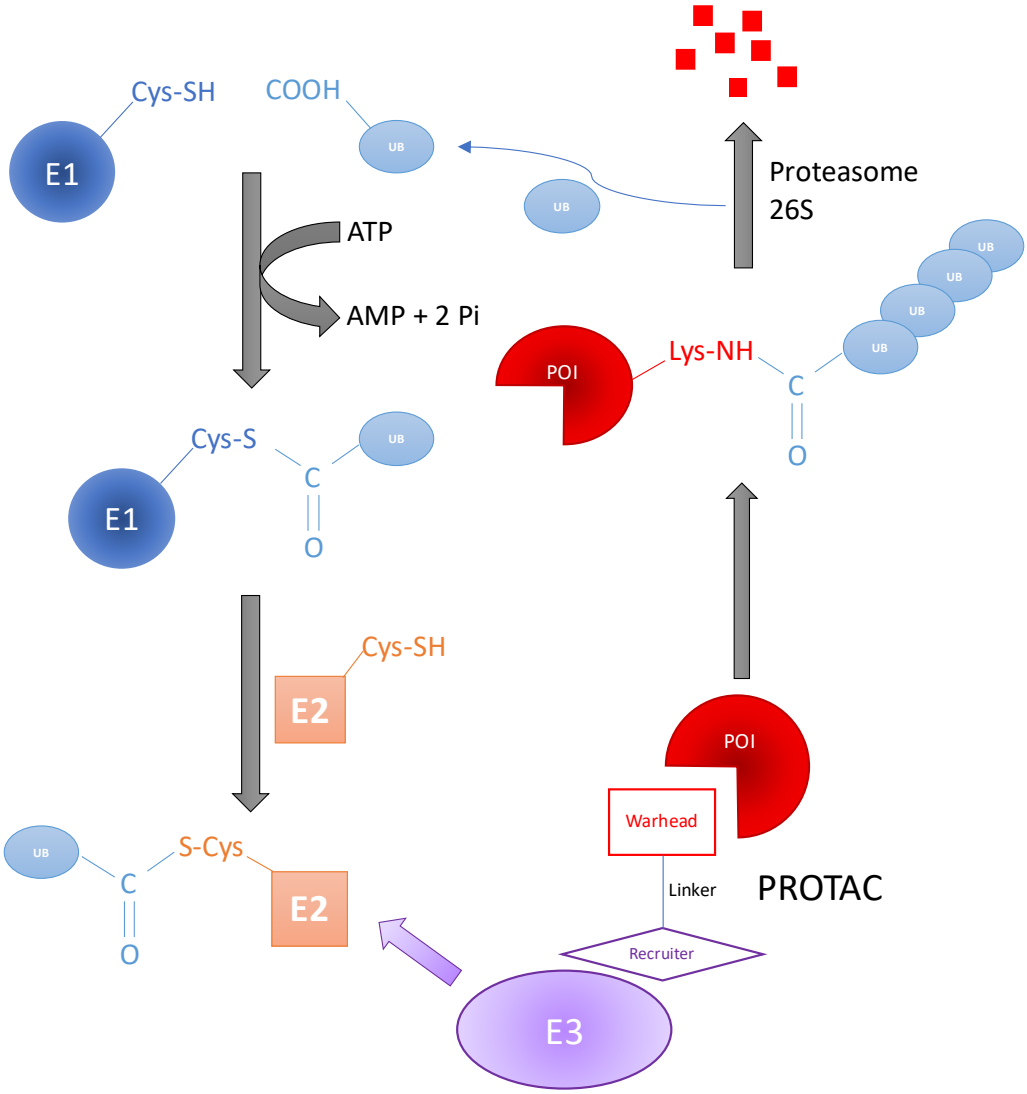

Figure 7: Schematic representation of the PROTAC-mediated protein degradation.

E1: Ubiquitin-Activating Enzyme, E2: Ubiquitin-Conjugating Enzyme, E3: E3 ligase; POI: Protein of Interest, UB: Ubiquitin units, PROTAC: Proteolysis Targeting Chimera. PROTACs are heterobifunctional molecules that consist of three parts: first, a warhead, which is a small molecule or motif that interacts shortly and superficially with a Protein of Interest, second, a linker of varying composition and length that tethers the third component, a Recruiter, another small molecule or motif that interacts with an E3 ligase, bringing it to the proximity of the Protein of Interest to induce its proteasomal degradation driven by the UPS.

1.4.1. Chronology of PROTACs

2001

This sophisticated mechanism was first used to target a Protein of Interest (POI) 20 years ago, with a proof-of-concept perspective. Crew and co-workers linked to a moiety of the small molecule ovalicin (an angiogenesis inhibitor) to a phosphopeptide derived from NF-κB inhibitor-α (IκBα) that binds to the E3 ligase F-box protein β-Transducin Repeat-Containing Protein (βTRCP), to degrade Methionine Aminopeptidase-2 (MetAP-2) in cell extracts. This molecule, called PROTAC-1, proved to be heterobifunctional, for it covalently bound to the POI, MetAP2, through one end (ovalicin), while it recruited an E3 ligase from the other, resulting in the degradation of MetAP2 in the micromolar range.

Despite its two main disadvantages (poor cell permeability and dependence on cellular phosphatases for the phosphorylation needed to recruit the E3 ligase), this project gave rise to the Proteolysis Targeting Chimera (PROTAC) technology (Lai & Crews, 2017; Sakamoto et al., 2001).

2003

The next achievement in the development of the PROTAC technology occurred when the ERα was targeted again for degradation, now using this technology. The Androgen Receptor (AR) is another hormone nuclear receptor, which responds to endogenous ligands such as 5α-dihydrotestosterone (DHT) and testosterone and is associated to prostate cancer. It can also be regulated by small molecules, e.g., flutamide, bicalutamide and enzalutamide.(Bondeson & Crews, 2017; Bradbury et al., 2011). Both nuclear receptors were successfully targeted for degradation by PROTACs in 2003. The PROTACs were micro-injected into the cells, thus degrading the nuclear receptors in intact cells. For this purpose, Sakamoto and co-workers also used the same 10 amino acid phosphopeptide from IκBα to recruit βTRCP, a member of the S-phase kinase-associated protein 1 (SKP1)-cullin 1- F-box E3 ligase complex ($SCF^{\beta TRCP}$), and estradiol and DHT to target the ERα and AR, respectively (Sakamoto et al., 2003).

2004

Then, the next step in the development of the technology was taken, the first cell permeable PROTACs. Instead of using the polypeptide derived from IκBα, a fragment from the Hypoxia Inducible Factor (HIFα), a cell permeable-sequence of seven amino acids (ALAPYIP) with a preserved proline residue (P^{564}), was used which, upon hydroxylation of this proline residue, binds to the Von Hippel-Lindau tumor suppressor (pVHL) E3 ligase. To further improve the cell permeability, a poly-D-arginine sequence was incorporated. This set up was used with AP21988 to target and successfully degrade FK506 Binding Protein ($FKBP12^{F36V}$); and with DHT to degrade AR (An & Fu, 2018; Buckley & Crews, 2014; J. S. Schneekloth, Jr. et al., 2004).

A similar approach was used to target other proteins. The ER was targeted for degradation, using again estradiol as the ligand, and a similar octapeptide containing hydroxyproline ($MLAP^{OH}YIPM$) was used; while MetAP-2 was again subjected to degradation using the same octapeptide to recruit pVHL and fumagilol to bind MetAP-2 (Bargagna-Mohan, et al., 2005; D. Zhang, et al., 2004).

2007

The next PROTAC developed in this format consisted in a shorter peptide that also had a benzyl ester at the C-terminus of the hydroxyproline containing peptide ($LAP^{OH}YIOBn$) to recruit pVHL, and the flavonoid apigenin to target the Aryl Hydrocarbon Receptor (AHR), which was successfully degraded with this approach with micromolar concentrations of the PROTAC (H. Lee, et al., 2007).

2008

The last of these peptidic PROTACs were developed against, once more, ERα and AR. The ligands to the POI were again 17β-estradiol and DHT, while the pVHL-recruiting motif was the peptide $LAP^{OH}YIGGa\text{-}D\text{-}Arg_9$. Both had activities in the lower micromolar

range in ERα- and AR-dependent breast and prostate cancer, respectively (Rodriguez-Gonzalez et al., 2008).

The next improvement in the field was the development of a full small-molecule PROTAC. It consisted in nutlin, a ligand to recruit the E3 ligase Mouse Double Minute 2 Homolog (MDM2), and a Specific Androgen Receptor Modulator (SARD) to target the AR, given that it was a nuclear protein that had repeatedly successfully been targeted and degraded. This time, the linker was a small soluble PEG chain. As a result, AR was degraded in cells at a concentration of 10 μM in a time as short as 7 hours (A. R. Schneekloth, et al., 2008).

2010

It had been observed that bestatin methyl esters bound to and promoted autoubiquitination of the E3 ligase cellular Inhibitor of Apoptosis Protein 1 (cIAP1). Thus, Hashimoto and co- workers produced a PROTAC using these small molecules to recruit cIAP1 to degrade Cellular Retinol- and Retinoic Acid-Binding Proteins I and II (CRABP-I and -II) (Itoh, et al., 2010).
After this PROTAC, several more cIAP1-based arose and are commonly known as Specific and Nonspecific IAP-dependent Protein Erasers (SNIPERs).

2011

The next 3 PROTACs (SNIPERs) were all developed against, again ERα and AR, and against Retinoic Acid Receptors using as ligands to the POIs estrone, DHT, and Ch55, respectively. In all cases methyl bestatin were utilized to recruit cIAP1 (Itoh, et al., 2011).

2012

Another ERα-degrading SNIPER was produced, utilizing a bestatin ester to recruit cIAP1 and 4-hydroxy-N-desmethyltamoxifen to target the nuclear receptor (Demizu et al., 2012). Nonetheless SNIPERs had two big disadvantages: first, bestatin esters have poor specificity and they also interact with and arginyl aminopeptidase and leukotriene A4 hydrolase and second, bestatins may destabilize and cause autoubiquitination of cIAP1, thus diminishing the PROTACs' potency (Buckley & Crews, 2014; Lai & Crews, 2017).

2014

The next SNIPER to be developed to target the Spindle Regulatory Protein Transforming Acidic Coiled-coil-3 (TACC3), utilizing KHS101 as its ligand. This SNIPER proved novelty not only in targeting a new protein for proteasomal degradation, but also in a new E3 ligase recruited. Initially, it was expected that cIAP1 would mediate degradation, yet it was found out that it was the Anaphase-promoting Complex/Cyclosome in complex with CDH1 (APC^{CDH1}) the E3 ligase involved in the ubiquitination process (Ohoka et al., 2014).
In this same year, another innovative approach came into the field. Wang's team produced three protein degraders, that have the same structure of PROTACs: a warhead to target the POI and a ligand that triggers degradation, in this case Chaperone-Mediated Autophagy (CMA), a specific form of autophagy, where proteins with a pentapeptide motif related to lysine-phenylalanine-glutamate-arginine-glutamine

(KFERQ) are subjected to lysosomal degradation. The first two degraders of this publication consist of a peptide derived from the C terminus of the N-methyl-D-aspartate (NMDA) receptor GluN2B subunit ($GluN2Bct_{1292-1304}$). This motif contains both a sequence that can recruit the CMA and a sequence that binds to Death-Associated Protein Kinase 1 (DAPK1) and Postsynaptic density proteins 95 (PSD-95) as POIs. The third degrader of this work consists of a similar peptide (βsynCTM) that successfully mediated the degradation of α-synuclein. All the degraders also contain the cell-penetrating sequence TAT (Fan, et al., 2014). The last PROTAC developed in 2014 targeted the viral X-Protein, which not only was able to degrade to protein, but also to inhibit it. X-Protein is known to dimerize. Thus, to target it, the PROTAC consisted in the fusion of the N-terminus oligomerization domain, and the C-terminus instability domain, as well as the cell-permeable poly-D-arginine peptide. A similar PROTAC was produced in the same publication, where the instability domain was exchanged for the hydroxyproline-containing peptide from HIF-1α to recruit pVHL as previously described for earlier PROTACs, leading to comparable results (Montrose & Krissansen, 2014).

2015

The field had the next big step the year after. It had been discovered a few years before, that Immunomodulatory imide Drugs (IMiDs), such as thalidomide, lenalidomide, and pomalidomide were able to recruit the E3 ligase cereblon (CRBN), and thus, were used in a series of PROTACs in 2015 and on. In this year, several PROTACs were developed practically simultaneously, taking advantage of this discovery. Bradner's group named their PROTAC dBET1, which consisted of an inhibitor (JQ1) of the Bromodomain and Extra-terminal (BRD/BET) protein family (BRD2, BRD3, BRD4 and BRDT (He, et al., 2020) and thalidomide as a CRBN recruiter, linked by 7-atom long moiety. This PROTAC was also the first reported to operate at nanomolar concentrations with over 95% depletion of protein abundance. In the same paper, a very similar set up was used to target FKBP12, also using thalidomide as a CRBN recruiter, and two linkers of different length to produce dFKBP-1 and -2, both of which depleted the POI at low nanomolar concentrations (Winter et al., 2015).

The Crews' lab also developed ARV-825, a PROTAC that uses OTX015 as a BRD4 binding unit and, pomalidomide as a CRBN recruiter, united by a flexible polyethylene glycol linker. This PROTAC showed even higher potency, requiring concentrations below 1 nM to be effective. Nonetheless, the degrader was not selective enough to spare BRD2 and BRD3 (J. Lu et al., 2015).

The Ciulli's group designed a series of PROTACs using the drug-like ligands VHL-1 and VHL-2 to recruit the VHL E3 ligase, the inhibitor JQ1 to target BRD proteins, and linkers with either three or four ethylene glycol units. As a result, the PROTAC MZ1 was produced which was surprisingly selective to BRD4 in lower concentrations, while all 3 BRD2, BRD3, and BRD4 were degraded as concentration of MZ1 increased. This increased selectivity implied an advantage over the other BRD-protein degraders described before. On the other side, the potency was more discrete, in comparison (Zengerle, et al., 2015).

In the same year, the first subdivision of the PROTAC technology was developed. A hydroxyproline derivative was used as a small molecule to recruit VHL attached to a chloroalkane linker, which can bind covalently to HaloTag7 (HT7), a modified bacterial dehalogenase. This system, named HaloPROTAC, can target ectopically expressed

proteins engineered to contain HT7. The principle was proved by targeting and degrading GFP-HT7 using low nanomolar concentration of the HaloPROTAC (Buckley et al., 2015).
This same year, the Crews group developed two more PROTACs based on a hydroxyproline-based small molecule to recruit VHL. Each one of them used linkers of different lengths, the shorter one bound to 2 to target ERRα, while the longer one had vandenatib as warhead against the serine-threonine kinase RIPK2. Both PROTACs displayed high selectivity and potencies in the lower and middle nano molar range, respectively (Bondeson et al., 2015).

2016

At the beginning of this year the Crews' group published a very interesting piece of scientific work, where they targeted the fusion oncoprotein BCR-ABL for the first time. To do so, they produced PROTACs with different Tyrosine Kinase Inhibitors (TKI), namely imatinib, dasatinib and bosutinib, using in all cases a hydroxyproline derivative to recruit VHL E3 ligase, and as linkers they used mixed moieties of hydrophobic alkane chains followed by hydrophilic polyethylene glycol chains of varying lengths. The PROTACs containing imatinib and bosutinib were all ineffective, while the PROTAC DAS-6-2-2-6-VHL was effective at a concentration of 1 μM with over 65% of c-ABL degradation, but no degradation of the fusion protein whatsoever. In response, they produced the same PROTACs exchanging the E3 ligase recruiters for thalidomide, lenalidomide and pomalidomide to recruit CRBN E3 ligase instead. Results were observed with pomalidomide, and the dasatinib-containing DAS-6-2-2-6-CRBN and the bosutinib-containing BOS-6-2-2-6-CRBN PROTACs, with DC_{50} values of 1 μM and 2.5 μM, respectively and efficacies of over 85% and 90%, respectively against c-ABL, and the same DC_{50} values against BCR-ABL, with efficacies of over 60% and 90%, respectively (Lai et al., 2016).

Chu and co-workers developed the first PROTAC against the Tau protein, responsible for the development of Alzheimer disease. This PROTAC was fully peptide-based, using a peptide called TH006 (YQQYQDATADEQG) as a Tau protein ligand, the peptide ALAPYIP previously described before, that can recognize and recruit VHL for polyubiquitination, and the tetrapeptide GSGS as a linker to increase the flexibility, which also had attached a Boc_3Arg moiety to increase the cell permeability. Despite the peptidic nature of the PROTAC, the DC_{50} was as low as 0.4 μM (Chu et al., 2016).
In the same year another PROTAC was developed to degrade another protein for the first time in this context, SMAD3. The PROTAC consisted of the small molecule EN300-72284 as a warhead, the pentapeptide LAPYI as pVHL E3 ligase recruiter, using as linker 1,6-diamidehexane. The PROTAC displayed a DC_{50} value of 4.5 nM (Wang et al., 2016).

The next PROTAC also represents a completely new different approach to the technology. To target the POI, Akt, a Protein-Catalyzed Capture agent (PCC) was used, which is a class of ligands that are built in situ by click chemistry. They have similar properties to antibodies, but they are considerably smaller, therefore, cell permeable. This anti-Akt PCC was linked to the hexapeptide ALAPYIP to recruit VHL E3 ligase to produce the PROTAC CPP-tri_a-PR which degraded the POI with a DC_{50} of 128 ± 9 μM (Henning et al., 2016).

That same year the Crews group produced yet another PROTAC, this time against BRD2/3/4 proteins. This PROTAC, ARV-771 targeted BRD proteins using the BET inhibitor JQ1, a peptide derived from HIF-1α containing an (R)-hydroxyproline residue to recruit VHL E3 ligase, and an 8-atom long linker. The POI degradation was achieved with DC_{50} values bellow 5 nM and an efficacy of over 90% (Raina et al., 2016).

The last PROTAC in this year also represents a significant contribution to the research in the field. This PROTAC also targets BRD4 using the BET inhibitor JQ1, and thalidomide as a recruiter of CRBN E3 ligase. The difference is that it is built inside treated cells. This In-cell Click-formed PROteolysis Targeting Chimera (CLIPTAC) relies on the "reverse electron demand Diels-Alder cycloaddition between tetrazine and trans-cyclo octene (TCO)" (Lebraud, Wright, Johnson, & Heightman, 2016). Thus, thalidomide was chemically modified to be tetrazine-tagged (Tz-thalidomide), and JQ1 to be TCO-tagged (JQ1-TCO), being bonded by a 25-bond long linker. Cells were treated for 18 hours with the separate components, at a concentration of 10 μM each. POI degradation was observable as soon as 16 hours after the addition of the second component, and complete depletion was observed after 24 hours. The system was modified to target the Extracellular Signal-Regulated kinases 1 and 2 (ERK1/2) using the namely Probe 1 to target the oncoprotein. JQ1-CLIPTAC 3 and ERK-CLIPTAC 6 were also produced extracellularly, and then used to treat cells. No degradation was observed, suggesting that the molecules are too large to permeate into cells, being only functional if assembled within the cells (Lebraud et al., 2016).

2017

This year began with the development of new SNIPERs, namely SNIPER(ER)-87, SNIPER(ABL)-38, SNIPER(BRD4)-1 and SNIPER(PDE4)-9. The first one targets ERRα, the second one the oncoprotein complex BCR-ABL, the third one targets the oncoprotein BRD4, and the last one targets phosphodiesterase-4 (PDE4). To recruit the mentioned POIs, the following ligands were used: 4-hydroxytamoxifen, dasatinib, JQ1, and PDE4 inhibitor respectively. In all cases the LCL161 derivative was used to recruit XIAP E3 ligase, with more affinity to any other member of the IAP family. The DC_{50} values and efficacies of these SNIPERs are 1-3 nM and over 70% of ERRα degradation; 3-10 nM with more than 90% of BCR-ABL protein degradation; 3-10 nM with more than 70% of BRD4 depletion; and around 1 nM and an approximate 60% of PDE4 degradation (An & Fu, 2018; Ohoka et al., 2017).

The next PROTAC to be developed is another BRD4 targeting molecule. Based on the previously published MZ1 PROTAC in 2015, Ciulli's group produced the PROTAC AT1 with an impressive level of detail, given that the crystal structure of the ternary complex POI-PROTAC-E3 ligase had been resolved, and the design of AT1 could be fine-tuned at intermolecular docking. AT1 also consisted of JQ1 to recruit BRD proteins, while VH032 was used as a very potent ligand of the VHL E3 ligase, united by a PEG linker. The DC_{50} value was in the lower nanomolar range with over 90% of protein degradation (An & Fu, 2018; Gadd et al., 2017)

dBRD9 was the next PROTAC to be produced, which targets the Bromodomain-containing protein 9 (BRD9). This PROTAC had the small molecule BI-7273 as a warhead against BRD9, pomalidomide was used as a CRBN E3 ligase recruiter, and the two ligands

were linked by a PEG chain. Remarkable BRD9 depletion was reported at concentrations lower than 50 nM (An & Fu, 2018; Remillard et al., 2017).

TANK-Binding Kinase 1 (TBK1) was the next protein to be targeted with a PROTAC named 3i, developed by the Crew's lab. This PROTAC used the VHL ligand 2 to recruit the E3 ligase, and a TBK1 inhibitor as warhead, while the linker combined hydrophobic and hydrophilic moieties within the 14-atom long linker. 3i proved to be very potent with a DC_{50} value of 12 nM and a D_{max} of 96% (Crew et al., 2018).

Next, Cyclin-Dependent Kinase 9 was successfully and selectively degraded, being able to rule out the analogs CDK2 and CDK5. Robb and colleagues proved that CDK proteins are structurally very similar, making it hard to find selective inhibitors. They produced a series of amino pyrazole derivatives to find a suitable candidate. They also found that the lysine residues necessary for polyubiquitination tagging and subsequent degradation are, nonetheless, oriented differently among the proteins, making it an opportunity to improve selectivity. Thalidomide was used to recruit CRBN E3 ligase linked to the warhead by a 5-carbon long hydrophobic chain, resulting in a PROTAC active at concentrations 10 and 20 μM leading to about 56% and 65% protein degradation rates, respectively (Robb et al., 2017).

Dihydroorotate Dehydrogenase (DHODH) was the next POI in the list. To tag it for proteasomal degradation, a PROTAC was developed, which consisted of Brequinar as an inhibitor and warhead, a short polyethylene glycol chain as linker connecting to a hydroxyproline derivative to bind to VHL E3 ligase. The resulting degrader had reported IC_{50} value of 5.2 μM in HCT-116 cells, and 3.7 μM in MiaPaca-2 cells. The authors conclude the publication with a need to further optimize the linker and warhead (Madak, et al., 2017).

This year concludes with a PROTAC that starts a new sub-technology in the field, HomoPROTACs. These are heterobifunctional molecules designed to dimerize with E3 ligases, causing ultimately self-polyubiquitination and degradation by the 26S proteasome. CM11 was the resulting PROTAC to produce chemically induced dimerization, which contains two hydroxyproline ligands, namely VH032 and VH298, making it a double ligand to VHL E3 ligase. PEG chains of 3, 4 and 5 units were tested, being the longest one the most effective. CM11 showed preferential degradation of pVHL30, over other isoforms such as pVHL19, with complete depletion of pVHL30 at a concentration of 1 μM and 10 hours of treatment (Maniaci et al., 2017).

2018

During and after this year, the development of new PROTACs grew remarkably. This year alone 26 new PROTACs were produced, some of them targeting proteins that had already been degraded by other PROTACs, and most of them using the same E3 ligases. Even though all of them made contributions to the field, out of practicality, only those which represent the most novel inputs will be described.

The Kelch-like ECH-associated Protein-1 (Keap1) E3 ligase was used for the first time to produce a PROTAC to degrade the non-enzymatic protein Tau. Keap1 cooperates with

Cul3-Rbx1 complex to produce the polyubiquitinating activity. This PROTAC consisted of the polypeptide Ac-LDPETGEYL-OH as a strong binder to Keap1, while the peptide YQQYQDATADEQG was used a ligand to the Tau protein, a small tetrapeptide GSGS was used as a linker. Finally, the Arg_8 motif was fused to enhance cell permeability. The peptide was effective from concentrations as low as 1 µM with a maximal activity at 50 µM, achieving up to 83.92% of protein degradation (M. Lu et al., 2018).

The next degraders were developed by the Crew's group, where they report the first transmembrane-protein targeting PROTACs, against Receptor Tyrosine Kinases (RTK) Epidermal Growth Factor Receptor (EGFR), Human Epidermal Growth Factor 2 (HER2) and c-Met. First, they produced Compound 1 by tethering lapatinib to a hydroxyproline derivative to recruit VHL E3 ligase, through a diethylene glycol linker, which was capable of degrading both EGFR WT and the 20 exon insertion mutant with DC_{50} values of 392 nM and 763.1 nM, respectively and with corresponding D_{max} values of 97.6% and 68.8%. Nevertheless, it was also observed that Compound 1 was able to degrade HER2 at concentrations lower than 100 nM to almost complete depletion. To increase the selectivity, an additional ethylene glycol unit was added to the linker, making the now namely Compound 5, an EGFR degrader only (Burslem et al., 2018).
Compound 3 had gefitinib as warhead instead, making it capable of degrading both EGFR with a 19 exon insertion mutation and the L858R point mutation, leaving the WT protein untouched. The degradation mediated by Compound 3 had a DC_{50} 11.7 nM and 22.3 nM for the corresponding mutations, and D_{max} values of 98.9% and 96.8%, respectively. The warhead was changed once more, this time to afatinib, thus producing Compound 4 which degraded EGFR with the double mutation L858R/T790, with a CD_{50} value of 215.8 nM and 79.1% of efficacy (Burslem et al., 2018).
Last, Compound 7 was produced by using as POI ligand foretinib, which degraded c-Met pronouncedly at concentrations lower than 500 nM. More interestingly, the protein depletion was sustained up to 48 hours upon withdrawal of the PROTAC and a washing step (Burslem et al., 2018).

TRIM24 was targeted for the first time by PROTAC-mediated degradation using the PROTAC dTRIM24, where the targeting molecule was the dimethylbenzimidazolone inhibitor IACS-9571 and VL-269 the VHL ligand, tethered together by a diethylene glycol chain. The DC_{50} ranged from 2.5 to 5 nM exhibiting an efficacy of about 70% (Gechijian et al., 2018).

BRD2/3/4 proteins were targeted once more, the difference is that the PROTACs developed for this purpose are the first reported to degrade proteins at the middle-high picomolar range. Zhou and colleagues produced a series of compounds combining either thalidomide or lenalidomide, hydrophobic linkers of various lengths tethering to HJB97 as a high affinity BET ligand. The compounds with lenalidomide were the most successful, being the best overall PROTACs Compounds 21 and 23 with IC_{50} values of 0.037 nM and 0.05 nM, respectively for BRD4, with near complete depletion (B. Zhou et al., 2018).

Next, a very novel PROTAC is described, not only because is the first one that targets an epigenetic eraser, but also because it is the first one to be obtained by the

organometallic cycloaddition of a modified form of thalidomide to a ligand of the POI, Sirt2. Sirtuin Rearranging Ligands (SirReals) are Sirtuin inhibitors that produce a rearrangement in the active site upon binding. Among them, triazole-based SirReals also show better water solubility. Thus, PROTAC 12 was produced by Cu(I)-catalyzed cycloaddition of an azido-thalidomide derivative to a SirReal. This CRBN-recruiting PROTAC was effective with over 90% of protein depletion at concentrations ranging from 0.2 to 1 μM (Schiedel et al., 2018).

Another PROTAC to degrade an epigenetic eraser was developed this year. Yang and co-workers developed a series of compounds that interacted unselectively to several members of the zinc-dependent Histone Deacetylases (HDACs) family, namely HDAC1, HDASC2, HDAC4, and HDAC6. By tethering one of these inhibitors to thalidomide through a triethylene glycol linker, this group achieved the selective degradation of HDAC6 over the other isoforms, with a DC_{50} 34 nM with an efficacy of 70.5% of protein depletion (K. Yang et al., 2018).

Anaplastic Lymphoma Kinase (ALK) was the next POI to be explored and successfully degraded by the PROTACS MS4077 and MS4078, both with pomalidomide as CRBN recruiter, and ceritinib as the warhead. A series of linkers with different lengths and compositions were tested, being the most effective a long PEG linker and a short hydrocarbon chain. The authors suggested that the longer linker folded into a shorter conformation, making it comparable to the shorter one. Nevertheless were the PROTACS effective against ALK fusion proteins, MS4077 with DC_{50} values of 3 ± 1 nM for NMP-ALK and 34 ± 9 nM for EML-ALK with efficacies of over 90% in both cases, and MS4078 with DC_{50} values of 11 ± 2 nM for NMP-ALK and 59 ± 16 nm for EML-ALK, also with an efficacy of over 90% in both cases (An & Fu, 2018; C. Zhang et al., 2018).

2019

The Mouse Double Minute 2 homolog (MDM2) is an E3 ligase involved in the protein stability of p53, a well-known protein in different tumors. The Crews group targeted MDM2 for 26S proteasome-mediated degradation by developing two PROTACs, using the well-known CRBN E3 ligase recruiters thalidomide and lenalidomide either of the attached to a short hydrophobic hydrocarbon chain and the self-designed MDM2 inhibitor MI-1061. The resulting PROTACs, MD-222 and MD-224 were both very successful at depleting MDM2, being MD-224 the most of potent of them, with an DC_{50} of less that 1 nM within 2 hours of treatment and with a D_{max} of near to complete depletion (Y. Li, Yang, et al., 2019).

Ironically, almost in parallel, also the Crews group developed a PROTAC that recruited MDM2 as a degrader of BRD4. The PROTAC consisted of BET inhibitor JQ1 in one end of a 13-aton long PEG linker, and MDM2 inhibitor idasanutlin at the other end. The resulting molecule, named A 1874 was successful in degrading BRD4 with a maximum activity at 100 nM and with an efficacy of over 98% of protein degradation. On addition to this, the PROTAC was also able to stabilize p53, acting in a synergistic manner with two different mechanisms and two different pathways, leading to tumor suppression (Hines, et al., 2019)

Wang and co-workers produced two PROTACs simultaneously in one publication with a very interesting feature. Both degraders contain pomalidomide as the CRBN E3 ligase recruiter, and the Mcl-1/BCL2 dual inhibitors S1-6 and Nap-1. One of them, the PROTAC C3 contained a 6-atom long hydrocarbon link, resulting in a DC_{50} value of 0.7 μM for Mcl-1 degradation; while the other, the PROTAC C5 had a diethylene glycol chain as linker, leading to a DC_{50} value of 3 μM for BCL2 degradation, with efficacies of 70 and 90%, respectively (Z. Wang et al., 2019).

Interleukin-1 Receptor-Associated Kinase 4 (IRAK4) was targeted for the first time for proteasomal degradation using a PROTAC developed by Nunes and colleagues, which consisted in a hydroxyproline derivative as a ligand to VHL E3 ligase, a 12-atom long hydrophobic linker, and as warhead an IRAK4 ligand named PF-0665833. This PROTAC, named Compound 9, was able to degrade IRAK4 in peripheral blood mononuclear cells and dermal fibroblasts with potencies of DC_{50} values of 151 nM and 36 nM, respectively. Nevertheless, the publication concludes with remarks of the need of further studies to understand the biology of the PROTAC more thoroughly (Nunes et al., 2019).

Burslem and colleagues developed the PROTAC GMB-475, consisting of the BCR-ABL inhibitor GNF5, an hydroxyproline derivative as recruiter of the VHL E3 ligase, and an ethylene glycol derivative as linker. This PROTAC exhibited a DC_{50} value of 340 nM and a D_{max} of over 95% (Burslem et al., 2019).

The PROTAC SD-16 was produced in Wang's group to target the Signal Transducer and Activator of Transcription 3 (STAT3) for proteasomal degradation. Lenalidomide was used for the purpose of recruiting CRBN E3 ligase in one of the ends of a 10-carbon long hydrophobic linker containing an ethynyl moiety, and SI-109, a STAT3 SH2 domain inhibitor, at the other end of the linker. Protein degradation was achieved with a potency of 0.06 μM and an efficacy of over 95% after 1 hour of treatment only, and up to 90% still after 72% of having initiated the treatment. This PROTAC was also able to degrade the phosphorylated form of the protein $pSTAT3^{Y705}$ with similar results (H. Zhou et al., 2019).

The Ciulli's group did a very extensive piece of scientific work to produce a highly optimized BRD9 PROTAC. First, they explored with three possible E3 ligases to be recruited: CRBN, VHL, and DCAF15. The linker was also intensively researched on, while the BRD9 inhibitor was the small molecule named BrdL1. As a result, 64 compounds were produced and tested. Although several of them had remarkable activities, VZ185 stood out, having a hydroxyproline derivative to recruit VHL, a 5-atom hydrocarbon linker. This PROTAC was not only able to degrade BRD9, but also BRD7, which had so far escaped targeted degradation. VZ185 displayed a DC_{50} value of 1.8 nM for BRD9, and 4.5 nM for BRD7 with efficacies of over 95% in both cases (Zoppi et al., 2019).

A very similar approach was followed by Su and co-workers when the produced a series of degraders with the purpose of targeting CDK6. CRBN, VHL, and cIAP, out of which only CRBN proved to be effective for CDK6 degradation, being recruited by pomalidomide. Different options for the warhead were also tested, being Palbociclib the most effective. Different linkers in composition and length were also tested, where

shorter, yet flexible linkers were proved to be more effective in degrading CDK6. CP-10 was the resulting PROTAC, able to degrade CDK6 sparing other members of the protein family, with a DC_{50} of 2.1 nM with a D_{max} of 89% at a concentration of 100 nM (Su et al., 2019).

The oncoprotein $BRAF^{V600E}$ was chosen as a POI by Posternak and colleagues. They developed in total 16 different degraders following a similar strategy of various E3 ligase recruiters and linkers of different compositions, lengths, and flexibilities. The most successful was P4B, consisting of pomalidomide as the CRBN E3 ligase recruiter, a linker made of 4 PEG units, and BI 882370 as the warhead. P4B degraded the POI with good selectivity over other associated proteins, with a potency of 15 nM and a D_{max} of 82%. Remarkably, the PROTAC was able to degrade other small-molecule resistant mutants of BRAF (Posternak et al., 2020).

Zhang and co-workers produced a PROTAC able to target for 26s proteasomal degradation B-Cell Lymphoma Protein Extra Large ($BCL\text{-}X_L$), a protein that has escaped effective clinical inhibition because of pronounced thrombocytopenia as side effect. This group built up from ABT263, a BCL2/$BCL\text{-}X_L$ inhibitor, connecting it to a hydroxyproline derivative to recruit VHL E3 ligase, united by a short pentane linker, resulting in the PROTAC DT2216, which was able to degrade the POI with a potency of 63 nM and an efficacy of 90.8% (Khan et al., 2019).

2020

This year was remarkably productive in the PROTAC field, at least 50 new of them were developed this year alone. Due to this, only some of those with very novel targets or technologies will be mentioned in this work.

Two PROTACs were designed to degrade the subunits EDD, EZH2, and SUZ12 of the PCR2 complex, based on the warhead US20160176882A1, an EDD inhibitor, and an hydroxyproline derivative as VHL E3 ligase recruiter, and two linkers of different lengths and compositions. The result was PROTAC 1 and PROTAC 2, both effective in degrading all the proteins simultaneously, starting from a concentration of 0.1 μM, and with treatments of 1 hour. Protein degradations were observable starting at one hour and with a maximum at 24 hours. Almost complete depletion of EDD is observed at 24 hours, and more discrete protein degradation was observed for the other two units, with PROTAC 2. With PROTAC 1, the degradation pattern is very similar, but with more moderate protein degradation efficacies (Hsu et al., 2020).

The signal transducing protein TGF-β1 was targeted for proteasomal degradation intracellularly with the PROTAC DT-6 which was able to bind and recruit CRBN E3 ligase through thalidomide in one end of its pentane linker, and at the other end the TGF-β1 inhibitor P144, a peptide from the type III TGF-β receptor, with the sequence (TSLDASIIWAMMQN) as a warhead. TGF-β1 degradation was observed starting at 0.1 μM, with a maximum degradation rate at 5 μM after 18 hours of treatment in cell lines like U87, MCF-7m and A549, but in other cell lines, such as HepG2, THP-1, and BV2, degradation was observed starting from concentrations ten times higher (Feng et al., 2020).

A G protein-coupled receptor was targeted por 26S proteasomal degradation for the first time with the development of Compound 9c, a CRBN E3 ligase-recruiting PROTAC consisting of pomalidomide and the α_1-adrenergic receptor inhibitor prazosin, tethered together by a diethylene glycol linker. Compound 9c exhibited a DC_{50} of 2.8 µM and a D_{max} of 90% upon treatment with 10 µM of Compound 9c for 12 hours (Z. Li et al., 2020).

A new sub-technology of PROTACs emerged early this year. Trauner's research group developed a series of small molecules that combined the PROTAC technology with photopharmacology to produce the PHOtochemically Targeting Chimeras (PHOTACs). These degraders had incorporated in their structures azobenzene moieties, that have a cis conformation in the dark, and isomerize to a trans conformation upon exposure to blue and violet light wavelengths (380-400 nm). At higher wavelengths the change of conformation reverses up 70%, and completely upon withdrawal of light. This conformational change is key for the proper positioning of the ligands within the PHOTACs to interact with their targets. The first PHOTAC of this series was PHOTAC-I-3, having lenalidomide as CRBN E3 recruiter, JQ1 BET inhibitor as BRD2/3/4 ligand linked at either side of a 5-atom log hydrocarbon chain. In cell viability assays, the PHOTAC had potencies of EC_{50} values of 88.5 nM when exposed to flashes of 100 ms every 10 s at 390 nm, and 631 nM in the dark. At the protein degradation level, the group reported for this PHOTAC remarkable BRD4 degradation after for 4 hours of treatment with the previously described light exposures. BRD3 also was remarkably degraded in a range of concentration from 100 nm to 3 µM and when exposed to violet light, while BRD2 degradation was slower. The second series of PHOTACs developed were aimed to target FKBP12, by incorporating a CRBN-targeting glutarimide and SFL, a synthetic ligand of FKBP. The most outstanding of these compounds were PHOTAC-II-5 and PHOTAC-II-6, both effective in degrading the POI, although at a lower rate, compared to the PHOTACs of the first series, observing the absences of the POI between 6 and 12 hours. Interestingly PHOTAC-II-6 exhibited minor activity in the dark after 24 hours of treatment (Reynders et al., 2020).

Almost simultaneously Jiang's group developed protein degraders with an almost identical strategy. Small molecule-based degraders that have azobenzene moieties that can switch from cis to trans conformation upon exposure of light at a certain wavelength, which would orientate lenalidomide and a warhead appropriately for interaction with CRBN E3 ligase and a POI. This group named, nonetheless, their technology azoPROTACs. In this case the warhead was dasatinib to target ABL and BCR-ABL proteins. After optimization of the linker, a 4-atom long hydrocarbon chain, azoPROTAC-4C resulted in a trifunctional molecule with a trans configuration maximum at λ_{max} of 361 nm. After 1 hour of exposure to this wavelength, complete cis to trans conformation was observed, while the conversion needed for 4 hours to be completed upon white light exposure. Additionally, it was reported that azoPROTAC-4C was stable for 5 switch cycles. The IC_{50} in a cell viability assay was 68 nM and the EC_{50} had a value of 28 nM. At the protein level, the best degradation rates in Western Blot were observed with exposures to white light. Observable BCR-ABL protein degradation started at 25 nM, which became remarkable in ABL and BCR-ABL at a concentration of 100 nM. No degradation was observed with the cis conformation of azoPROTAC-4C.

Significant protein degradation was observed after 10 hours of treatment, and up 90% of protein degradation was obtained after 32 hours of treatment (Jin et al., 2020).

Cheng and colleagues worked in developing a series of PROTACs purposed to target the programmed cell death-ligand 1 protein (PD-L1). To design the PROTAC several lengths and compositions of the linker were tested, as well as different warheads, being two of the most effective PROTACs P22 and P33, which have as warhead the small molecule BMS-8, while pomalidomide was the CRBN E3 ligase recruiting element of these degraders linked together by a rigid piperazine linker. These PROTACS had DC_{50} values of 39.2 nM and 25.2 nM, respectively. Interestingly, it was observed that P22 could also moderately decrease the POI levels through the lysosome pathway (B. Cheng, et al., 2020).

Next, the protein isoforms p38α and p38β were targeted for proteasomal degradation by a PROTAC, NR-1c based on thalidomide as CRBN E3 ligase ligand, the ATP competitive inhibitor PH-797804 as warhead. Linker optimization was the core point of this work, resulting in 24 different combinations. The outcome was that the ideal linker for the two ligands chosen had 16-17 atoms of length, resulting in two most effective PROTACs, NR-7h and NR-6 with efficacies of around 90% in different cell lines in both cases. NR-7h was determined to have DC_{50} values of 2.9 nM in T47D cells and 18.4 nM in MB-MDA-231 cells, while the values of NR-6a were 24 nM for T47D cells 27.2 nM in MB-MDA-231 cells (Donoghue et al., 2020).

A series of 6 PROTACs were developed to target the Vascular Endothelial Growth Factor Receptor-2 (VEGFR-2), based on the VHL E3 ligase ligand VH032, 3 linkers of different lengths, and the angiogenesis inhibitors Tie-2 and EphB4. PROTACs 2 and 5 proved to be the most effective, with potency DC_{50} values of 32.8 ± 5 μM and 38.7 ± 4 μM, respectively (Shan et al., 2020).

Next, another Histone Deacetylase was targeted for PROTAC-mediated proteasomal degradation. PROTACs against HDAC3 were based on degradation mediated by CRBN E3 ligase recruited by pomalidomide and o-aminoanilide-based class I HDAC inhibitors. HD-TAC7, the most successful of them, with a short 6-atom hydrocarbon chain, had a potency of DC_{50} 0.32 μM, with a maximum effect at 6 hours, lasting for at least 2 days (F. Cao et al., 2020).

The following piece of science is another entry in the list of technologies derived from the main concept of PROTAC, antibody coupled PROTACs. Interestingly, there were a few examples of this technology during this year, and this publication represents an example of them only. Maneiro and colleagues develop a PROTAC conjugated to trastuzumab in a ratio 4:1. The PROTAC consisted of the BET inhibitor JQ1, and a hydroxyproline derivative to recruit VHL E3 ligase, which was attached to an azido PEG chain in one end of the linker, through the free hydroxyl group at the proline residue. Yet, this linker is not the classical linker between E3 ligase recruiter and warhead, but a tether to trastuzumab at the other side of the linker, through re-bridging the disulfide bonds within the antibody. Once that PROTAC-loaded trastuzumab interacts with HER2, the complex is endocytosed for lysosomal degradation, and the ester bond between the

linker and the hydroxyl group of the VHL ligand is hydrolyzed, and thus, the PROTAC released, making sure that the degrader remains caged in the antibody until it is released into HER2+ cells only. Not only was The PROTAC found to be effective in HER2+ cells only, but also to be BRD4 selective, degrading it to almost full depletion at 100 nM in 4 hours, and remarkable degradation was also observable at 50 nM. It was also observed, that upon 1 hour treatment with the ab-PROTAC conjugate, protein degradation is still observable 23 hours after the treatment (Maneiro et al., 2020).

Hematopoietic Progenitor Kinase1 (HPK1) was subjected to 26S proteasomal degradation upon treatment with the optimized PROTAC SS47 at a concentration of 100 nM, with observable degradation at 12 hours and maximal degradation, yet moderate, at 24 hours. SS47 consisted of the HPK1 inhibitor ZYF0033 united to the CRBN E3 ligase recruiter thalidomide, by a pentaethylene glycol chain (Si et al., 2020).

PROTAC-mediated degradation of CDK proteins had previously reported. Yet, the PROTAC to be next described was capable of degrading simultaneously CDK2/4/6 and was also administered and bioavailable orally. The Compound 3 described from this publication consisted in pomalidomide as de recruiter of CRBN E3 ligase, while Ribociclib was the warhead to target the POIs. The linker is a 9-atom long hydrocarbon chain with an amide moiety at the end with Ribociclib and a secondary amine on the side linking to pomalidomide. Compound 3 had a IC_{50} value of 0.097 μM in B16F20 cells, and 0.166 μM in A375 cells (Wei et al., 2021).

Glycogen Synthase Kinase 3 (GSK-3β) was targeted for proteasomal degradation for the first time. The PROTAC PG21 was the best out of 23 different molecules, which was able to recruit CRBN E3 ligase having in one end thalidomide and the small molecule G1 at the other end of an n-octane linker. This PROTAC could selectively degrade GSK-3β, sparing GSK-3α with an efficacy of 44.2% of protein degradation and a moderate potency of 2.8 μM (Jiang et al., 2021).

2021

It is important to mention, that, once more, not only will very novel PROTACs be considered for description in the section, but also only those reported until April of 2021, when this written doctoral thesis started.

A new strategy was developed at the beginning of this year. RNA-PROTACs that target RNA-Binding Proteins (RBP) for 26S proteasomal degradation. The targeting elements were “short oligonucleotides that are iso-sequential with the RNA consensus binding element of an RBP”. The targets of the RNA-PROTACs developed were the stem cell factor Lin28 and the splicing Factor RBFOX1. As VHL E3 ligase recruiter the LAPYI pentapeptide was used, while the oligonucleotide sequence AGGAGAU was used as a warhead. The RNA-PROTAC $ORN3P_1$ was observed to produce 50% of Lin28A degradation at a concentration of 2 μM, while Lin28B was not altered. The VHL ligand was changed to VH032 to produce $ORN3VH_{032}$ which produced similar results. To target RBFOX1 the same set up was followed (using the peptidic VHL E3 ligase ligand) and the sequence GCCAUCU as warhead. Also 50% of protein degradation was observed at a

concentration of 2 µM. The authors report that further optimization of the linker and the E3-ligand system is required to obtain quantitative results (Ghidini, et al., 2021).

The PROTAC next described combines both a novel target protein, which is incidentally an E3 ligase, and a novel small molecule warhead. The degrader XD2-149 targets the E3 ligase ZFP91 using napabucasin to target the protein, pomalidomide as a CRBN E3 ligase recruiter and an alkyl linker that contains a piperidine moiety with a total length of 11 atoms. The protein degradation was achieved with a potency of DC_{50} 60-80 nM, depending on the cell line, after 16 hours of treatment, achieving maximal degradation at a concentration of 1 µM for 24 hours. No D_{max} is reported (Hanafi, et al., 2021).

Pomalidomide was next used to recruit CRBN E3 ligase to degrade Hematopoietic Prostaglandin D Synthase (H-PGDS), targeted by the small molecule TFC-OO7. These small molecules were attached to either side of a tetraethylene glycol chain. The resulting degrader, PROTAC(H-PGDS)-1 produced observable protein degradation at concentrations lower than 10 nM and exhibited a maximum activity in the range go 100-1000 nM. Nevertheless, almost complete depletion was observed upon treatment at concentrations lower than 10 nM over 6 to 24 hours of treatment (Yokoo et al., 2021).

Even though the Androgen Receptor (AR) had long before been targeted for proteasomal degradation, the next PROTAC was capable of degrading not only the full-length proteins, but also the splice variants AR-V7, and to a minor extent AR-567. The degrader consisted of a hydroxyproline derivative as a ligand to the VHL E3 ligase, a 9-atom long alkyl linker with primary amides at either side. The warhead consisted of a small molecule binding to the DNA-Binding domain of the AR. The PROTAC MTX-23 exhibits a DC_{50} value of 0.37 µM for AR-V7 and 2 µM for AR full-length, upon a 24-hour treatment. When administered in animal models, MTX-23 demonstrated to produce almost complete depletion of both forms of the protein in WB from tumor lysate (G. T. Lee et al., 2021).

In the past years the development of PROTACs has grown exponentially. Just due April 29th, 2021, there were around 50 resulting publications when “PROTAC” was used in PubMed’s search bar, being most of them new actual entries to the PROTAC list. To date there are over 2 000 reported PROTACs, being the examples mentioned and described in this section a very small fraction of all the work that has been done.
For a thorough reference and literature research on the topic, the following data base is recommended, where the chemical, biological and clinical information of registered PROTACs is compilated: http://cadd.zju.edu.cn/protacdb/ (Link added on October 22nd 2021).

Figure 8 summarizes this chronology in a timeline from the first PROTAC developed to April 2021.

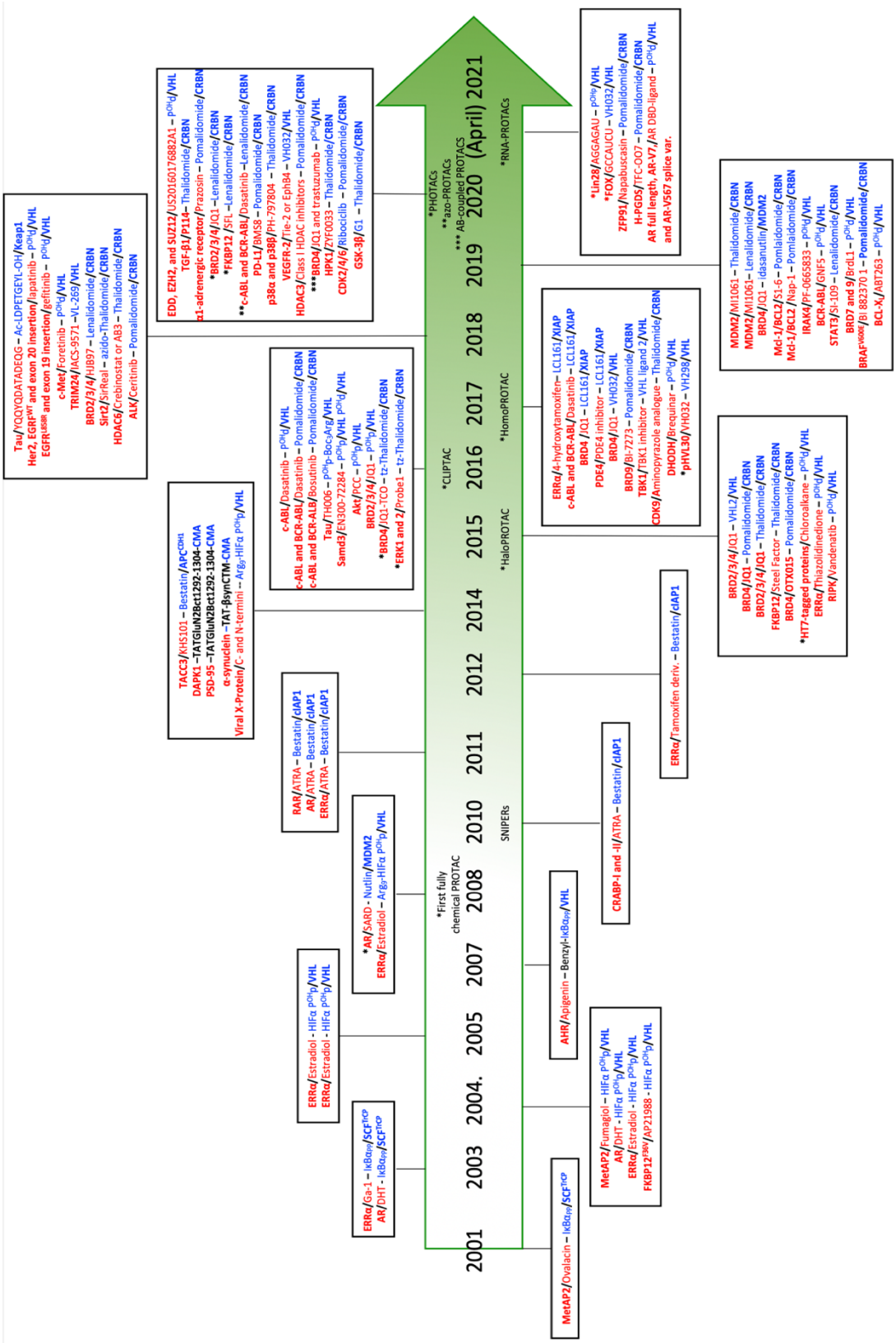

Figure 8: Timeline of PROTAC development.

Entries in **bold red** font represent the targeted proteins, entries in red font are the warheads used to target the Proteins of Interest, components in blue font are the E3 ligase Recruiters, and elements in **blue bold** font are the E3 ligases recruited with these PROTACs. In 2014, three PROTACs are listed with entries in **black bold** font, these represent moieties that worked both as warhead and E3 ligase recruiters. The list showed here is complete until 2018. After that point, the number of PROTACs developed is too large to be fully represented. Instead, the most innovative examples are mentioned here. The meaning of all abbreviations can be found in Table 1: list of abbreviations, of this work.

1.4.2. Aspects to Consider During PROTAC Design

During the past 20 years of PROTAC development, all research groups have made contributions to the understanding of PROTAC design and function. Piece by piece, the aspects that make PROTACs successful or ineffective have been understood, and probably more are yet to come. In the following paragraphs these aspects are described, for they must be kept in mind during the design, optimization, and test of new PROTACs.

- Lipinski's Rule of 5

  Traditionally, it is understood that small molecule drugs comply with Lipinski's rule of 5, to be both pharmacologically bioavailable and effective. The rule of 5 comprises the following characteristics:

  - A molecular weight of up to 500 g/mol
  - A number of hydrogen bond donors equal to or higher than 5
  - A number of hydrogen bond receptors equal to or higher than 10
  - A polar surface area (PSA) higher than 200 Å

  In medicinal chemistry, these characteristics are almost a consensus for drug design (Cecchini, et al., 2021; Churcher, 2018). PROTACs are much larger molecules, mostly falling into the range from 700 to 1 000 Da, with some having molecular weights even higher than 1 000 Da, with reported poor cell permeability profiles. Also, few PROTACs exceed 6 hydrogen bond donors. Bulky and hydrophobic moieties may block polar motifs, affecting their solubility profile (Cecchini et al., 2021).
  It is also commonly agreed on, that passive transport across the cell membrane is the main internalization mechanism for large chemicals. It has been reported that cyano-acrylamide motifs may facilitate permeation through covalent reversible chemistry. This occurs between electrophilic groups in PROTACs or other chemicals and cysteine residues on the cell surface, making it possible for thioester and thioether bonds to occur, thus fostering small molecule permeation (Cecchini et al., 2021).
  There are several ways in which the intracellular concentrations of small molecule drug-candidates can be regulated, such as the 49 identified ATP-Bindig Cassettes (ABC) and Solute Carriers (SLC) efflux transporter superfamilies. These proteins are significantly involved in the internalization of chemicals beyond the Lipinski's Rule of 5, such as PROTACs (Cecchini et al., 2021).
  In addition to that, larger molecules are more prone to undergo metabolic modification, mostly through the first-pass effect. This phenomenon is technically hard to study in cell culture, being these very isolated and artificial models, and can mostly be observed when studied in vivo (An & Fu, 2018; Lai & Crews, 2017).

- Hook Effect

  The Hook Effect consists of a phenomenon broadly observed among PROTACs in which the degraders lose their effectiveness beyond a concentration threshold. This is, PROTAC-mediated protein degradation is, in most cases, a concentration-dependent

process until a maximum point, after which the degrader loses effectiveness, making the dose-response curve bell-shaped. For a PROTAC to be effective, the ternary complex E3 ligase-PROTAC-POI must occur. At higher concentrations of PROTACs, the equilibrium among the three components is overridden and inactive PROTAC-E3 ligase and PROTAC-POI tend to occur instead. This phenomenon is hard to prevent and is often observed at concentrations between 1 and 10 μM. Most of early PROTACs, having heavily peptidic profiles, fell into this range, and several newer PROTACs have an upper limit of activity in this range (An & Fu, 2018; Churcher, 2018; Pettersson & Crews, 2019).
Another problem that can arise from the formation of the dimers mentioned before, is off-targeted protein degradation. The PROTAC-E3 ligase dimer may target proteins other than the POI through the warhead, causing side effects. The UPS constitutes a very tightly controlled homeostatic mechanism. The loss of its equilibrium may result in safety problems, reducing the clinical applicability of the developed degraders (Burslem et al., 2018).

The Hook effect may also be problematic to find adequate dosing regimens and administration forms of PROTAC, given that too high doses will lead to high intracellular concentrations, thus to a loss of activity. Subcutaneous administration can be an option to deliver the drug gradually starting from low volumes, to avoid the rapid accumulation of PROTAC in the target tissue (Neklesa et al., 2017).

- Cooperativity α value

In some cases, the Hook Effect is not observed even in concentrations within the range previously mentioned. When the interaction between the E3 ligase and the target protein are very favorable, the Hook effect may not take place. The cooperativity value α is higher than 1 when the protein-protein interactions between the target protein and the E3 ligase promote or facilitate the ternary complex formation. When the interactions are repulsive or strong steric hinderance occurs the α value is lower than 1 (Pettersson & Crews, 2019).

Cooperativity is often determining for the success of PROTACs. Some PROTACs have been reported to have a much greater degrading potency compared to the affinity of their parental warhead towards the POI. That is, the IC_{50} of a ligand to a its POI has a significantly higher value than the resulting EC_{50} of the PROTAC developed with it. The opposite phenomenon has also been observed. When the protein-protein interactions do not favor the ternary complex formation, even PROTACs containing warheads with very high affinities fail to degrade the POI. However, some successful PROTACs with very little to no cooperativity have also been developed (Liu et al., 2020; Pettersson & Crews, 2019).
This intrinsically means that the choice of the E3 ligase is also determinant for the success of a PROTAC. In several of the PROTACs mentioned before, a crucial part of the development was testing more the one ligand to different E3 ligases. As previously described, some linker-warhead configurations proved to be ineffective with a E3 ligase, e.g., VHL, but could degrade the protein of interest when CRBN was recruited

instead. Some E3 ligases may interact with the POI better than others, in a certain linker-ligand set up

- Chemistry and length of the linker

  In several of the PROTACs described before in this work, optimization of the linker was crucial. As crystal structures of the ternary complexes started being resolved, a closer look into the binding sites was accessible, opening the door for deeper optimization. As the exact amino acid residues interacting with specific moieties of the PROTACs could be observed, the distance between the interacting motifs could be improved by changing the length of the linker, bringing the parts involved into a more adequate proximity.

  The composition of the linker also plays a very important role in PROTAC activity. In some cases, interactions between the proteins involved (E3 ligase and POI) and the linker have been observed (Pettersson & Crews, 2019). Hydrophobic or hydrophilic motifs may make a difference to increase the number of interactions that favor the ternary complex formation.

  The chemistry can also directly convert a PROTAC from ineffective to a successful degrader, being PHOTACs, also published as azoPROTACs the clearest examples of it. In cis conformation, the ligands present in the PROTAC are too distant from the target protein, either the E3 ligase or the POI, while when shifting to their trans conformation, the ligands are properly aligned and positioned to interact with their intended proteins.

  Last in this regard, the combination of both composition and length may be crucial. As described in the PROTACs ARV-825 (J. Lu et al., 2015) and CP-10 (Su et al., 2019), the flexibility of the linker was key for successful degradation, allowing the PROTAC to adapt a favorable conformation to allow the necessary interactions for ternary complex formation.

- Sub-stoichiometry and Covalent PROTACs

  Sub-stoichiometric activity is very often observed in PROTACs and confers them one of their most advantageous characteristics. Given the PROTACs do not need a binding pocket or active site to degrade a POI, but else only a short superficial interaction, one PROTAC molecule can quickly induce the polyubiquitination of the POI and then leave to interact with another POI unit. This is broadly known as “event-driven pharmacology” (Cecchini et al., 2021). Thus, the amount of PROTAC to degrade the pool of intercellular POI is much smaller compared to the stoichiometry needed in occupancy-driven pharmacology. This can be seen in the often nanomolar and even picomolar potencies of some PROTACs (Cecchini et al., 2021; Neklesa et al., 2017; B. Zhou et al., 2018).
  Also, eliminating the need of an active site or binding pocket make proteins lacking them accessible for targeted proteasomal degradation, making it possible to modulate their intracellular abundances and, therefore, their activity, thus expanding the

potential clinical opportunities beyond kinases and other enzymes (Neklesa et al., 2017; Pettersson & Crews, 2019).
In addition to this, the high potencies and high efficacies of PROTACs also make it possible to reduce the dose significantly, and in the case of proteins with slow turnover cycles, to also reduce the dosing frequency, thus minimizing the side effects and improving clinical safety (Churcher, 2018; He, Koch, et al., 2020).

Despite the common agreement in the PROTAC field that the activity of these molecules is intrinsically sub-stoichiometric, successful covalent PROTACs have also been developed. Covalent, irreversible forms of BTK degraders proved to have excellent activity, while non-covalent forms of the degraders had previously poorer performance. Some studies have been conducted to compare reversible non-covalent, reversible covalent and irreversible covalent modes of action. Successful examples of all cases have been reported, thus the paradigm that PROTACs must work catalytically has been broken, and non-covalency is not a strict rule to follow during PROTAC design (Cecchini et al., 2021).

- Resistance

As in many other drug treatments, the development of resistance to PROTACs has also been reported. Initially, this was not expected from PROTACs, given the fact that a specific binding site is not required for PROTAC-mediated protein degradation. In other most of cases, point or shift mutations at the active site lead to resistance to a drug treatment. However, reports of genomic alteration in one or more of the components the UPS can affect in the efficacy of these protein degraders (Cecchini et al., 2021; He, Khan, et al., 2020). For instance, loss or loss-of-function of E2, E3 or Cullin proteins have been observed. Chromosomal deletion of CRBN, for example, has been reported (Ocana & Pandiella, 2020).

1.5. Development and Biological Testing of Two New PROTACs. Objectives of this Doctoral Work

The present doctoral work is based on the development of two novel PROTACs, one targeting Cas proteins, those that constitute the CRISPR/Cas9 system, and the related proteins dCas9, Cas12 and Cas 13 (Gama-Brambila, et al., 2021); the second PROTAC targets for protein degradation of the Splicing Factor 3b Subunit 1 (SF3B1) (Gama-Brambila, et al., 2021). The chemical syntheses and designs of these two PROTACs are not covered in this work, but the cell and molecular biology work to test them and elucidate their action mechanisms.
The paragraphs in the following sub-sections provide more specific background information on these POIs and are meant to provide understanding and justify the significance of targeting them for proteasomal degradation.
In both cases, the main goal was to verify the proof of concept, proof of protein degradation in cells and verification that the mechanism of degradation is UPS-dependent.

1.5.1. Cas Proteins: A new target of PROTACs

The CRISPR-Associated (Cas) proteins belong to a family of nucleases that constitute the adaptive immune response of prokaryotes against invasive genetic material, such as bacteriophages (Garcia-Doval & Jinek, 2017). After destruction of such invading material, the resulting fragments are incorporated and used as CRISPR RNA (crRNA), serving as a guide of Cas nucleases to target and cleave related invading phages and plasmids in the future (Esvelt et al., 2013; Garcia-Doval & Jinek, 2017). Cas nucleases are categorized into two classes and six types, according to their molecular mechanisms. Given that class 2 Cas proteins (types II, V, and VI) operate as simpler single-protein-single guide RNA (sgRNA) complexes, compared to class I proteins, these nucleases have attracted more attention among molecular biologists and biotechnologist (Doudna & Charpentier, 2014; Garcia-Doval & Jinek, 2017). The most often used type II protein is Cas9 from Streptococcus pyogenes (spCas9), although the protein derived from other species of bacteria has also been used with comparable activity (Esvelt et al., 2013). Once Cas9 associated with crRNA, it undergoes important conformational rearrangement, and then detects and binds to double-stranded DNA (dsDNA) of the invading or targeted genomic material, where its function is to cause double strand breaks (DSB) in it to ultimately produce genomic deletions. The cleaved dsDNA has two alternative repair mechanisms, either Nonhomologous End Joining Repair, or Homologous Recombination, which can then give place to gene replacement or insertions (Doudna & Charpentier, 2014). The most common example of type V proteins is Cas12 (a and b) from Prevotella buccae and Francisella novicida, which also detect dsDNA and produce DSB. Cas12 proteins operate in a very similar fashion, with minor mechanistic differences, mainly, that Cas12 is also capable of detection of single-stranded DNA (ssDNA), where it can produce trans-cleavages. Thus, Cas12 proteins offer advantages in additional applications (Y. Li, Li, Wang, & Liu, 2019). Class VI proteins (Cas13a, Cas13b, and Cas13c), are RNA-guided ribonucleases responsible of detecting and degrading single-stranded RNA (ssRNA) by utilizing two Higher Eukaryote and Prokaryote Nucleotide-Binding Domain (HEPN), with the ultimate purpose of regulating the gene expression at the post-transcriptional level. These proteins derived from Leptotrichia sp and Provetella sp, and other species may serve several other purposes in molecular biology, such as identification and tracking of plant and mammalian transcripts (Cox et al., 2017; O'Connell, 2019; Wolter & Puchta, 2018).

Despite the revolution the CRISPR/Cas systems has been representing in biology and the access they gave to genetic manipulation and engineering; disadvantages and flaws have also been observed, commonly off-target mutations (Fu et al., 2013). Aiming to modulate Cas9 proteins to improve the accuracy and reduce the off-target activities, research on engineering to modify these proteins, and research on anti-CRISPR/Cas9 proteins has been conducted (Hu et al., 2018; Kleinstiver et al., 2015; Slaymaker et al., 2016). These anti-CRISPR proteins naturally occur in bacteria as a mechanism to block or diminish the activity of Cas9 proteins, and thus regulate their function, which, otherwise, would be lethal in self-targeting CRISPR sequences. Following this approach, anti-CRISPR/Cas12 inhibitors have also been identified (Watters, et al., 2018).

Lenalidomide was used in this work as a CBRN (E3) ligand to ultimately target Cas9, Cas12, and Cas13 proteins and stabilize them at the cell culture level. Lenalidomide was fused to a perfluoroaromatic ringed motif, for this moiety has been proved to bind very selectively to the thiol group of the cysteine residue (Cys) in the sequence phenylalanine-cysteine-proline-phenylalanine (FCPF by the one-letter amino acid code; Phe-Cys-Pro-Phe, by the three-letter amino acid code) in a nucleophilic aromatic substitution reaction S_NAr. The side chains of the two Phe residues form a π-clamp that creates the microenvironment that make the thiol group of Cys selectively reactive to perfluoroaromatic rings in an one-step reaction at mild, close-to-physiological conditions (C. Zhang et al., 2016). The C-termini of Cas9, dCas9, Cas12, and Cas13 were engineered to contain the Phe-Cys-Pro-Phe sequence, to make them reactive to the lenalidomide-perfluoroaromatic ring (PROTAC-FCPF) to, ultimately, trigger the polyubiquitination signals against the Cas^{FCPF} proteins in mammalian cells. Our results show that the PROTAC-FCPF was indeed able to target and destabilize the engineered Cas^{FCPF} proteins regulating the gene editing activity timely. Figure 9 shows the chemical structure of PROTAC-FCPF.

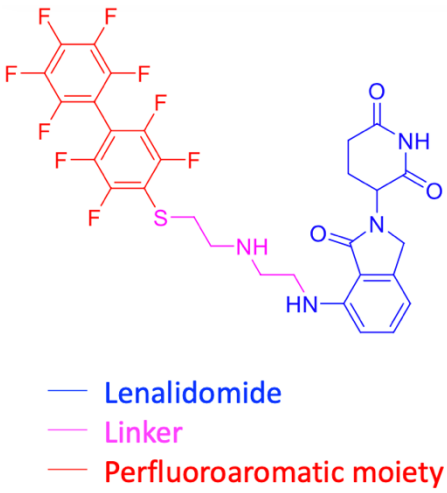

Figure 9: Chemical structure of PROTAC-FCPF

Lenalidomide in blue is the E3 ligase recruiter of this molecule, while the perfluoroaromatic moiety in red is the warhead. The linker is showed in magenta.

1.5.2. SF3B1: another target of PROTACs

Gene expression is a fundamental process for the production, regulation, and maintenance of the machinery necessary for all the cellular processes. In bacteria the messenger RNA (mRNA) resulting from transcription can directly be translated for protein expression, while in eukaryotes the transcript is an unmature RNA mix of exons an introns. The transcript must undergo excision of introns, non-coding sequences, followed by the ligation of exons, the coding sequences. Once the process, named splicing, is complete, the mRNA is mature and ready for translation (Effenberger, et al., 2017).

The spliceosome is a complex machinery of small nuclear RNA (snRNA) and a family of enzymes, such as the splicing factor 3B subunit 1 (SF3B1), which is crucial within the multiprotein complex SF3B, responsible for the recognition of 3' sites between introns and exons (Golas, et al., 2003).

There are some small molecules in use to inhibit spliceosome-mediated alternative splicing, such as pladienolide B and spliceostatin A. These chemicals have been used to induce apoptosis in several cancer cells (Eskens et al., 2013; Kaida et al., 2007; Kakeya et al., 2016; Kotake et al., 2007; Seiler et al., 2018).

However, even though chemical inhibition has been reported, no PROTAC-mediated degradation had been published until recently (Gama-Brambila, et al., 2021).

One section of this doctoral work is based on the biological testing and mechanism elucidation of a PROTAC, which used as warhead O4I2, a small molecule that was initially developed as a chemical inducer of Oct4, one of the Yamanaka transcription factors that is essential for the reprogramming of somatic cells into human induced Pluripotent Cells, commonly known as hiPSCs (Bishop, Buttery, & Polak, 2002; Theunissen & Jaenisch, 2014). For the mentioned work, a collection of chemicals was screened using High Throughput Screening techniques, finding, among other small molecules, the Oct4-Inducing Compound 2 (O4I2), which succeeded in triggering Oct4 pathways, thus, supporting the generation and maintenance of hiPSCs. (X. Cheng, et al., 2015; X. Cheng, et al., 2015; Dabiri et al., 2019).

As part of this piece of research, proteomics analysis of cells treated with O4I2 revealed several hits, among them SF3B1. Hence O4I2 is repurposed in the present work as a warhead, with the goal of targeting SF3B1 for protein degradation. Thalidomide was used to recruit CRBN in the PROTAC-O4I2, which successfully degraded SF3B1 and inhibited cancer cell proliferation. Figure 10. Shows the chemical structure of PROTAC-O4I2.

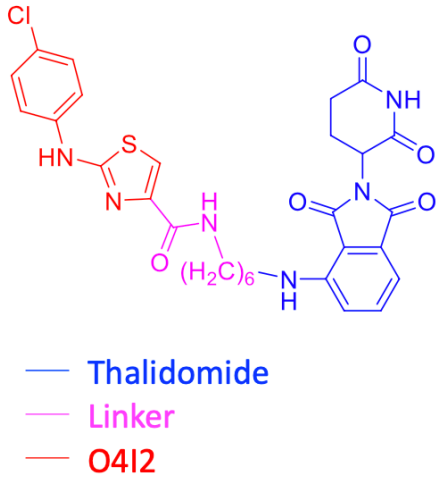

Figure 10: Chemical Structure of PROTAC-O4I2.

Thalidomide in blue is the E3 recruiter of this PROTAC, while O4I2 in red is the warhead. The linker is showed in magenta.

2. AIMS OF THE PROJECT AND HYPOTHESIS

Because historically the development of small molecules to target proteins has been limited to target mostly kinases and other enzymes, the number of compounds targeting other proteins, that can be equally pathogenic, is limited, it is the purpose of this project to:

- Develop two new PROTACs capable of degrading two new Proteins of Interest, by utilizing small molecules, which have not been used in the field to date to contribute to the expansion of de degradome with clinically relevant Proteins of Interest.
- Utilize the binding of a perfluoroaromate to a short FCPF target peptide to develop a perfluoroaromatic-based PROTAC, that can target a protein of interest, by inserting the peptide FCPF in its sequence, to develop a new strategy for targeted proteasomal degradation utilizing the FCPF sequence as degradation tag.
- To repurpose a small molecule identified by High Through Put Screening as a warhead to a clinically relevant protein to ultimately mediate its degradation driven by the PROTAC technology, as an example of this strategy to expand the warhead library.

To achieve the use of the sequence FCPF as a tag for a given protein to mediate its proteasomal degradation, it was inserted into Cas9, dCas9, Cas12 and Cas13. This sequence

contains a π-clamp making the sulfhydryl side chain in the cysteine of the peptide highly reactive to perfluoroaromatic moieties in a nucleophilic aromatic substitution reaction. Bound to Lenalidomide, a cereblon E3 ligase recruiter, the resulting perfluoroaromatic-based PROTAC-FCPF is thought to be able to bind covalently to $Cas9^{FCPF}$, $dCas9^{FCPF}$, $Cas12^{FCPF}$, and $Cas13^{FCPF}$ in cells, and recruit the E3 ligase cereblon to mediate the proteasomal degradation of these proteins.

By using High Throughput Screening techniques, it was found that the Oct4 Inducing Compound 2 (O4I2) interacts with SF3B1. Thus, by linking it to Thalidomide, a cereblon E3 ligase recruiter, the resulting PROTAC-O4I2 can interact shortly and reversibly with SF3B1 to trigger its proteasomal degradation, proving that High Throughput Screening techniques can be used to repurpose a small molecule as a warhead for a PROTAC.

3. RESULTS

The data acquired to support this work and that proves these two new PROTACs are effective new entries to the targeted protein degradation field are next described in two corresponding parts. However, the data shown here are just part of the entire research that was required, and some experiments fall beyond the scope of this work. Thus, they will be mentioned in this section only and acknowledged accordingly.
In both cases, Dr.rer.nat.habil. Xinlai Cheng designed the molecules; Dr. Jie Chen carried out the syntheses and purifications of the degraders, Václav Němec contributed to procedures part of the chemical synthesis of PROTAC-FCPF; Georg Tascher and Christian Münch performed the proteomics experiments; and Jun Zhou conducted the experiments in vivo. None of these parts will be described in this doctoral thesis but are referred to the corresponding publications (Gama-Brambila, Chen, Dabiri, et al., 2021; Gama-Brambila, Chen, Zhou, et al., 2021). The establishment of the $HeLa^{CRBN\ KO}$ and $K562^{CRBN\ KO}$ cell lines was also conducted by Dr.rer.nat.habil. Xinlai Cheng.

As well, all figures shown in this doctoral thesis are taken and modified from the above-mentioned publications.

3.1. Part I: PROTAC-FCPF

3.1.1. The activity of PROTAC-FCPF in cells

The π-clamp has already been used to target proteins engineered to contain the sequence Phe-Cys-Pro-Phe or else FCPF (C. Zhang et al., 2016). Thus, proving that this targeting strategy worked in the experimental conditions for the intended purpose was the first step. Hence, HeLa cells were transfected to express the Green Fluorescent Protein (GFP), which served as positive control. Then, $HeLa^{WT}$ cells were transfected to express the bacterial protein Cas9, in which the sequence FCPF had been inserted at the C-terminus. After transfection, the cells were treated with a synthetic derivative of the fluorophore NHS-activated 6-fluorescein isothiocyanate (FITC). This derivative also contained the perfluoro-1,1'-byphenyl moiety (together referred at FITC-FCPF), which is responsible of binding to the cysteine residue in the FCPF sequence, in a nucleophilic aromatic substitution (S_NAr) reaction. Given that Excitation/Emission wavelengths of FITC (495/519 nm) are very similar to those of GFP (509/540 nm) Cas9 fused to this fluorescent protein was used as a positive control, for the fluorescent signals from each source are reasonably comparable. In the other hand, having coupled the perfluoroaromatic motif to GFP itself would not have been practical, given that the fluorescent protein would have very probably not been incorporated into cells, because of its large size. The schematic representation of the perfluoroaromatic-FCPF recognition and tagging, and the structure of FITC-FCPF is shown in Figure 11A.

After $HeLa^{Cas9\text{-}FCPF}$ cells were treated with FITC-FCPF 10 μM for two hours, the cells were observed under a fluorescence microscope, as well as the positive control $HeLa^{GFP}$ and $HeLa^{WT}$ cells as negative control. No fluorescence is expected in WT cells because no specific protein containing the target FCPF sequence was overexpressed. Nevertheless, this must be verified, because it is not known whether any of the native proteins naturally have this sequence exposed and available for interaction. Images of living cells were taken at 10x and 63x amplifications in brightfield and a green channel for the detection of GFP and FITC. The panel B of Figure 11 shows representative images taken, where no remarkable difference between the fluorescence signals and intensities from ectopic GFP and internalized FITC can be observed. Thus proving, that the modified fluorophore FITC-FCPF can be internalized into cells and tag ectopically expressed $Cas9^{FCPF}$ within living cells.

To confirm this observation, a similar experimental set up was used for a Fluorescence-Activated Cell Sorting (FACS) experiment. $HeLa^{WT}$ cells were used as negative control, $HeLa^{GFP}$ cells as positive control, and $HeLa^{Cas9\text{-}FCPF}$ were treated with FITC-FCPF 10 μM for two hours. After the treatment, cells were washed with pre-warmed and sterile DPBS, to remove all residual FITC that may give strong background signal. After that, cells were prepared as described in 6.3.14 FACS (from 6. Materials and Methods). Fluorescent signals from ectopic GFP and FITC-FCPF-tagged ectopic $Cas9^{FCPF}$ were comparable, and both 20-fold higher than that of $HeLa^{WT}$, as shown in Figure 11C. The experiment was reproduced in four biological

replicates, confirming the observation from microscopy. Two-way ANOVA analysis was used, where *** represents a $p < 0.001$.

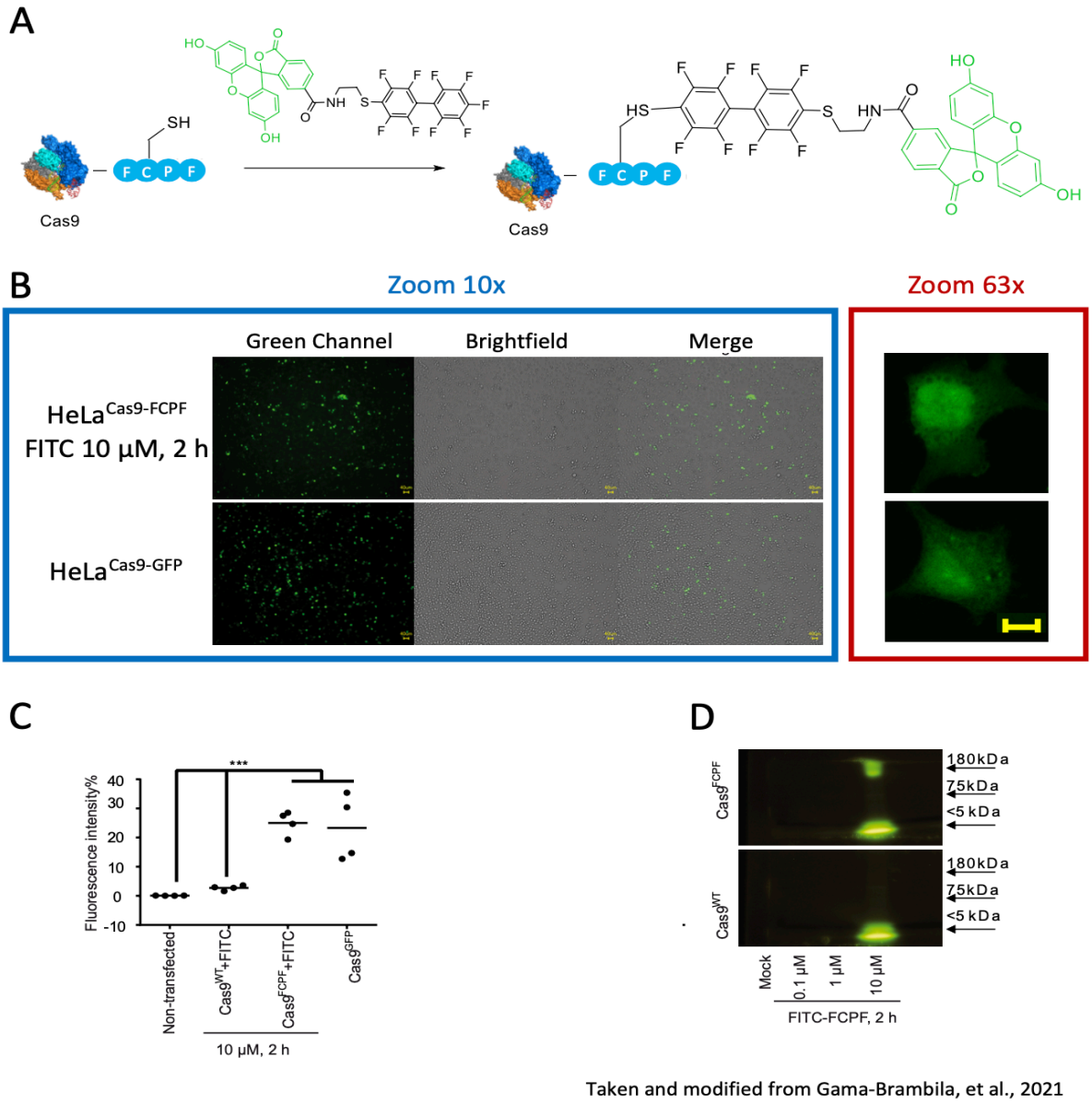

Taken and modified from Gama-Brambila, et al., 2021

Figure 11: Proof of concept. The FCPF sequence can be targeted in live HeLa cells.

Panel A: schematic representation of the S_NAr reaction between the perfluoroaromatic motif and the sulfhydryl moiety in the cysteine residue of the π clamp (FCPF sequence) present at the C-terminus of the engineered $Cas9^{FCPF}$ protein. **Upper panel B**: $HeLa^{WT}$ cells were transfected with $Cas9^{FCPF}$ overnight, followed by 24 hours of recovery in DMEM medium with FCS 10% and P/S 1%. After recovery, $HeLa^{Cas9\text{-}FCPF}$ cells were treated with FCPF bound to the perfluoroaromatic motif (FITC-FCPF), at a concentration of 10 µM for 2 hours. Ectopically expressed $Cas9^{FCPF}$ bound to FITC was observed in fluorescence microscopy. Magnifications 10x and 63x are presented. **Lower panel B**: $HeLa^{WT}$ cells were transfected with Cas9-GFP as fluorescence and transfection positive control. Transfection occurred in the same conditions and no treatment took place. $HeLa^{Cas9\text{-}GFP}$ were also observed in green fluorescence microscopy. Magnifications 10x and 63x are displayed. The scale bar in yellow represents 40 µm. **Panel C**: $HeLa^{WT}$ cells were transfected with either $Cas9^{WT}$ or $Cas9^{FCPF}$ or $Cas9^{GFP}$ overnight, followed by 24 hours of recovery in DMEM medium with FCS 10% and P/S 1%. Each cell type was treated with FITC-FCPF for 2 hours at a concentration of 10 µM. Cells were trypsinized and prepared for FACS analysis. The plot consists of 4 biological, independent replicates. Every point represents a replicate, while the bar represents the median. The data were analyzed with two-way ANOVA, where *** $p < 0.001$. **Panel D**: $HeLa^{WT}$ cells were transfected with either $Cas9^{WT}$ or $Cas9^{FCPF}$ under the conditions previously described. After recovery, each cell type was treated with FITC-FCPF 0.1, 1 and 10 µM for 2 hours. Then whole cell lysates were resolved in an 8% polyacrylamide gel to detect $Cas9^{FCPF}$ bound to FITC-FCPF.

To further support the concept HeLa^{WT} cells and HeLa$^{Cas9\text{-}FCPF}$ cells were both treated with FITC-FCPF 0.1 µM, 1 µM and 10 µM for two hours in all cases. Then, the cells were washed with DPBS three times, and then lysed with Urea Buffer, and the lysates were run through SDS PAGE in a polyacrylamide gel 8%. Only lysates from HeLa$^{Cas9\text{-}FCPF}$ showed a distinctive signal at about 150 kDa (the molecular weight of Cas9). Also, as shown in Figure 11D, only the highest concentration (10 µM) was effective in 2 hours. Given the relatively large molecular weight of Cas9, a bigger pore size was required to visualize the protein. Strictly, the concentration of acrylamide should not be determinant in this experiment, because it was not the purpose to resolve Cas9 from a protein pool, and only Cas9^{FCPF}-FITC-FCPF is expected to have fluorescent activity from the protein pool. Yet, this experiment, indirectly, provided evidence that no other proteins is predominantly being target by the modified die. It is also important to mention that SDS PAGE could be used in this experiment, because the fluorescence was not emitted by the protein, but by a fluorophore. GFP would have denatured in these conditions and would not have served as a positive control Should this be necessary, a native gel (lacking SDS) must be used instead to keep the integrity of the 3-dimensional structure of the fluorescent protein, and thus its capacity to emit fluorescence.
All together, these experiments prove that FITC-FCPF can be internalized in cells, where it reacts selectively with the ectopically expressed Cas9^{FCPF} protein, with a concentration of 10 µM for 2 hours.

3.1.2. PROTAC-FCPF inhibits the activity of Cas9^{FCPF} through degradation

Once proved that the perfluoroaromatic derivative can be internalized into cells, the next step was to test PROTAC-FCPF, which is based on the same principle of FITC-FCPF. As discussed in earlier sections of this work, several small molecules have been utilized to target proteins for proteasomal degradation. One of the most used ligands are the Immunomodulatory imide Drugs (IMiDs) thalidomide, lenalidomide and pomalidomide (Bondeson & Crews, 2017; Winter et al., 2015). Lenalidomide was the chosen ligand to PROTAC-FCPP as seen in Figure 9. The first experiment consisted in proving that PROTAC-FCPF could target Cas9^{FCPF} and lead to its degradation. Thus, HeLa^{WT} cells, used as negative control, and HeLa$^{Cas9\text{-}FCPF}$ were treated with PROTAC-FCPF 10 µM and lysates were produced at 2, 4, 6, 8 and 24 hours, by lysing cells in Urea buffer. This buffer has the purpose to inhibit the activity of all enzymes, including proteases, ultimately protecting the integrity of the protein pool. The WT cells were lysed only after 24 hours, for it is not expected to observe protein degradations from these cells. Thus, only the latest time point was used for the control. As shown in Figure 12A, Cas9^{FCPF} degradation was observable after 6 hours of treatment, and the protein seemed completely depleted after 8 hours, while no protein loss was observed in the negative control. To further investigate the time-dependence of Cas9^{FCPF} degradation, the experiment was repeated for an extended time of 72 hours with the sample collection points every 24 hours. HeLa$^{Cas9\text{-}FCPF}$ non-treated did not show protein degradation at any point within the 72 hours, while the

protein was absent in lysates from the treated cells. Non-transfected cells treated with PROTAC-FCPF were used as control and as expected, there is no observable amount of proteins, for Cas9, being prokaryotic, is naturally completely absent in human cells.

The targeted degradation of Cas9 has already been published, using the dTag technology. The degrader showed a potency in the low micromolar range (Sreekanth et al., 2020). Hence, and once that it was observed that PROTAC-FCPF could degrade Cas9^{FCPF}, the next goal was to determine the potency of the PROTAC. HeLa$^{Cas9\text{-}FCPF}$ cells were obtained by transfecting

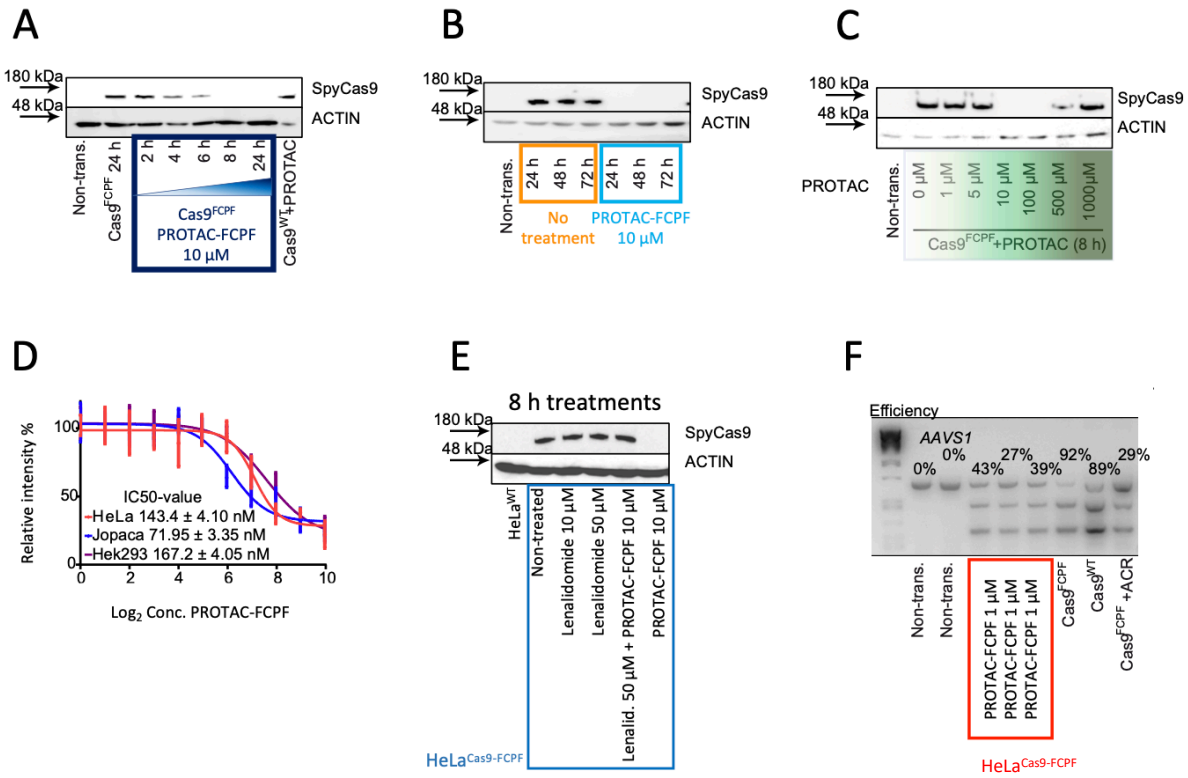

Taken and modified from Gama-Brambila, et al., 2021

Figure 12: The protein-degrading activity of PROTAC-FCPF in HeLa$^{Cas9\text{-}FCPF}$ cells.

Panel A: HeLa^{WT} cells were transfected with Cas9^{FCPF} overnight, followed by 24 hours of recovery in DMEM with FCS 10% and P/S 1%. After that, the cells were treated with PROTAC-FCPF 10 µM, taking samples a different time point. Cell lysates were immunoblotted, showing the time dependence of Cas9^{FCPF} degradation. **Panel B**: HeLa^{WT} cells were transfected as previously described, followed by the same treatment as in panel A for extended periods of time. The protein degradation was sustained up to 72 hours. **Panel C**: HeLa^{WT} cells were transfected to ectopically express Cas9^{FCPF}. After recovery, HeLa^{FCPF} cells were treated with several concentrations of PROTAC-FCPF in a range from 0 to 1 000 µM for 8 hours. The concentration dependence of Cas9^{FCPF} degradation was observed. **Panel D**: HeLa^{WT}, Jopaca-1^{WT}, and Hek293^{WT} cells were transfected to express ectopically Cas9^{FCPF} as previously described. After recovery, cells were treated with a range concentration of PROTAC-FCPF for 24 hours. Upon treatment, cells were lysed for immunoblotting. The signals from residual Cas9^{FCPF} were used to plot the half-degrading concentration (DC_{50}). The concentration-response curve shown represents four independent replicates, where the error bars are ± SD. **Panel E**: HeLa$^{Cas9\text{-}FCPF}$ were produced as earlier described. Lenalidomide was used as treatment of the free E3 ligase recruiter at concentrations of 10 and 50 µM or in combination with PROTAC-FCPF 10 µM, at a concentration of 50 µM. Cells were treated with only PROTAC-FCPF as positive control, and all treatments took place for 8 hours. The free E3 ligand failed to degrade Cas9^{FCPF}, as well as it rescued the protein by competing with PROTAC-FCPF. **Panel F**: The gene-editing activity of Cas9^{FCPF} was tested on gene AAVS1 using the T7E1 assay in the presence or absence of PROTAC-FCPF, and the activity of Cas9^{WT} was used as control. HeLa$^{Cas9\text{-}FCPF}$ were obtained as described before with either Cas9^{WT} or Cas9^{FCPF}. Co-transfection of Cas9^{FCPF} with Anti-CRISPR-Cas9 Protein AcrIIIA4 was used as positive control. The gene editing efficiency is reported as percentage from biological, independent triplicates. **A-E**: all experiments consist of independent triplicates.

overnight with the $Cas9^{FCPF}$ plasmid. Then the culture medium with the transfection mix was aspirated and replaced by fresh DMEM FCS 10% and P/S 1 %, for 24 hours as a recovery step. The next day, cells were treated for 8 hours with PROTAC-FCPF 0, 1, 5, 10, 100 and 500 µM, using $HeLa^{WT}$ cells as negative control. Figure 11C shows that the first effective concentration within the range and at this time point was 10 µM and the effect carried on until 100 µM. It can also be observed in 11C that near-complete to complete protein degradation was achieved. After that point the protein degradation lost effectiveness until no degradation at all was observable at a concentration of 1 000 µM. Figure 12C then, clearly shows a Hook Effect for PROTAC-FCPF, a phenomenon previously described in this work, that is often observed both in covalent and non-covalent PROTACs. The Hook effect is often, but not exclusively reported at concentrations starting at concentrations around 10 µM, which is not only much lower than the effect being observed in this case, but is also the first effective concentration of this PROTAC (Bondeson et al., 2015; Douglass, et al., 2013; Gabizon et al., 2020).

Next, PROTAC-FCPF was tested in three different cell lines transfected to ectopically express $Cas9^{FCPF}$: HeLa, Jopaca-1, and Hek293. These cells were all treated over 24 hours with a range of concentrations of PROTAC-FCPF within the middle-nanomolar range, to produce three concentration-response curves. Thus, not only was it possible to observe that the degrader worked in more than one cell line, but also was it possible to obtain DC_{50} values. The DC_{50} value in $HeLa^{Cas9\text{-}FCPF}$ was 143.4 ± 10 nM, in Jopaca-$1^{Cas9\text{-}FCPF}$ 71.95 ± 3.35 nM, and in $Hek293^{Cas9\text{-}FCPF}$ 167.2 ± 4.05 nM. The corresponding plot is shown in Figure 12D. The vslues found in HeLa and Hek293 cells are comparable in the middle-low nanomolar range, which is neither remarkably high nor low in the PROTAC field. It is important to remark at this point, that the DC_{50} determined in Jopaca-1 cells is almost 50% lower. Jopaca-1 are primary cells derived from poorly differentiated ductal adenocarcinoma, while the other two examples are established cell lines, making this finding of higher relevance for the applicability of the PROTAC-FCPF (X. Cheng et al., 2016).

Given that it was hypothesized that lenalidomide would trigger the protein degradation by recruiting CRBN3 ligase, it was necessary to prove that the PROTAC-FCPC also obeyed this specific mode of action. $HeLa^{Cas9\text{-}FCPF}$ were obtained as previously mentioned, cells were treated with Lenalidomide at concentrations of 10 and 50 µM, to show that the degradation is not mediated by the free warhead, instead of the PROTAC. In parallel, $HeLa^{Cas9\text{-}FCPF}$ cells were pre-treated with the free CRBN ligand at a concentration of 50 µM, and then PROTAC-FCPF was added as a co-treatment at a concentration of 10 µM for 8 hours. This pre-treatment had the purpose of saturating the cell microenvironment and cytoplasm with the free CRBN recruiter. $HeLa^{WT}$ cells were used as negative control, while $HeLa^{Cas9\text{-}FCPF}$ cells treated with PROTAC-FCPF 10 µM for 8 hours served as positive control, for it had already been proved that under these conditions, there is proved $Cas9^{FCPF}$ degradation. As expected, Lenalidomide did not mediate observable protein degradation, and the lysate from cells treated with the degrader did not have observable amounts of $Cas9^{FCPF}$. The lysate from cells with the co-

treatment had no apparent $Cas9^{FCPF}$ degraded, implying that the free ligand as pre-treatment in high concentrations must have competed for CRBN E3 ligase, rescuing the POI. As shown in the Western Blot in Figure 12E.

Determination of the efficiency of CRISPR/Cas9-mediated genome editing is a common practice, when such system is used, and the T7E1 assay is also often utilized to achieve this (Bubeck et al., 2018; Kim, et al., 2014). As explained in the first section of this work, the main purpose of protein degradation strategies is to deplete the pool of a POI, to ultimately exert control on its activity and, given that the CRISPR/Cas9 system has been repurposed as a very powerful gene editing technique, it is necessary to prove that the genome editing activity of $Cas9^{FCPF}$ consequentially stops upon PROTAC-FCPF-mediated degradation, specifically in this experiment on the gene AAVS1, as previously reported (Aschenbrenner et al., 2020). There was no significant difference in the activity of $Cas9^{FCPF}$ compared to that of Cas^{WT}, meaning that the insertion of the FCPF sequence did not alter the genome-editing activity of the system. In other words, that the insertion of the tetrapeptide in the C-terminus does not affect the activity substantially, nor that the engineered sequence alters importantly the integrity of the protein. $HeLa^{WT}$ cells were co-transfected with $Cas9^{FCPF}$, the anti-CRISPR/Cas9 protein (AcrIIA4), and AAVS1 sgRNA. Upon treatment with PROTAC-FCPF 1 µM for 24 hours, on three independent biological replicates, a reduction of the cleavage of AAVS1 was observed, ranging from 27% to 42%. The off-target gene editing was calculated to have been reduced from 12.1% to 3.56%. This experiment corresponds to Figure 12.F. The resulting reduction of the protein activity as a consequence of treatment with PROTAC-FCPF is comparable to the reduction observed with the Anti-CRISPR-Cas9 Protein AcrIIIA4. This implies that protein degradation does not offer a more powerful technique, given that similar results were obtained. However, the difference lies on the practicality of the technique. While using AcrIIIA4 requires a more complicated transfection system, storage conditions, and higher expenses, the protein degradation approach requires the addition of PROTAC-FCPF as drug treatment only.

More concisely, the experiments of this section together prove that PROTAC-FCPF mediates the degradation of $Cas9^{FCPF}$ in a time- and concentration-dependent manner to, apparently, full depletion. The protein degradation is sustained up to, at least, 72 hours at a concentration of 72 hours. In a time frame of 24 hours, the least investigated effective concentration for full depletion is 10 µM, and the Hoof effect occurs from, at least, a concentration of 500 µM. Lenalidomide as a free CRBN ligand does not lead to the degradation of $Cas9^{FCPF}$. The calculated DC_{50} from three different cell lines ranges from 72 to 167 nM, with the important remark that the lowest DC_{50} value was observed in primary cells. Last, the activity of $Cas9^{FCPF}$ is compromised as a result of treatment with PROTAC-FCPF with an effect comparable to that of the Anti-CRISPR-Cas9 Protein AcrIIIA4.

3.1.3. The mechanism of PROTAC-FCPF

To assess PROTAC-FCPF as a true PROTAC, the reliance on the UPS must be proved. The following experiments were carried out with such a purpose. Figure 13A shows an immunoblot that serves for a few important points. HeLa^{WT}, HeLa$^{Cas9\ WT}$, and HeLa$^{Cas9\text{-}FCPF}$ cells were all treated with PROTAC-FCPF 10 µM for 8 hours, conditions previously found as effective for full protein depletion. Hence these two cell types are then negative control and positive control, respectively, while non-treated of each of these cells functioned as negative controls. Cas9 was detected using two different primary antibodies: anti-Cas9 and anti-FLAG. Cas9 was detected in lysates from cells transfected with either Cas9^{WT} or Cas9^{FCPF} but not treated with PROTAC-FCPF. While no detectable protein was observed in HeLa^{WT} cells HeLa$^{Cas9\text{-}FCPF}$ treated with PROTAC-FCPF. This experiment proves that the addition of the FCPF sequences does not interfere with the epitope of Cas9, and therefore its detection with a primary antibody, thus the WT and the mutated protein can equally and comparably be detected. Yet, this experiment also proves that Cas9^{WT} Is no affected by the treatment with PROTAC-FCPF, implying that the degradation of Cas9 relies exclusively on the presence of the sequence FCPF. Ubiquitinated proteins, and more importantly, ubiquitinated Cas9 protein were barely observed in lysates from HeLa$^{Cas9\text{-}FCPF}$ treated with PROTAC-FCPF, while no Cas9^{FCPF} protein was detected in the same sample. This observation, together with the time point, at which it had already been proved Cas9 depletion occurred, suggests that the POI was already mostly degraded, and very little ubiquitinated protein was left. To confirm this, the proteasome inhibitor MG132 was added as a co-treatment at a concentration of 5 µM. As expected, Cas9 was rescued by MG132, but also there was a significant increase in the signal from the anti-ubiquitin antibody. MG132, being a proteasome inhibitor, does not prevent all the previous steps occurring at the E1-E2-E3 axis. In other words, MG132 does not prevent neither the activation step mediated by E1 enzymes, nor the transfer of ubiquitin to E2 enzymes for the attachment of ubiquitin to the client protein mediated by E3 ligases. Hence, upon treatment with MG132 ubiquitinated proteins are not expected to be present in the protein pool, but to be accumulated, given that the step ubiquitin is detached from the client protein prior to its degradation is being inhibited. Thus, ubiquitinated proteins, and significantly ubiquitinated forms of Cas9, accumulated, proving that PROTAC-FCPF mediates the ubiquitination of Cas9^{FCPF}.

Once that ubiquitination of Cas9 was proved, the immediate following step was to show that the ubiquitination depends on CRBN E3 ligase, for Lenalidomide is the CRBN-recruiting ligand of PROTAC-FCPF. The experiment to prove it was based on two different cell sets, first HeLa$^{Cas9\text{-}FCPF}$ and the other one co-transfected cells with the plasmid to ectopically express Cas9^{FCPF} and CRBN siRNA to generate a CRBN knockdown (HeLa$^{Cas9\text{-}FCPF/CRBN\ KD}$). Both cell types were treated with PROTAC-FCPF 0, 1, 5, and 10 µM for 8 hours. Figure 13B shows that in the KD cells, the intracellular pool of CRBN decreased remarkably compared to the cells transfected with the Cas9^{FCPF} plasmid only. The levels of Cas9 in the CRBN KD cells were

considerably higher, compared to those of HeLa$^{Cas9\text{-}FCPF}$, implying that absence of CRBN impacts negatively in Cas9 degradation.

To further prove the involvement of CRBN in the ubiquitination and degradation of Cas9^{FCPF} mediated by PROTAC-FCPF, an *in vitro* ubiquitination experiment was carried out. CRISPR/Cas9 CRBN-Knockout HeLa cells, that is, HeLa cells where CRBN is completely and irreversibly absent, were transfected with either Cas9^{WT} or Cas9^{FCPF}, while non-transfected HeLa$^{CRBN\ KO}$ cells were used as negative control. Cells were lysed 48 hours after transfection with Urea Buffer. It is expected in this protein pool that no native CRBN is present, but ectopically expressed Cas9^{WT} and Cas9^{FCPF} are present. In parallel HeLa^{WT} cells were transfected with either FLAG-CRBN^{WT} or FLAG-CRBN^{m}. The latter corresponds to the loss-of-function double-mutant (Y383A and W385A), previously reported (G. Lu et al., 2014). After transfection, both FLAG-CRBN^{WT} and FLAG-CRBN^{m} were immunoprecipitated and then purified, taking advantage of their FLAG tags. The thorough description of the procedure can be found in 6. Materials and Methods (6.3.3 *In vitro* Ubiquitination Assay for Cas proteins). The lysates from HeLa$^{CRBN\ KO}$ (CRBN-negative control), HeLa$^{Cas9\ WT/CRBN\ KO}$ (CRBN and Cas9 negative control) and HeLa$^{Cas9\text{-}FCPF/CRBN\ KO}$ cells were prepared for in vitro polyubiquitination, by addition of the component of the kit (full details can be found in 6.3.3. *in vitro* Ubiquitination assay for Cas proteins), as well as PROTAC-FCPF 100 µM was added to lysates from HeLa$^{Cas9\ WT/CRBN\ KO}$ (Cas9 and CRBN negative control) and HeLa$^{Cas9\text{-}FCPF/CRBN\ KO}$ cells, and last, a co-treatment of PROTAC-FCPF 100 µM and Lenalidomide 100 µM was added to the lysate from HeLa$^{Cas9\text{-}FCPF/CRBN\ KO}$ cells. The reaction started with the addition of purified FLAG-CRBN^{WT} and FLAG-CRBN^{m} proteins to the preparations. After 90 minutes, the luminescence signal was measured as an indirect method to measure the ubiquitination process. Figure 13C shows the results of at least two technical replicates of three biological, independent replicates of the experiment. Concisely, the luminescent signal increases importantly only in the lysate from HeLa$^{Cas9\text{-}FCPF/CRBN\ KO}$ cells in the presence of purified CRBN^{WT} and PROTAC-FCPF. As expected, no considerable luminescence intensity was detected in any of the samples where CRBN^{m} was present, given that is a loss-of-function mutant, with which no ubiquitination of the client protein is expected. Luminescence was not observed in HeLa$^{Cas9\ WT/CRBN\ KO}$ lysates treated with PROTAC-FCPF, because of the absence of the targetable FCPF sequence in the ectopically expressed protein. In the presence of the free E3 ligase ligand, the luminescence signal was attenuated, supporting the observation of free Lenalidomide competing with PROTAC-FCPF for CRBN^{WT}. It is also important to notice, that the attenuation was partial, while in the previous subsection (2.1.2 PROTAC-FCPF inhibits the activity of Cas9^{FCPF} through degradation, Figure 12C), no protein degradation was observed at all. This difference may be related to the levels of sensitivity of the methods and that, in the experiment corresponding to Figure 12C the proportion Lenalidomide to PROTAC-FCPF was 5:1, while in the experiment being discussed, the proportion of these two components is 1:1. Suggesting that higher concentrations of Lenalidomide are necessary to fully suppress the activity of PROTAC-FCPF. The data were analyzed as Two-way ANOVA.

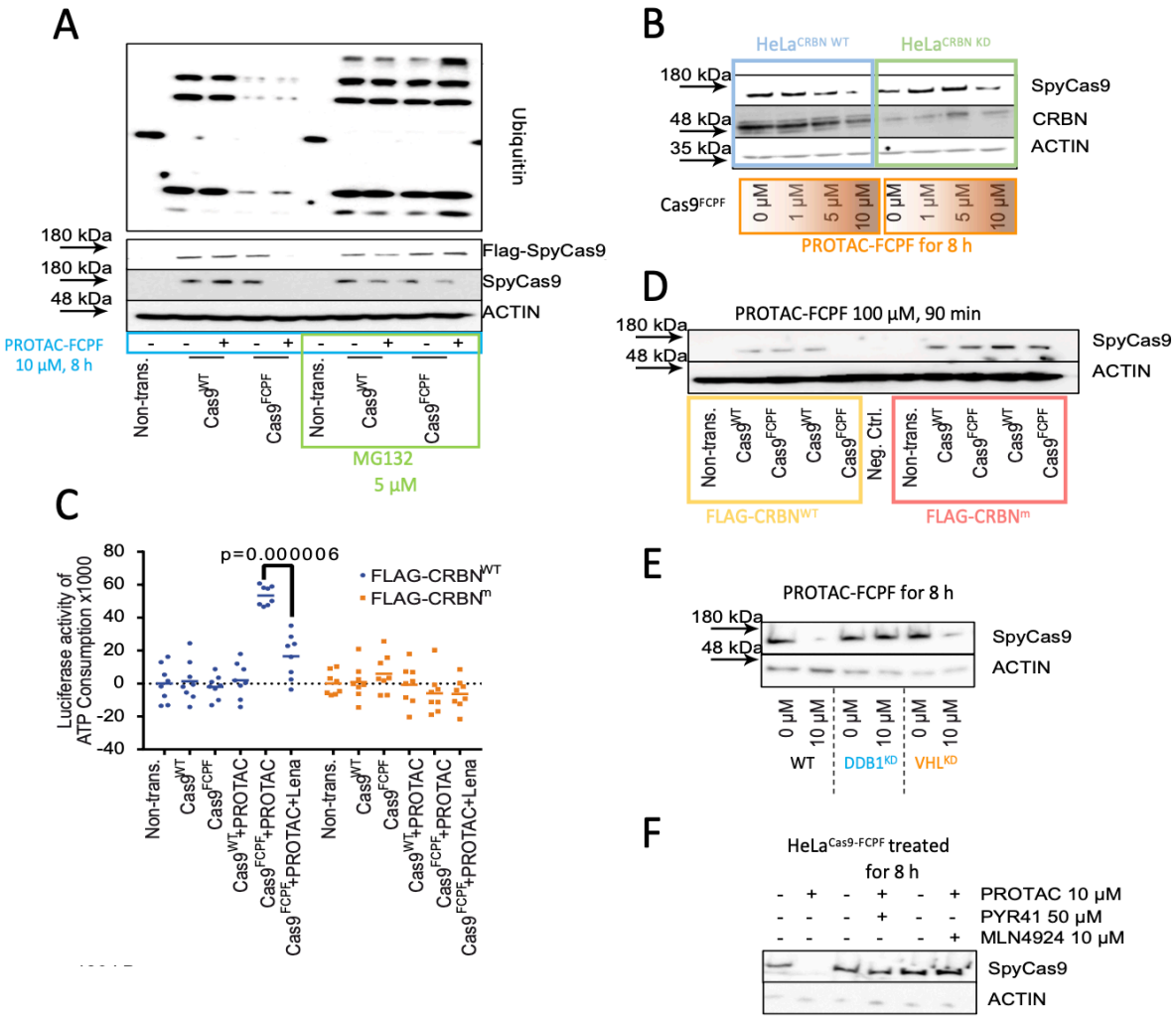

Taken and modified from Gama-Brambila, et al., 2021

Figure 13: The protein degradation mechanism of PROTAC-FCPF is based on the UPS.

Panel A: HeLa^{WT} cells were transfected to express either FLAG-Cas9^{WT} or FLAG-Cas9^{FCPF} overnight, with a following recovering time of 34 hours, while non-transfected cells were used as negative control. After recovery, all cells were treated with PROTAC-FCPF 10 µM for 8 hours in the presence or absence of MG 132 at a concentration of 5 µM. Cells were lysed after treatment, and FLAG-Cas9^{WT} and FLAG-Cas9^{FCPF} were immunoprecipitated for immunoblotting with FLAG, Cas9, and Ubiquitin primary antibodies. **Panel B**: HeLa^{WT} were transfected as previously described with Cas9^{FCPF} in the presence or absence of CRBN siRNA. After the recovery time, all cells were treated with PROTAC-FCPF 0, 1, 5, and 10 µM for 8 hours, after which whole cell lysates were immunoblotted. **Panel C and D**: HeLa$^{CRBN\ KO}$ cells were transfected with wither FLAG-Cas9^{WT} or FLAG-Cas9^{FCPF} as previously explained, while non-transfected HeLa$^{CRBN\ KO}$ were used as control. After recovery, all cells were lysed and FLAG proteins immunoprecipitated to be further purified. (**C**) Once pure, a fraction of each protein solution was mixed either with previously purified FLAG-CRBN^{WT} or FLAG-CRBN^{m}. Non-treated samples were used as positive control, while PROTAC-FCPF 100 µM was added along in samples of both FLAG-Cas9^{WT} and FLAG-Cas9^{FCPF}, and an additional sample was generated with co-treatment with Lenalidomide 100 µM in lysates from HeLa$^{CRBN\ KO/FLAG\text{-}Cas9\text{-}FCPF}$. All samples with all components were incubated at 37 ˚C for 90 minutes, after which, the samples were prepared for ATP-dependent in vitro ubiquitination assay measured by luciferase activity. The experiment consists of a technical triplicate of three independent, biological replicates. Every dot in the plot represents a datum point and the bar represents the average value. Data were analyzed with two-way ANOVA. (**D**) The rest of the purified FLAG-Cas9 proteins were treated with PROTAC-FCPF 100 µM and either FLAG-CRBN^{WT} or FLAG-CRBN^{m} for 90 minutes at 37 ˚C. After the incubation, samples were immunoblotted for Cas9 detection. **Panel E**: HeLa^{WT} cells were transfected with either DDB1 siRNA or VHL siRNA as previously described, using crtl. siRNA as negative control. Upon recovery, all cells were treated with PROTAC-FCPF 10 µM for 8 hours, and non-treated cells were kept as control. After the treatment all cells were lysed and whole lysates were immunoblotted. **Panel F**: HeLa$^{CAS9\text{-}FCPF}$ cells were produced as explained before. Non-treated cells were used as negative control, while the rest of the cells were co-treated with PROTAC-FCPF 10 µM for 8 hours with either PYR41 50 µM or MLN4924 10 µM. After the treatments, all cells were lysed and whole cell lysates were used for Western Blot to detect Cas9.

The same procedure was used for WB. The lysates from HeLa$^{CRBN\ KO}$, HeLa$^{Cas9\ WT/CRBN\ KO}$ and HeLa$^{Cas9\text{-}FCPF/CRBN\ KO}$ cells were treated with PROTAC-FCPF for 90 minutes at a concentration of 100 µM each at 37 ˚C in the presence of either CRBN^{WT} or CRBN^{m}. The preparations were used for immunoblotting as shown in Figure 13D. There, it is also possible to see that no degradation was observed in the presence of the double mutant CRBN^{m}, while Cas9^{FCPF} degradation was observed in in lysates treated with PROTAC-FCPF in the presence of CRBN^{WT}. No protein degradation is observed in lysates from cells expressing Cas9$^{WT.}$

Once it was proved that CRBN is determinant in the mechanism of PROTAC-FCPF, the next necessary step is to rule out alternative E3 ligases involved in the proteasomal degradation. The following experiment consists of the siRNA-mediated knockdown of proteins related to CRBN. CUL4 and DDB1 are fundamental components of the CRBN E3 ligase complex, as previously mentioned in Section 1.3. Targeted Protein Degradation Strategies. HeLa^{WT} cells were transfected with DDB1 and VHL siRNA, first to validate the need of the entire DDB1-Rbx1-CRL4-N8-CRBN E3 ligase complex, second to discard that the degradation may be consequence of the activity of VHL E3 ligase, the other most employed route in the PROTAC field. Figure 13E shows in a Western Blot that lysates from HeLa$^{Cas9\text{-}FCPF/DDB1\ KD}$ cells treated with PROTAC-FCPF failed to degrade Cas9^{FCPF}, implying that the absence of DDB1 defunctionalized the E3 complex, while HeLa$^{Cas9\text{-}FCPF/VHL\ KD}$ accomplished the depletion of the POI, yet to a minor extent. A possible explanation for this, is that the degradation of proteins may not be completely selective, VHL may contribute to a small fraction of the total Cas9^{FCPF} proteolysis. PROTACs manipulate a naturally occurring process, therefore the natural degradation of the protein may have more than one alternative. To confirm the last sentence more experiments focusing on this issue could be performed in the future, such as the knocking down of other members of the VHL E3 ligase complex but fall beyond of the scope of this work.

Last for this section, the E1 inhibitor PYR-41 (Y. Yang et al., 2007) and MLN4925 (Soucy et al., 2009), an inhibitor of the NED8-Activating Enzyme, needed for full activity of the CUL4A-DDB1-Rbx1-N8-CRBN complex were used to investigate whether the protein degradation process would be interrupted if inhibitors of early steps of the UPS pathway were used, opposite to the experiment performed with MG132. Therefore, the protein degradation is expected to be inhibited by suppressing the ubiquitinating activity at the first and third steps. HeLa$^{Cas9\text{-}FCPF}$ were pre-treated with either PYR-41 at a concentration of 50 µM or MLN4925 10 µM, followed by treatment with PROTAC-FCPF 10 µM for 8 hours. Figure 13F showed that only lysates from HeLa$^{Cas9\text{-}FCPF}$ cells with single PROTAC-FCPF treatment lack Cas9^{FCPF}, while the lysates from pre-treated cells failed to degrade the POI.

3.1.4. PROTAC-FCPF activity in other Cas proteins

The last experiments with PROTAC-FCFP had the goal to prove its efficacy against other proteins tagged with the sequence FCPF, and that this new approach to targeted protein degradation is not limited to Cas9. As well as Cas9, the related proteins dCas9, Cas12 and Cas13 were engineered to have the mentioned tetrapeptide inserted at their C-termini, namely proteins dCas9^{FCPF}, Cas12^{FCPF} and Cas13^{FCPF}. Figure 14A shows the concentration-dependent degradation of dCas9^{FCPF} after treatment with PROTAC-FCPF, with observable degradation starting at a concentration of 1 µM, and very important, comparable, almost full protein degradations at 5 and 10 µM in an 8-hour treatment.

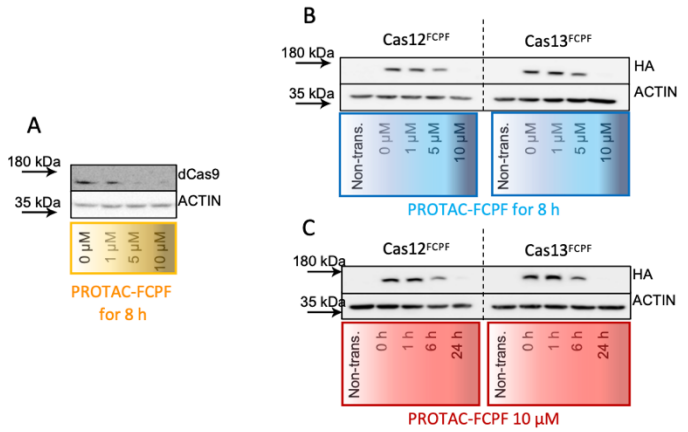

Taken and modified from Gama-Brambila, et al., 2021

Figure 14: The Activity of PROTAC-FCPF in other proteins tagged with the FCPF sequence.

Panel A: HeLa^{WT} cells were transfected to express ectopically dCas9-FCPF overnight, followed by 24 hours of recovery in DMEM FCS 10% and P/S 1%. After recovery, transfected cells were treated with PROTAC - FCPF 0, 1, 5, and 10 µM for 8 hours, after which all cells were lysed to be immunoblotted to detect dCas9. **Panel B** similarly for a concentration-dependence experiment, HeLa$^{Cas12\text{-}FCPF}$ and HeLa$^{Cas13\text{-}FCPF}$ were obtained. After recovery, cells were treated with PROTAC-FCPF 0, 1, 5, and 10 µM for 8 hours, followed by cell lysis and Western Blot analysis to detect Cas12 and Cas13. **Panel C**: HeLa$^{Cas12\text{-}FCPF}$ and HeLa$^{Cas13\text{-}FCPF}$ were obtained as mentioned before, and treated with PROTAC 10 µM for 0, 1, 6 and 24 hours. After treatments, all samples were immunoblotted to detect Cas12 and Cas13 to prove the time-dependence of protein degradation. All experiments were done in biological, independent triplicates.

HeLa^{WT} cells were transfected to ectopically express Cas12^{FCPF} and Cas13^{FCPF}, and were also treated with PROTAC-FCPF 0, 1, 5, and 10 µM for 8 hours. In both cases, protein degradation started being obvious at a concentration of 5 µM and reached apparent full depletion at a concentration of 10 µM upon treatment for 8 hours, as shown In Figure 14B, a result that is like that observed in Cas9^{FCPF}, except that the concentration 5 µM seemed completely ineffective in that first case. Hence, it can be said that proteins Cas12^{FCPF} and Cas13^{FCPF} are slightly more susceptible to PROTAC-FCPF.

Last, the time-dependence was studied in HeLa$^{Cas12\text{-}FCPF}$ and HeLa$^{Cas13\text{-}FCPF}$ cells, using the same concentration of PROTAC-FCPF (10 µM). Figure 14C shows as Western Blot, where it was found that degradation was observable at 6 hours, and after 24 hours, complete depletion had been achieved.

3.2. Part II: PROTAC-O4I2

3.2.1. O4I2 activity in RNA synthesis

As previously mentioned at the start the Section 3. Results, SF3B1 was found as one of the hits during the proteomics analysis of cells treated with O4I2. Therefore, the first step in this part of the experimental work is to focus on the real activity of O4I2 on SF3B1. The first experiment was the tracking of newly synthesized RNA with a fluorophore. Should the hypothesis that O4I2 binds to SF3B1 be correct, the result would be an impact in the splicing activity, and by consequence, the synthesis of RNA. It has been previously reported that 5-ethynyl uridine can substitute or replace uridine during RNA synthesis (Jao & Salic, 2008). Then, using click chemistry, an azide-containing fluorophore can be attached to 5-ethynyl uridine, making it visualizable in fluorescence microscopy, and cells can be quantified by FACS.

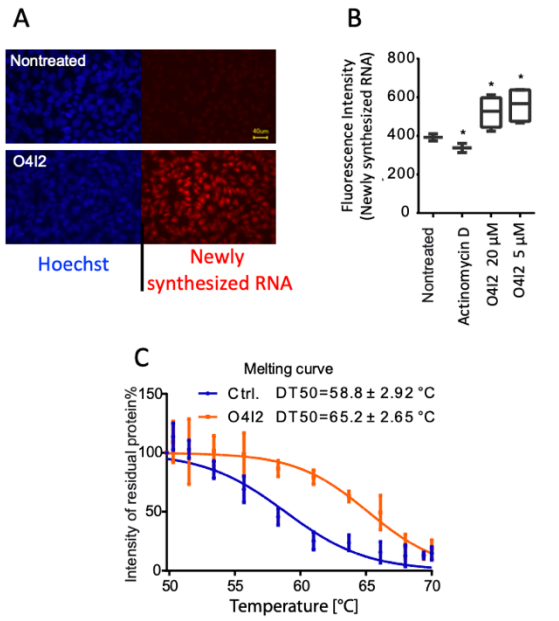

Taken and modified from Gama-Brambila, et al., 2021

Figure 15: in vitro activity of O4I2 with SF3B1.

Panel A and B: 5-ethynyl uridine was added to the cell culture medium of Human Fibroblasts. Then cells were treated with O4I2 10 µM for 4 hours, after which images were taken in fluorescence microscopy, where red is the newly synthesized RNA and blue is the Hoechst 33342 die, used as control. The scale bar represents 40 µM. **Panel B**: 5-ethynyl uridine was added to the cell culture medium of Human Fibroblasts. Then cells were treated with O4I2 either 5 or 20 µM, or with Actinomycin D for 4 hours. After treatment, cells were trypsinized and analyzed with FACS. The experiment consists of 4 biological, independent experiments. Data were analyzed with two-way ANOVA. The upper and lower edges of the boxes represent the highest and lowest values, respective, while the middle bar represents the median. Error bars are ±S.D. * $p < 0.05$. **Panel C**: Hek293^{WT} cells were transfected to express FLAG-SF3B1 overnight, followed by 24 hours of recovery in DMEM FCS 10% and P/S 1%. Then cells were lysed and FLAG-SF3B1 purified (10 mg/mL). The protein was treated with O4I2 20 µM for 30 minutes. And then incubated at various temperatures for 20 minutes, after which the proteins samples were immunoblotted. Three replicates were done. The signal was used to plot a thermal stability curve, analyzing the data with two-way ANOVA. Error bars are ± S.D.

Human fibroblasts were treated with O4I2 10 µM for 4 hours. After that, the EzClick global RNA synthesis assay kit was used to label the newly synthesized RNA. Figure 15A shows fluorescence microscopy images of cells with and without treatment with O4I2. A very important increase in the synthesis of RNA can be observed in the treated cells (red) in comparison to the non-treated. The die Hoechst33342 was used as control. It can be seen in Figure 15A that the fluorescence intensity in the blue channel, that is the Hoechst33342-stained nuclei is comparable between non-treated and treated cells with O4I2, while in non-treated cells there is no substantial red fluorescence. This does not mean that no new RNA is being synthesize in non-treated cells, but rather that the base-lone synthesis is too low to be detected in with this microscope, while the red fluorescence intensity in cells treated with O4I2 is remarkably higher, implying that the RNA

synthesis was heavily enhanced. The same experiment was repeated for FACS analysis, using O4I2 at 5 and 20 µM, and fibroblasts treated with Actinomycin D, an RNA polymerase inhibitor (Jao & Salic, 2008) as negative control. In this case, two different concentrations were used, one under and one above of the concentration used for microscopy, to distinguish between two different point, because FACS has significantly more sensitivity. Figure 14B is a box plot that shows the quantification of FACS analysis of 4 biological, independent experiments analyzed with Two-way ANOVA, where * represents a p value of 0.05. The upper and lower edges of the boxes represent the maximum and minimum measurements, respectively, while the bar in the middle is the median. There is a notorious increase in the fluorescence signal from cells treated with O4I2, compared to that of cells treated with the negative control. These two experiments together imply that O4I2 induces the RNA synthesis, probably by inducing SF3B1.

To further prove that O4I2 interacts with SF3B1 a melting curve assay was carried out, for it is known that the thermal stability of a protein tends to increase when bound to a ligand. FLAG-SF3B1 was ectopically expressed in Hek293T cells. After transfection, the cells were lysed and FLAG-SF3B1 immunoprecipitated to be then purified taking advantage of the FLAG tag. Then, the purified protein, with a concentration of 10 µg/mL in a total volume of 25 µL of protein solution, was treated with O4I2 in a gradient of temperatures ranging from 50 to 70 ˚C, and then incubated for 20 minutes. Then the supernatants were collected and immunoblotted. With the relative intensity of the Western Blot signals, a melting curve was plotted as a concentration-response curve (Figure 15C) comparing the lysates with O4I2 and without it, as negative controls. The curves were analyzed with Two-way ANOVA from three independent experiments and yielded a DT_{50} value of 58.8 ± 2.92 ˚C for the non-treated protein, and 65.2 ± 2.65 ˚C for the treated protein, observing a roughly 6 ˚C-increase in the melting curve. Thus, it can be affirmed that O4I2 does interact and bind to SF3B1, for it increased the thermal stability of the protein.

3.2.2. PROTAC-O4I2 protein-degrading activity in human cancer cells

To transform O4I2, an SF3B1 inducer, into a degrader, the compound was attached to a 6-atom long alkyl linker in one side, and Thalidomide was bound to opposite end of the linker, as a CRBN E3 ligase recruiter. The resulting chemical was named PROTAC-O4I2. To test it, K562 cells were transfected to ectopically express SF3B1, then treated with a range of concentrations of PROTAC-O4I2 up to 5 µM for 24 hours. After the treatment, cell lysates were immunoblotted as shown in Figure 16A. Protein degradation was observable at a concentration as low as 0.5 nM. The protein degradation as sustained up to a concentration of 5 µM and the Hook effect started appearing at a concentration of 10 µM (not shown). The calculated DC_{50} from this curve has a value of 0.244 µM. The experiment consisted of a

biological triplicate, and the relative signals were plotted as a protein degradation curve, analyzed with two-way ANOVA.

The next point was to prove that PROTAC-O4I2 was driving the degradation of SF3B1 and not the free warhead. The next experiment consists of Hek293^{WT}, HepG2^{WT}, K562^{WT} and HeLa^{WT} cells transfected to overexpress SF3B1, using the respective WTs as negative control. Then, both WT and transfected cells were treated with either 10 µM of the free warhead, or 1 µM of PROTAC-O4I2. Figure 16B shows the resulting immunoblot after all cells were lysed. SF3B1 was detected with both anti-SF3B1 primary antibody for the endogenous protein, and anti-FLAG primary anti-body for the ectopically expressed protein. It can also be seen that the signal from SF3B1 antibody is much stronger than that of the FLAG antibody. There are a few probable explanations for that, but most probably, the signal from the SF3B1 antibody is the addition of the ectopically expressed protein and the endogenous protein, while the FLAG antibody detects only exogenous SF3B1. Nevertheless, it is also worth mentioning that it was

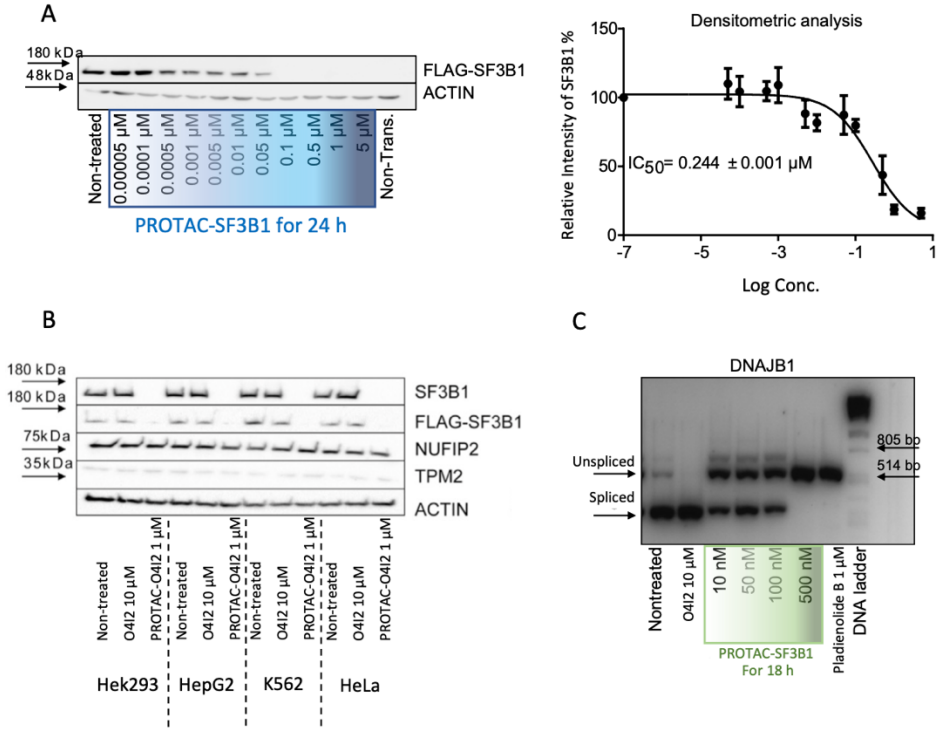

Taken and modified from Gama-Brambila, et al., 2021

Figure 16: Effects of PROTAC-O4I2 in cancer cells.

Panel A: K562^{WT} cells were transfected to ectopically express FLAG-SF3B1 overnight, then cells were allowed to recover for 24 hours in RPMI 1640 with FCS 10% and P.S 1%, after which treatment with PROTAC-O4I2 took place at a gradient of concentrations for 24 hours. After treatment cells were lysed and whole cell lysates were immunoblotted. The experiment was carried out in a biological triplicate, and the Western Blot signals were used to produce the concentration-response curve on the right side, and the DC_{50} calculated. The data were analyzed with two-way ANOVA, where the error bars are ±S.D. **Panel B**: Hek293^{WT}, HepG2^{WT}, K562^{WT}, and HeLa^{WT} were al transfected as previously described, then treated with either O4i2 10 µM or PROTAC-O4I2 1 µM 24 hours, while non-treated cells were used as negative control. After treatment whole cell lysates were immunoblotted against SF3B1, FLAG, NUFIP2, TPM2 and β-actin primary antibodies. **Panel C**: K562^{WT} cells were treated with either O4I2 10 µM, Pladienolide B 1 µM as positive control, or with PROTAC-O4I2 10, 50, 100 or 500 nM, while non-treated cells were negative control All treatments took place for 18 hours, after which cells were lysed for RNA extraction, followed by cDNA synthesis. PCR was used to amplify DNAJB1, and products were resolved in a 2% agarose gel. The experiment was performed in a biological triplicate.

observed that no signal was obtained at all from the FLAG antibody when the protein lysates were blotted and imaged after one week from the lysis day. Thus, it is highly recommended to carry out the Western Blot experiment as soon as possible from the lysis day. In all cell lines degradation was just observed in lysates from cells treated with PROTAC-O4I2 only. Both endogenous and exogenous SF3B1 were degraded. The Western Blot image also show proteins NUFIP2 and TPM2, two other hits during the proteomics analysis (data not shown here, but available in the corresponding publication), none of which was affected by PROTAC-O4I2. It is also important to notice that there does not seem to be a difference in the amounts of any of the proteins among the cell lines, except a slightly increased β-actin amount form Hek293 cells and slightly decreased in K562 cells. The importance of this observation is that the proportion in the expression of these proteins is comparable throughout the sample set, making this set of cell lines a suitable comparison system.

To investigate the effects of degrading SF3B1, the next experiment was based on the splicing of DNAJB1. A DNAJB1-splicing follow up has already been reported (Kotake et al., 2007). $K562^{WT}$ cells were treated with either the free warhead O4I2 at a concentration of 10 µM, with Pladienolide B, a reported SF3B1 inhibitor, therefore used in this experiment as negative control, at a concentration of 1 µM or with PROTAC-O4I2 at concentrations of 10, 50, 100, and 500 nM for 18 hours. After that, the total RNA was isolated and the respective cDNA syntheses carried out. The genetic materials were amplified by PCR, and the products run in an agarose gel. Figure 16C shows an image of the gel, where it can be observed that, as expected, free O4I2 increased the splicing of the gene of interest, while PROTAC-O4I2 clearly prevented splicing even at the lowest concentration tested, having a maximum effect at 500 nM, comparable to that of the inhibitor Pladienolide B. The difference in the effect at concentrations 10, 50, and 100 is not easy to distinguish, but the splicing is completely inhibited at the highest tested concentration.

3.2.3. The mechanism of PROTAC-O4I2

For PROTAC-O4I2 to be classified as a PROTAC, it also must be proven that the degradation of SF3B1 is mediated by the UPS. For the first experiment with this purpose K562 cells were transfected with CRBN siRNA to produce $K562^{CRBN\ KD}$, while $K562^{WT}$ were used as negative control. Both cell types were treated with different concentrations of PROTAC-O4I2 at concentrations of 0.01, 0.1, and 1 µM for 24 hours. After the treatment all cells were lysed for Western Blot. Figure 17A shows that degradation of SF3B1 had concentration dependence in $K562^{CRBN\ WT}$ cells, almost reaching close to 50% depletion with the concentration 0.1 µM and almost full depletion with the highest concentration, while in $K562^{CRBN\ KD}$ cells exhibited much lower degradation levels, not even reaching 50% of relative degradation. This plot consists of 3 independent, biological triplicates, analyzed with Two-way ANOVA, followed by post hoc Turkey test. Therefore, even partial absence of CRBN diminished the POI

degradation. The upper and lower limits of the box correspond to the highest and lower measured values, respectively, while the bar within the box represents the median.

The next step in the understanding the mechanism behind PROTAC-O4I2 is determining whether ubiquitination occurs upon treatment with the degrader. $K562^{FLAG\text{-}SF3B1}$ cells were obtained as previously described and then treated with either the free warhead O4I2 at a concentration of 10 µM or with PROTAC-O4I2 at a concentration of 1 µM for 24 hours. These samples were produced in duplicates and one of the sample set was co-treated with the proteasome inhibitor MG132 at a concentration of 2.5 µM. The protein levels in the lysate from cells treated with the free warhead were, as expected, comparable to those of the non-treated (negative control). It is important to mention that only FLAG-SF3B1 was detected in this experiment. Therefore, the endogenous protein levels were not considered. FLAG-SF3B1 was not detected in the sample from cells treated with PROTAC-O4I2, and polyubiquitinated forms of the protein were absent, as well. Because of the treatment and time point, probably all the protein had already been degraded and there was polyubiquitinated protein to observe. The negative control from the MG132 sample set and the sample from cells co-treated with the free warhead and MG132 are comparable to those of the MG132-free sample set. That it, FLAG-SF3B1 was detected with no changes in the abundance, and ubiquitinated forms of the protein were observed. But as it can be observed in Figure 17B MG132 rescued SF3B1 from PROTAC-O4I2-driven degradation as well as the ubiquitinated forms of the protein. Given that MG132 is a proteasome inhibitor, ubiquitination steps are not inhibited and are expected to be present and accumulated in the sample, when the ubiquitin-detaching step, and the subsequent protein degradation are inhibited. It can indeed be seen that the intensity of the ubiquitinated proteins is slightly stronger than in any other sample and only in this sample (PROTAC-O4I2 in co-treatment with MG132) polyubiquitinated proteins are observed.

Free Thalidomide was used to test whether it could compete with PROTAC-O4I2 for CRBN. FLAG-SF3B1 was overexpressed in K562 cells, using the WT cells as negative control. To test it, three pre-incubations took place, all for 1 hour: free warhead (O4I2) at a concentration of 10 µM, free Thalidomide 10 µM, and the combination of the two free ligands both at 10 µM. To all these samples PROTAC-O4I2 was added at a concentration of 1 µM for 24 hours. Additional samples of non-treated, treatment with O4I2 10 µM for 24 hours and treatment with PROTAC-O4I2 1 µM for 24 hours were included as negative and positive controls. After all treatments were over, all cells were lysed and immunoblotted as shown in Figure 17C. As expected, degradation of SF3B1 was not or observed in samples with pre-treatments, confirming competition of Thalidomide for CRBN with PROTAC-O4I2, while the presence of

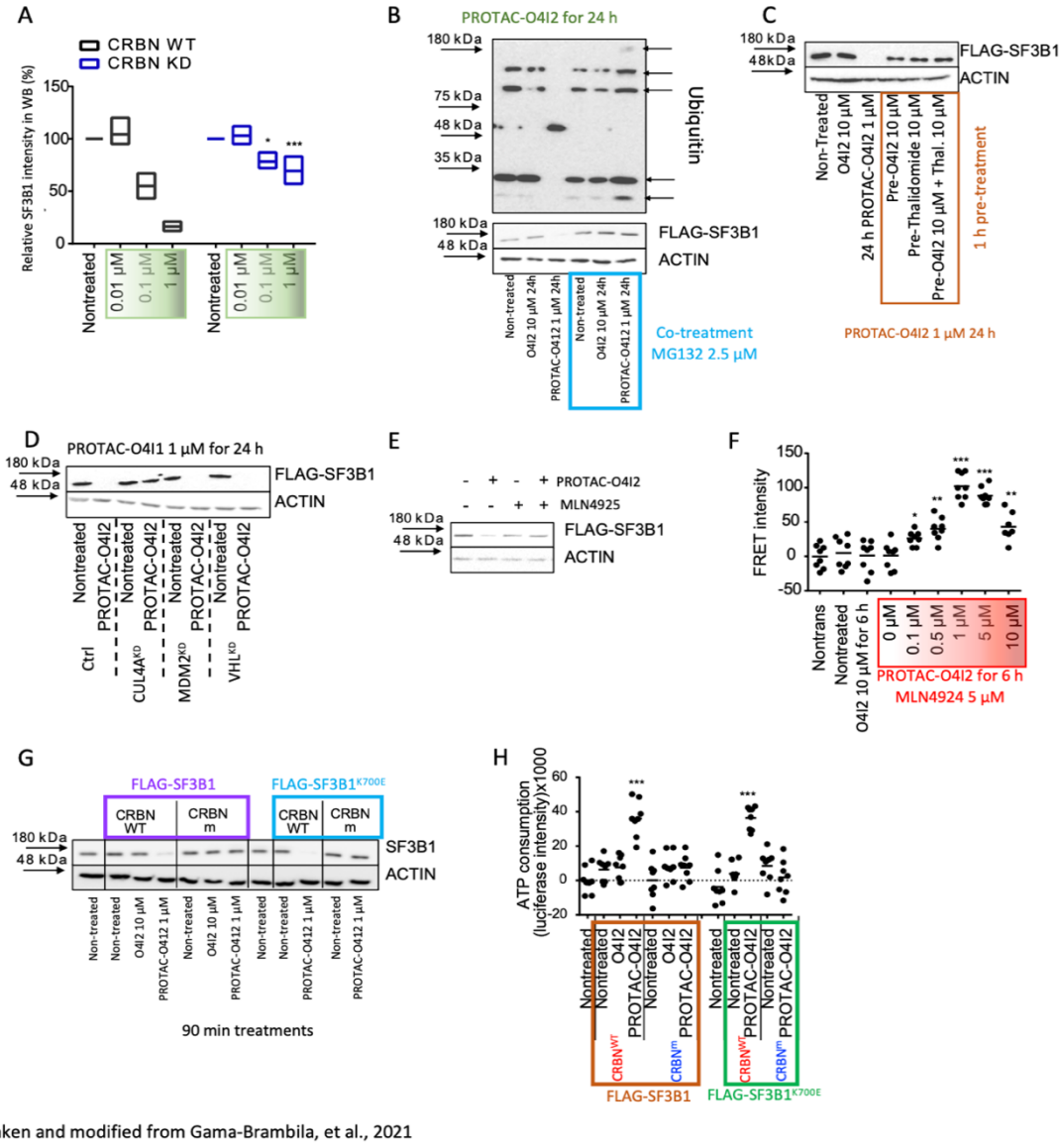

Taken and modified from Gama-Brambila, et al., 2021

Figure 17: Elucidating the action mechanism of PROTAC-O4I2.

Panel A: K562^{WT}cells were transfected with FLA-SF3B1 plasmid in the presence or absence of CRBN siRNA overnight, followed by 24 hours of recovery in RPMI 1640 FCS 10% and P/S 1%. Upon recovery, cells were treated with PROTAC-O4I2 0.01, 0.1 or 1 µM for 24 hours. Cell lysates were immunoblotted and the data from three biological replicates were analyzed with two-way ANOVA and post hoc Tukey test. The upper and lower edges of the boxes represent the highest and lowest value, respectively, while the middle bar represents the median. * $p < 0.05$ and *** $p < 0.001$. **Panel B**: K562$^{FLAG\text{-}SF3B1}$ were produced as previously described, then these cells were treated with O4I2 10 µM or PROTAC-O4I2 1 µM for 24 hours in the presence or absence of MG132 2.5 µM, while non-treated cells were used as negative control. After treatment, cells were lysed and FLAG-SF3B1 immunoprecipitated for further purification. Once purified, both the protein and the residual lysate were immunoblotted for FLAG and Ubiquitin, respectively. **Panel C**: K562$^{FLAG\text{-}SF3B1}$ cells were produced as previously described. After recovery, cells were pre-treated with either O4I2 10 µM (negative or thalidomide 10 µM, or the combination of both for 1 hour, then PROTAC-O4I2 was added (1 µM) for 24 hours. Cells treated with only PROTAC-O4I2 were used as positive control. After treatment, cells were lysed and whole lysates were immunoblotted. **Panel D**: K562^{WT} were co-transfected as previously described with FLAG-SF3B1 plasmid and either Crtl siRNA, or CUL4A si RNA, or MDM2 siRNA, or VHL siRNA. After the recovery time, cells were treated with PROTAC-O4I2 1 µM for 24 hours. **Panel E**: K562$^{FLAG\text{-}SF3B1}$ were obtained as previously mentioned. After recovery cells were treated with PROTAC-O4I2 1 µM in the presence or absence of MLN4924 5 µM for 24 hours. After the treatment cells were lysed and whole lysates were immunoblotted. **Panel F**: K562 cells were co-transfected with CRBN-GFP and SF3B1-OFP as previously described, WT cells were used as negative control. Once recovered, wells were treated with either O4I2 10 µM or PROTAC-O4I2 in a range of concentrations in combination with MLN4924 5 µM for 6 hours. After treatment FRET signal was measured in a plate reader with Ex/Em 485/573 nm. The experiment consists of 6 independent replicates, each represented by a dot. * $p < 0.05$, ** $P < 0.01$, *** $p < 0.001$. **Panels G and H**: K562$^{CRBN\ KO}$ cells were transfected with either

FLAG-SF3B1^{WT} or FLAG-SF3B1^{K700E} as previously explained, while non-transfected K562$^{CRBN\ KO}$ were used as control. After recovery, all cells were lysed and FLAG proteins immunoprecipitated to be further purified. Once pure, a fraction of each protein solution was mixed either with previously purified FLAG-CRBN^{WT} or FLAG-CRBN^{m}. Non-treated samples were used as positive control, while either O4I2 10 µM or PROTAC-OI42 1 µM was added along in samples of both FLAG-SF3B1^{WT} and FLAG-SF3B1^{K700E}. All samples with all components were incubated at 37 ˚C for 90 minutes, after which, (**G**) a fraction of the preparations was used to detect residual SF3B1 in Western Blot, (**H**) while the rest was prepared for ATP-dependent in vitro ubiquitination assay measured by luciferase activity. The experiment consists of a technical triplicate of three independent, biological replicates. Every dot in the plot represents a datum point and the bar represents the average value. Data were analyzed with two-way ANOVA with a sample size of 8 independent replicates.

O4I2 alone seemed to be irrelevant. It can be observed that the intensity of the signal in O4I2 alone seemed to be irrelevant. It can be observed that the intensity of the signal in samples with pre-treatments is indeed slightly weaker, compared to the negative controls. Which suggests that the presence of the free ligands does not inhibit the protein degradation completely. Probably the free ligands compete for their corresponding proteins but are not present in a concentration or proportion to completely override PROTAC-O4I2.

To confirm that PROTAC-O4I2 SF3B1 degradation does not have alternative routes to CRBN, K562 were double-transfected with the FLAG-SF3B1 expression plasmid and either CUL4A siRNA, or MDM2 siRNA, and or VHL siRNA. CUL4A is a component of the CRBN E3 ligase complex and is necessary for a fully functional complex, and for proper E3 ligase activity. MDM2 and specially VHL are other E3 ligases that are commonly recruited for proteasomal degradation in the PROTAC field. Thus, knocking them down has the purpose to discard their involvement in the degradation of SF3B1. Non-transfected cells were used as negative control, and K562$^{FLAG\text{-}SF3B1}$ were used as positive control. After transfections, all cells were treated with PROTAC-O4I2 at a concentration of 1 µM for 24 hours. Figure 17D, shows the resulting Western Blot image, where the absence of CUL4A compromised the integrity of the DDB1-CUL4A-Rbx1-N8-CRBN complex, thus impeding the degradation of SF3B1. The absence of VHL and MDM2 E3 ligases did not seem to interfere at all with the degradation of SF3B2 mediated by PROTAC-O4I2. These observations together point that a fully functional DDB1-CUL4A-Rbx1-N8-CRBN complex is necessary for the degradation of the POI, and that, from the tested E3 ligases, CRBN is the only responsible for the proteasomal degradation of SF3B1.

MLN4925, an inhibitor of the NED8-Activating Enzyme, needed for full activity of the CUL4A-DDB1-Rbx1-N8-CRBN complex, was also used in this case to prove entirely the involvement of the UPS pathway. The experiment was conducted with K562$^{FLAG\text{-}SF3B1}$ cells treated with PROTAC-O4I2 1 µM in the presence or absence of the NEDD8-Activating Enzyme inhibitor (MLN9425 5 µM). As expected, the inhibitor prevented the degradation of the POI, as shown in the immunoblot of Figure 17E, given that it inhibits the last step of the ubiquitination pathway.

To investigate the protein-protein (CRBN-SF3B1) interaction this with more detail, PROTAC-O4I2 was titrated in a Fluorescence Resonance Energy Transfer (FRET) assay. K562 cells seeded in a flat, transparent-bottom black 96 well-plate, and were then double transfected with CRBN-GFP and SF3B1-OFP expression plasmids, then treated with either O4I2 10 µM, or with PROTAC-O4I2 in a range of concentrations from 0.1 to 10 µM in co-treatment with MLN9425 5 µM (to inhibit the degradation but allowing the protein-protein interaction) for 5 hours (See Figure 16F). The fluorescence signals from living cells were read in a plate reader, which was set at Ex/Em 485/573 nm. The plot represents the values from at least six independent, biological replicates. The p values determined are the following: * $p < 0.05$, ** $p < 0.01$, *** $p < 0.001$. Every circle represents the datum of an individual measurement, while the bar represents the average value. The FRET assay shows that, indeed, the point of maximum interaction is at a concentration of PROTAC-O4I2 of 1 µM, while the interaction declines at 10 µM, probably owed to the Hook effect.

The last step to confirm the UPS-mediated mechanism was an in vitro ubiquitination assay. The acquisition of the purified FLAG-CRBN^{WT} and CRBN^{m} can be found as a general description in Sections 6.3.3 Briefly, K562^{WT} cells were transfected with either FLAG-CRBN^{WT} or FLAG-CRBN^{m} overnight, followed by a recovery stem in RPMI 1640 FCO 10% and P/S 1% for 24 hours Then cells were lysed in Urea Buffer and the FLAG-tagged proteins were immunoprecipitated and further purified. The mechanism of PROTAC-FCPF and thoroughly in 6.3.11. Immunoprecipitation and Ubiquitination (for SF3B1) K562$^{CRBN\ KO}$ were transfected with FLAG-SF3B1^{WT} and SF3B1^{K700E}, a common mutation found in up to 55% of patients with myelodysplastic syndromes (Papaemmanuil et al., 2011). After transfection, all cells were lysed and the lysates were prepared as follows: six samples from every SF3B1^{WT} were produced, one non-treated as negative control, another sample to be treated with O4I2 10 µM in the presence of purified FLAG-CRBN^{WT}, the next one to be treated with PROTAC-O4I2 1 µM in the presence of CRBN^{WT} and, the last three with the same treatments, but in the presence of FLAG-CRBN^{m}. From lysates with SF3B1^{K700E} four samples were prepared, one non-treated as negative control in the presence of FLAG-CRBN^{WT}, and the other one to be treated with PROTAC-O4I2 1 µM in the presence of FLAG-CRBN^{WT}. The other two, with the same treatments in the presence of FLAG-CRBN^{m}. All these samples were used for either Western Blot (Figure 17G) or Ubiquitination assay with further addition of reagents for luciferase assay (Figure 17H). In Western Blot no protein degradation was observed except for two samples: K562$^{FLAG\text{-}SF3B1\ WT}$ in the presence of FLAG-CRBN^{WT} treated with PROTAC-O4I2 and K562$^{FLAG\text{-}SF3B1\ K700E}$ in the presence of CRBN^{WT} and treated with PROTAC-O4I2. This means two important points. First, CRBN^{m}, as expected and previously observed in the experiments with PROTAC-FCPF, was not able to mediate the proteasomal degradation of SF3B1, for it is a loss-of-function mutant and, second, PROTAC-O4I2 does no distinguish between SF3B1^{WT} and the clinically relevant mutant SF3B1^{K700E}. Although there is a slight difference in the level of degradation. SF3B1^{K700E} seems to be completely depleted, while minimal residual WT protein could be observed.

The luciferase assay reported the same results: no luminescence was significantly detected except for the two samples treated with PROTAC-O4I2 1 µM in the presence of FLAG-CRBN^{WT}. Together, these results imply that, as expected, the protein degradation depends on the functional form of CRBN^{WT} but, interesting, the PROTAC-O4I2 had similar activity in both variants of SF3B1, meaning that the PROTAC may have clinical relevance. Opposite to the result observed in Western Blot, single datum points of luminescence from K562$^{FLAG\text{-}SF3B1\ WT}$ seem to be slightly higher than those of the mutant K562$^{FLAG\text{-}SF3B1\ K700E}$, although the average value seems the same in both samples.

3.2.4. Cytotoxicity of PROTAC-O4I2

RNA splicing has been related to the development of some tumors, associated with mutations in the spliceosome, which impact on the excision of introns or lack of it, modifying the sequence of some proteins, resulting in occasional gain-of-function mutations of oncoproteins or loss-of-function mutation in tumor supressing proteins (Dvinge, Kim, Abdel-Wahab, & Bradley, 2016). SF3B1 inhibitors have been used in *in vivo* and *in vitro* studies, showing antiproliferative activity of these small molecules (Cretu et al., 2018; Jimenez-Vacas et al., 2019; Seiler et al., 2018). To test the antiproliferative activity of PROTAC-O4I2, K562^{WT} cells were transfected to overexpress SF3B1^{WT} and SF3B1^{K700E}, and WT cells were used as negative control. Each cell type was treated with a range of concentrations of Pladienolide B, O4I2, and PROTAC-O4I2 to produce dose-response curves in an MTT cell viability assay. Figure 18A shows the resulting curves. The first curve shows that the cytotoxicity of O4I2 is neglectable, barely reaching 50% of survival with concentrations as high as 10 µM, while in WT cells Pladienolide B is about three times more cytotoxic than PROTAC-O4I2, with IC_{50} values of 76.4 ± 15.2 nM and 227.9 ± 23 nM, respectively. In K562 overexpressing SF3B1^{WT}, there is an inversion of the cytotoxicity profiles, making PROTAC-O4I2 twice as effective as Pladienolide B against cell viability, with IC_{50} values of 62.9 ± 13.5 nM and 133.5 ± 8.6 nM, respective. In K562 cells overexpressing SF3B1^{K700E} a similar effect was observed, with IC_{50} values of 90.2 ± 24.5 nM for PROTAC-O4I2 and 116.1 ± 17.5 nM for Pladienolide B, making the degrader slightly more effective. This experiment consisted of 5 biological, independent replicates. Interestingly, cells expressing the mutant SF3B1^{K700E} are slightly more sensitive to Pladienolide B, but less sensitive to PROTAC-O4I2, compared to cells expressing the WT protein. Yet, looking at the concentration-response curves together, the survival profile is very similar in both cases (Pladienolide B and PROTAC-O4I2) and it is only at the inflection point of the curve where the trends of the curves differ. At higher concentrations, there does not seem to be a difference in survival.

To further test the cytotoxicity of PROTAC-O4I2 both K562^{WT} and K562$^{CRBN\ KD}$ cells were treated with either PROTAC-O4I2 or Pladienolide B, both at a concentration of 1 µM for 72 hours. After the treatments, the cells were tested in an apoptosis assay with Annexin V/PI double staining. The experiment was performed in a biological triplicate resulting in Figure

18B. The assay shows that, as expected, Pladienolide B does not distinguish between the absence or presence of CRBN, while PROTAC-O4I2 does, having a cytotoxicity comparable to that of Pladienolide B in K562$^{CRBN\ WT}$ cells. The results imply that the induction of apoptosis is comparable with the two treatments, but only one, that derived from treatment with PROTAC-O4I2, is CRBN-dependent.

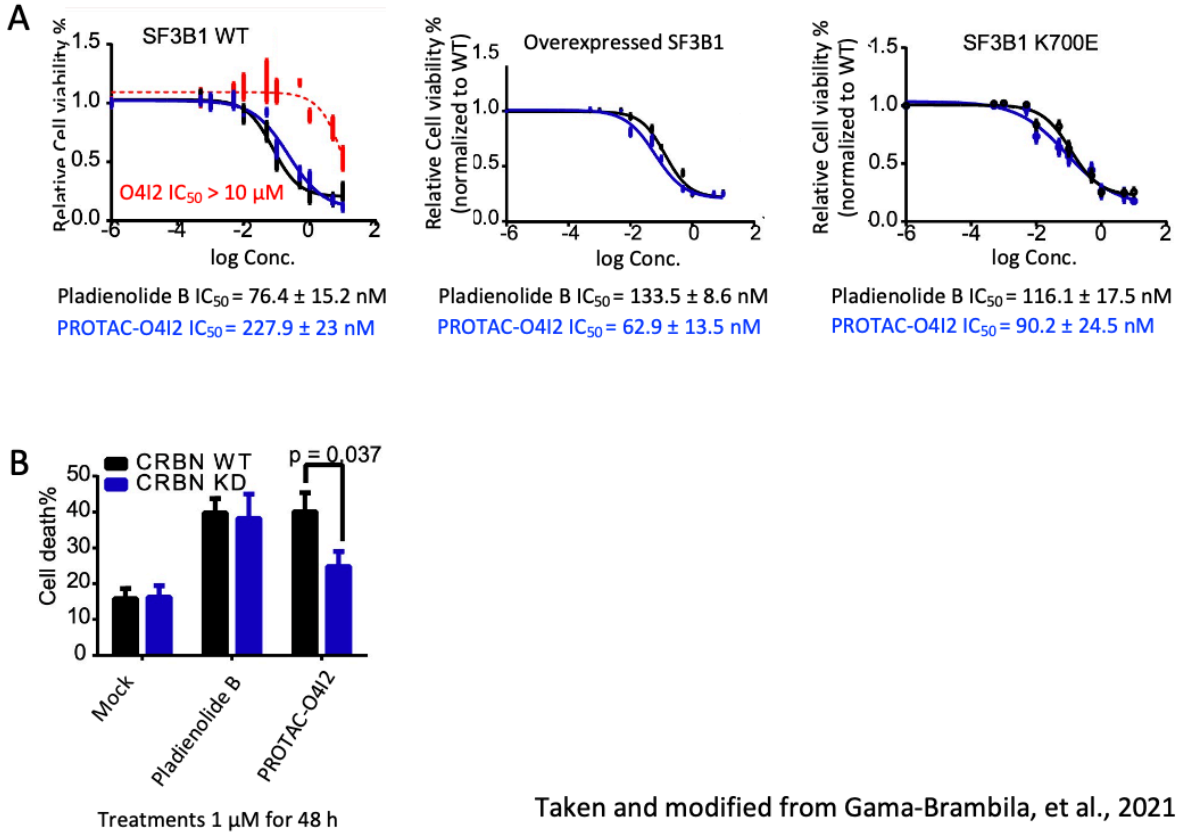

Figure 18: Antiproliferative effects of PROTAC-O4I2 in cancer cells.

Panel A: K562 were transfected to ectopically express either SF3B1^{WT} or S3B1^{K700E}. Every cell type was treated with a range of concentrations of Pladienolide B as positive control, or PROTAC-O4I2 for 72 hours. After treatment, the culture medium was changed to RPMI 1640 FCS 1% P/S 1% and MTT 0.5 mg/mL. The assay was run when purple precipitates were observable. The plate was read in a plate reader at a wavelength of 595 nm. The experiment consists of 5 replicates. The error bars in the survival curve represent ±S.D. **Panel B**: K562^{WT} cells were transfected with CRBN siRNA overnight, followed by a recovery step of 24 hours, while WT cells were used as negative control. After recovery each cell type was treated with either Pladienolide B 1 µM as positive control treatment or PROTAC -O4I2 1 µM for 72 hours. After treatments, the double die Annexin V/PI was added to label living cells, early apoptotic cells, and late apoptotic cells. Independent, biological triplicates of this experiment were analyzed with FACS being the error bars ± S.D.

4. DISCUSSION AND FUTURE PERSPECTIVES

During the last two decades the Proteolysis Targeting Chimeras (PROTACs) developed to become a revolutionizing technology in the branch of protein activity modulation for cell biology, chemical biology, pharmacology, and molecular biology research. These small molecules, broadly defined in the scientific literature as heterobifunctional molecules, that have two ligands tethered by a linker, one to target a protein of interest, commonly known as warhead, and the other to bind a recruit an E3 ligase, ultimately trigger the ubiquitination of the target protein, resulting in its degradation by the 26S proteasome (Krall, et al., 2016).

There are many other approached, technologies and techniques to regulate the activity, different to the occupancy-driven pharmacology, that has predominated the field of protein activity modulation ever since small molecules started being used to treat diseases. Most of these technologies and techniques are based on the temporary and reversible degradation of a Protein of Interest within cells, but not only. One example of it is the Ancho away technology, based on the re-localization of proteins away from their cite of action. An example of an Anchor Protein is Rpl13A, a ribosomal protein that enters the nucleus in the process of producing new ribosomes. The Anchor protein is fused to FKBP12, that, in the presence of rapamycin, an mTOR inhibitor, makes a complex to FRAP which is fused to a Protein of Interest. The main disadvantage of this methods is that it is mostly limited to nuclear proteins, significantly limiting the potential of the technique.

Most of the other techniques, such as dTag, HyT, deGradFP, SMASH, and AiD are based on the proteasomal degradation of the Protein of Interest. Even though, all of them mediate the protein degradation through the same pathway, they all have mechanistical differences. For example, HyT is based on the incorporation or fusion of a dehalogenase to the POI and the exposure to linker that has an adamantyl acetamide moiety, increasing the overall superficial hydrophobic area, mimicking a misfolded protein and thus, triggering the Unfolded Protein Response, ultimately resulting in proteasomal degradation of a protein. AiD relies on the ubiquitous expression of the SKP-Cullin-F-Box (SCF)-RING E3 ligase complex in eukaryotes. Thus, by fusing AID degron to the Protein of Interest, its proteasomal degradation is induced by the temporary and reversible treatment of phytohormones, such as IAA.

The technique deGradFP is a Protein degradation technique with very high specificity, given that it is based on the detection of GFP by a nanobody that is fused to an E3 ligase complex. Thus, only the Protein of Interest will be targeted for degradation by the modified E3 ligase. However, all these techniques have a major disadvantage for their clinical application: the require genetic manipulation to engineer the Protein of Interest and fused it to a degron or tag, and then introduce it into cells or a tissue to ectopically expressed them. Thus, these techniques are automatically discarded for their clinical use, yet they remain as very powerful techniques for research.

TRIM away is a different technique, although also based on proteasomal degradation of the Protein of Interest. TRIM21 is a protein that recognizes the F_C of IgGs that have been internalized into cells upon viral recognition and complexation. This E3 ligase has the natural

task to drive the degradation of the IgG-virus complex, which results in viral peptides, that Antigen-presenting cells will later use as part of the immune response. Thus, internalization of antibodies against Proteins of Interest, mostly by microinjection, leads to very efficient and fast proteasomal degradation of the desired proteins, However, the need of microinjection into cells makes this technique very unpractical for clinical used, and therefore, is also limited to research.

Unlike all the examples mentioned above, PROTACs, being small molecules, can simply be placed in the microenvironment of cells for natural uptake, despite their usually large size These degraders have proved to be very powerful tools, for they produce pronounced intracellular protein depletion at very low concentrations, which can be reversible and do not require genetic manipulation, opening possibilities for clinical applications. Currently, there are just two PROTACs in clinical trials: ARV-100 targeting the Androgen Receptor, in trial in patients with metastatic Castration-resistant Prostate Cancer, and ARV-471 targeting the Estrogen Receptor, in trial in patients with ER+/Her2- locally advanced or metastatic breast cancer (Chen et al., 2021).

Another one of the big advantages these molecules offer is that their activity is independent of active sites and hydrophobic binding pockets, which are characteristic of kinases. The need of these binding sites is one of the biggest obstacles that pharmacology has had to face, limiting the druggable fraction of the proteome to about 20%. Therefore, PROTACs, in theory, have the potential to cover the rest of the proteome and make it druggable, since they only need to interact with the target protein superficially and shortly (Bondeson & Crews, 2017; Neklesa et al., 2017; Pettersson & Crews, 2019).

Nevertheless, a big portion of the PROTACs developed up to date still targets the proteins that have been the focus of occupancy-driven pharmacology, mostly kinases, nuclear receptors, bromodomain and extra-terminal motif proteins consequently, because the design and development of chemicals to target proteins was limited to the need of interaction with a binding pocket. This, however, is an opportunity to give a second chance to many molecules that were discarded in the past, for not being table to fulfill the chemical and thermodynamic requisites of classical pharmacology and chemical biology (Bondeson & Crews, 2017; Neklesa et al., 2017).

Because of these reasons, not only is it necessary to develop more ligands that can be used for new PROTACs, but also new techniques to take advantage of already existing molecules and, thus expand the library or ligands that can be used for the design of PROTACs

This work presents two new PROTACS able to degrade not only novel proteins in the PROTAC field, but also protein types that do not fall in the spectrum of proteins targeted so far. In addition to that, these two new degraders were developed with two different approaches that can contribute to expand the library of ligands very importantly. The first, is the use of a generic perfluoroaromatic compound, that is, not a specific, already-existing small molecule, that binds covalently to the sulfhydryl motif in the side chain of the cysteine in the tetrapeptide Phe-Cys-Pro-Phe. The phenyl motifs in these two phenylalanine residues constitute a π-clamp that makes this sulfhydryl moiety more reactive to perfluoroaromatic

compounds in a Nucleophilic Aromatic Substitution Reaction. Thus, theoretically, any protein containing this peptidic sequence is prone to be bound (tagged) to a perfluoroaromatic moiety. If the mentioned compound linked to an E3 ligase, the FCPF-containing protein would then undergo proteasomal degradation. This would be a technique to, technically, tag any protein for UPS-driven degradation. In this work, this approach was tested with Cas proteins.

Cas proteins and the CRISPR/Cas9 system represent a turning point in the field of genome editing, molecular biology and cell biology. They made it possible to delete, substitute, and insert genes in a stable and irreversible fashion. However, over the years, flaws in the system have been reported, often related to off-target editing. Extensive research has been conducted, attempting to overcome these flaws, such as the development of inhibitors, engineered Cas proteins and the use of anti-CRISPR proteins (Hu et al., 2018; Kleinstiver et al., 2015; Slaymaker et al., 2016) .

The first PROTAC presented in this work consists of Lenalidomide as a CRBN E3 ligase recruiter and a perfluoroaromatic moiety that has been previously proved to target the tetrapeptide Phe-Cys-Pro-Phe through a nucleophilic aromatic substitution reaction (S_NAr) in physiological conditions, with the thiol group in the side chain of cysteine. This tetrapeptide, known as a π-clamp was inserted in the c-termini of Cas9, dCas9, Cas12, and Cas13.

PROTAC-FCPF has a molecular weight of 699.57 g/mol. Even though the structure is not particularly large, its high content of fluorine makes it much heavier. The molecule also has 8 heteroatoms with free pairs of electrons that can be acceptors of hydrogen bonds, while 20 protons are available within this molecule, relatively available to produce a hydrogen bond. Most of the chemical structure is planar, with a predominant number of carbon atoms and heteroatoms in sp^2 configuration. Then, most of the protons within the molecule lack important hinderance for hydrogen-bond formation. The Polar surface area was not estimated in this work, which would be necessary, particularly in this molecule with high content of heavy and very electronegative fluorine, to fully assess its profile according to Lipinski's Rule of 5. Nevertheless, with what is known about the molecule, it can be said that it is too heavy to be classifies as small molecule, but it has a good number of substituents that can either donate or accept hydrogen bonds. Most of PROTACs are reported to fall in the range of 700 to 1 000 g/mol in molecular weight (Neklesa et al., 2017), very close to that of PROTAC-FCPF, which may affect its uptake in cells.

However, the molecule proved to degrade the engineered proteins selectively in the low micromolar range in short treatments, and with a calculated DC_{50} value of 150 nM in a 24-hour treatment. The degradation effect was sustained for up to 72 hours. It was demonstrated that de degradation was dependent not only of CRBN E3 ligase, but also of the presence of DDB1, meaning that the integrity of the entire E3 ligase complex is necessary for the POI degradation. It was also proved that the activity of PROTAC-FCPF triggers ubiquitination, that degradation can be interrupted in the presence of E1 and E2 inhibitors, and the ubiquitinated POI accumulate in the presence of a proteasome inhibitor.

For this degrader to work, it requires the engineering of the POI to contain the sequence FCPF. Although, as discussed before, this sequence is too short to produce changes in conformation or activity, there requirement of genetic manipulation is present, a need that true PROTACs can, as matter of principle, override. Therefore, it is not totally clear whether this molecule should be named PROTAC, although it fulfills the commonly accepted profile of such molecules in the field. However, as effective as this molecule proved to be, there is room for improvement and optimization. It has been broadly reported in the scientific literature, and discussed earlier in this work, the optimization of the length and composition of the linker can be determining in the success and potency of the linker. With the information collected in this work, it is impossible to predict whether a different linker would improve or worsen the activity of PRTOAC-FCPF. Nevertheless, investigating this is a potential opportunity for improvement.

It was observed that the Hook effect took place on concentrations higher than 500 µM. Neither no experiment was carried out to study or estimate the α cooperativity value, nor were other E3 ligase recruited for Cas^{FCPF} degradation by utilizing other E3 ligase ligands. Thus, the degree protein-protein interactions and cooperativity between the Cas^{FCPF} proteins and CRBN remains completely unknown and is room for improvement in further work with this modality of FCPF-perfluoroaromatic compounds-triggered protein degradation. The obtainance of a crystal structure of the ternary complex could also help identify what the predominant interactions are between the proteins, and between each protein and the linker, thus making it clear what are the structure or design features that could be optimized in this degrader.

The mode of action of this degreader (PROTAC) makes it an irreversible, covalent degrader, making this system very suitable for proteins that must have activity only once and can safely be completely depleted without further consequences, or ese, for proteins with very slow turnover rates. It remains to be researched on what the consequences would be, should the system be applied to proteins that require activity in more than one event, and the difference between proteins with varying turnover rates.

In the second case High Through Put screenings revealed that the small molecule O4I2 was capable of chemically inducing Oct4, promoting the reprogramming of somatic cells and contributed to sustain the pluripotency of hiPSC. Proteomics analysis from cells treated with O4I2 showed that main hit was the spliceosome-element SF3B1. Thus, the use of these techniques was useful in finding an already existing molecule that could be repurposed to target a molecule that, so far, had escaped targeted degradation by PROTACs.

The second PROTAC reported in this work has Thalidomide as a ligand to recruit CRBN E3 ligase in one side of a 6-atom long alkyl linker, which tethers on the opposite end O4I2. This ligand was found to interact with, among other proteins, with SF3B1, a crucial member of the spliceosome, responsible of 3’ splice recognition sites at junctions occurring between non-coding introns and coding exons. This protein had not been targeted for PROTAC-mediated degradation before this work, which not only makes a novel target, but is also a clinically

relevant protein. Reports show, as earlier discussed in this written work, that mutations in the spliceosome may lead to alterations in the sequences of expressed proteins, possibly resulting in gain-of-function of oncoproteins and/or loss-of-function of tumor repressing proteins (Dvinge et al., 2016). An example of this is the $SF3B1^{K700E}$ mutant, that has been found to be related in tumorigenesis and is present in up to 55% of patients with myelodysplastic syndromes (Papaemmanuil et al., 2011; L. Wang et al., 2011).

PROTAC-O4I2 has a molecular weight of 593.1 g/mol, much closer to fall into the range of small molecules, but nonetheless slightly too heavy to be considered one. It has 12 heteroatoms with free pairs of electrons readily capable of hydrogen bond formation, while 26 protons within the molecule could potentially form hydrogen bonds. Unlike PROTAC-FCPF, the linker in this PROTAC is considerably longer, hydrophobic, and flexible, making the molecule much less planar, even though Thalidomide has predominantly atoms in sp^2 configuration, while the structure of the warhead is considerably planar, except for the secondary amine substituent connecting the two rings. The Total Polar Surface Area was not determined for this molecule either, but with the information known of it, it is possible to estimate that its profile is closer to that of a small molecule and has higher probabilities to be taken up by cells, which is probably the case, given that this PROTAC is active 10-fold lower concentrations, compared to PROTAC-FCPF.

PROTAC-O4I2 degraded both $SF3B1^{WT}$ and $SF3B1^{K7006}$ both in a concentration and time-dependent manner. Although it was proved that the free warhead O4I2 had activity in cancer cells impacting in the rate of RNA synthesis, neither of the free ligands induced protein degradation, unlike PROTAC-O4I2. The degradation was proved to be dependent on a fully functional CRBN-based E3 ligase complex, for the lack of one of the members of the complex, CUL4A, led to failure in degradation of the POI, while the depletion of the protein was independent of the absence of other E3 ligases (VHL and MDM2).

The Hook effect was also observed in this PROTAC at concentrations equal to or higher than 10 µM. Only one CRBN recruiter was used, thus it is unclear whether SF3B1 can better be degraded using other E3 ligases, which may hint how good or bad the protein-protein interactions, and therefore the α cooperativity value are. Yet, for this PROTAC the FRET assay was carried out to study the interactions of the proteins involved. Even though the α cooperativity value was not calculated, it was observed that the point of maximum proximity between the proteins is 1 µM, the most effective concentration. However, the FRET assay may have limitations such as the quenching of the fluorophores. A nonspecific, interfering effect of a component in the sample matrix on wither the donor or the acceptor of the energy may alter the ratio, and therefore lead to the wrong calculation (Liu et al., 2020). Another technique would have been useful as a complement, such as the Fluorescence Polarization assay, which has already been used to prove that a PROTAC can degrade the POI despite negative α cooperativity values (Liu et al., 2020).

It was also demonstrated that the process triggers ubiquitination of the protein of interest, that inhibition of the proteasome led to accumulation of the ubiquitinated protein, and inhibition of earlier stages of the UPS also led to failure of protein degradation. PROTAC-O4I2

degraded the target protein with a calculated DC_{50} of 0.244 µM, discriminating other proteins that interact with the free ligand O4I2.
The antiproliferative activity of PROTAC-O4I2 was researched on cells, proving that PROTAC-O4I2 is remarkably more cytotoxic than the free ligand, and slightly less potent than Pladienolide B, a known SF3B1 inhibitor. However, PROTAC-O4I2 was importantly more potent in cells transfected to overexpress $SF3B1^{WT}$ and moderately more potent in cells expressing the mutant $SF3B1^{K700E}$.
In vivo activity of PROTAC-O4I2 was indeed investigated but falls beyond the scope of this doctoral thesis (Gama-Brambila, et al., 2021).
No optimization work of the ligand was carried out. It remains to be researched on whether modifications in the length and composition of the ligand may affect positively or negatively on the activity of the PROTAC.

5. CONCLUSIONS

- Two new PROTACs (degraders) were successfully developed to degrade Proteins with relevance in clinical applications, which had not previously been degraded in the PROTAC field, using small molecules as warheads, that had not been previously used in the field.
- The FCPF-perfluoroaromartic compound system proved to be an effective approach to degrade proteins where the tetrapeptide Phe-Cys-Pro-Phe was engineered into, making it susceptible to covalent bond formation with the PROTAC and also to proteasomal degradation.
- PROTAC-FCPF was successful in degrading engineered proteins $Cas9^{FCPF}$, $dCas9^{FCPF}$, $Cas12^{FCPF}$, and $Cas13^{FCPF}$ in a time and concentration-dependent manner, by triggering the Ubiquitin-Proteasome System.
- The calculated DC_{50} average value of PROTAC-FCPF from three different cell lines is around 150 nM over 24 hours treatment.
- The mechanism of PROTAC-FCPF was proved to be triggered by ubiquitination of the target proteins, thus fulfilling the mechanistic requirements of PROTACs.
- The PROTAC-FCPF-mediated degradation was close to full depletion and was demonstrated to be sustained for up to 72 hours in cancer cells.
- The PROTAC-FCPF-mediated degradation of $Cas9^{FCPF}$ resulted in a reduction of off-target mutations of from 12.1% to 3.56%.
- The activity of PROTAC-FCPF was proved to be dependent on the complete, therefore, fully functional DDB1-CUL4A-Rbx1-N8-CRBN E3 ligase complex.
- The protein degradation activity of PROTAC-FCPF was interrupted when inhibitors for three different stages of the Ubiquitin-Proteasome System were used.
- It remains to be tested what the impact on the protein degradation activity would be if a linker between the perfluoroaromtic moiety and lenalidomide is modified. Should

it be the case, it remains necessary to optimize the length and composition of the linker.

- The activity and efficacy of PROTAC-FCPF on proteins acting in more than one-event and with different turnover rates remains to be researched on.
- High Through Put Screening and Proteomics were successfully used to repurpose an already existing small molecule as a warhead to develop a PROTAC to target $SF3B1^{WT}$ and the mutant $SF3B1^{K700E}$, proteins of clinical relevance.
- The free ligand O4I2 was proved to increase the RNA synthesis rate in cancer cells.
- PROTAC-O4I2 succeeded on degrading SF3B1 in a concentration and time-dependent manner.
- SF3B1 degradation mediated by PROTAC-O4I2 was successfully tested in four different cancer cell lines, reaching almost full depletion over 24 hours of treatment.
- The calculated DC_{50} of PROTAC-O4I2 in $K562^{FLAG\text{-}SF3B1}$ cells was 0.244 µM over 24 hours of treatment, with close-to-full depletion of the protein.
- Degradation of SF3B1 by PROTAC-O4I2 resulting in inhibition of splicing of DNAJB1 at a concentration of 500 µM after 18 hours of treatment.
- The degradation of SF3B1 by PROTAC-O4I2 was demonstrated to depend on ubiquitination and the integrity, therefore full functionality, of the DDB1-CUL4A-Rbx1-N8-CRBN E3 ligase complex.
- The degradation activity of PROTAC-O4I2 was proved to be independent of VHL and MDM2 E3 ligases.
- PROTAC-O4I2 failed to degrade SF3B1 in the presence of an NEDD8-Activating Enzyme inhibitor (MLN9425), confirming the requirement of a fully functional CRBN E3 ligase complex.
- Antiproliferative activity of PROTAC-O4I2 was demonstrated to be much higher than that of the parental warhead, and lower than the SF3B1 inhibitor Pladienolide B. K562 cells over expressing SF3B1 are more sensitive to PROTAC-O4I2 (IC_{50} value of 62.9 ± 13.5 nM) than to Pladienolide B (IC_{50} value of 133.5 ± 8.6 nM).
- PROTAC-O4I2 not only succeeded in degrading $SF3B1^{WY}$, but also in degrading the clinically relevant $SF3B^{K700E}$ mutant.
- K562 overexpressing the $SF3B1^{K700E}$ mutant were slightly more sensitive to PROTAC-O4I2 with an IC_{50} value of 90.2 ± 24.5 nM, compared to Pladienolide B, with an IC_{50} value of 116.1 ± 17.5 nM.
- The apoptosis-inducing activity of O4I2 was comparable to that of Pladienolide B, but unlike the latter, was sensitive to the presence or absence of CRBN E3 ligase.
- Further research on the optimization of length and composition of the linker remains to be conducted.

6. MATERIALS AND METHODS

6.1. Materials

The following tables list all the consumables and disposables used for this doctoral work.

Table 1: plastic ware and disposable supplies

Product Name	Specifications	Provider
Cell culture flask	25 cm^2	Greiner Bio-One
Cell culture flask	75 cm^2	Greiner Bio-One
Falcon tubes	15 mL	Corning
Falcon tubes	50 mL	Corning
Filter Pipette tips	0.2-10 µL	Starlabs
Flat bottom transparent well plate	Greiner Bio-One	Greiner Bio-One
Flat bottom transparent well plate	12 wells	Greiner Bio-One
Flat bottom transparent well plate	24 wells	Greiner Bio-One
Flat bottom transparent well plate	48 wells	Greiner Bio-One
Flat bottom transparent well plate	96 wells	Greiner Bio-One
Flat transparent bottom black well plate	96 wells	Greiner Bio-One
Flat transparent bottom black white plate	96 wells	Greiner Bio-One
Micropipette tips	0.5-10 µL	Starlabs
Micropipette tips	2-200 µL	Starlabs
Micropipette tips	100-1000 µL	Starlabs
Microreaction tubes	0.5 mL	Greiner Bio-One
Microreaction tubes	1.5 mL	Greiner Bio-One
Microreaction tubes	2 mL	Greiner Bio-One
Microreaction tubes (PCR)	200 µL	Greiner Bio-One
Microreaction tubes safe lock	1.5 mL	Eppendorf
Microreaction tubes safe lock	2 mL	Eppendorf
Plastic petri dish	96 mm	Greiner Bio-One
PVDF membrane	0.45 µm cut off	GE Healthcare Life Sciences
Serological pipettes	2 mL	Greiner Bio-One
Serological pipettes	5 mL	Greiner Bio-One
Serological pipettes	10 mL	Greiner Bio-One
Serological pipettes	25 mL	Greiner Bio-One
Serynge	50 mL	BD
Serynge Filters	0.22 µm	Starlab
Serynge Filters	0.45 µm	Starlab
Whatmann Filter Paper		GE Healthcare Life Sciences

Table 2: chemicals and reagents

Product Name	Specifications	Provider
6-aminohexanoic acid	minimum 99%	Carl Roth
Agaorse Ultra pure	for molecular biology	Sigma Aldrich
Ammonium persulfate	≥98 %, extra pure	Carl Roth
Aprotinin	3.0 PEU/mg	Carl Roth
BlueStar Plus Prestained Protein Marker	10-240 kDa	Nippon Genetics
Boric Acid	ACS reagent Ph.Eur. ≥99.8%	Sigma Aldrich
Bovin Serum Albumin Fraction V protease-free	≥98 %, for protein analysis and molecular biology	Carl Roth
Bradford reagent	for 0.1-1.4 mg/ml protein	Sigma Aldrich
Bromophenol Blue sodium salt	powder for molecular biology	Sigma Aldrich
Calcium chloride	≥99 %, Ph.Eur., USP	Carl Roth
Chloroform	≥99 %, p.a.	Carl Roth
Ethanol	≥99,8 %, p.a.	Carl Roth
Glacial acetic acid	ACS reagent Ph.Eur. ≥99.8%	Merck
Glycerine	≥98% water-free	Carl Roth
Glycine	≥99 %, Blotting Grade	Carl Roth
Hydrochloric acid	37% Ph.Eur.	Carl Roth
Hydrogen Peroxide	Ph.Eur., stabilised 30%	Carl Roth
Isopropanol	≥99,8 %, p.a., ACS, ISO	Carl Roth
Lipofectamine 3000 Transfection Reagent	N/A	Thermo Fisher Scientific
Lucigen QuickExtrac DNA Extraction Solution	N/A	Bioenzyme
Magnesium chloride	≥99 %, Ph.Eur., USP, BP	Carl Roth
Magnesium sulfate	≥99 %, Ph.Eur., USP, BP	Carl Roth
Methanol	>99.5 Ph.Eur.	Carl Roth
Milk Powder	Blotting grade	Carl Roth
MG132	>98%	Biomol
MLN4924	>98%	Biomol
MTT	Sigma Aldrich	M2128
Na_2 EDTA $2H_2O$	≥99 %, p.a., ACS	Carl Roth
Paraformaldehyde	DAC, 95.0-100.5%	Sigma Aldrich
Pepstatin A	≥98%	Carl Roth
Pladienolide B	>98%	Biomol
PMSF (Phenylmethylsulfonylfluoride)	≥99 %, for biochemistry	Carl Roth
Ponceau S	for histology and electrophoresis	Carl Roth
Potassium chloride	>99% Ph Eur., USP, BP	Carl Roth
Potassium dihydrogen phosphate	≥99 %, p.a., ACS	Carl Roth
PYR41	>98%	Biomol
QIAzol	200 mL	Thermo Fisher Scientific

qPCRBIO Sygreen Mix Lo-ROX	50x 1 mL	Nippon Genetics
Rotiphorese (acrylamide solution)	30%	Carl Roth
SDS powder	>99% Blotting-Grade	Carl Roth
Sodium Azide	99%, p.a.	Carl Roth
Sodium chloride	≥99,5 %, p.a., ACS, ISO	Carl Roth
Sodium fluoride	≥99 %, p.a., ACS, ISO	Carl Roth
Sodium hydrogen carbonate	≥99 %, Ph.Eur., extra pure	Carl Roth
Sodium hydrogen phosphate	≥99 %, p.a., ACS, anhydrous	Carl Roth
Sodium hydroxyde	ACS reagent Ph.Eur. ≥98%	Sigma Aldrich
Sodium pyrophosphate	≥99 %, p.a.	Carl Roth
Sodium Vanadate	≥99 %, pure	Carl Roth
SuperSignal West Pico Plus Chemiluminischent Substrate	200 mL	Thermo Fisher Scientific
SYBR Safe	10 000x in DMSO	Thermo Fisher Scientific
SYPRO Orange	5000x in DMSO	Thermo Fisher Scientific
TEMED	≥98.5% p.a.	Carl Roth
Thalidomide	>98%	Biomol
Tris (basic)	≥99.9% p.a.	Carl Roth
Triton X-100	100 mL	Sigma Aldrich
Tween-20	Ph.Eur.	Carl Roth
Urea	≥995 %, p.a., BioScience Grade	Carl Roth

Table 3: Cell culture media, supplements and reagents

Product Name	Specifications	Provider	Preparation/Stock
DMEM with Glutamax	500 mL	Thermo Fisher Scientific	W/O FCS 10%, P/S 1% v/v
DMSO 100 mL	BioUltra, for molecular biology, ≥99.5% (GC)	Sigma Aldrich	N/A
DPBS	500 mL	Thermo Fisher Scientific	N/A
Glutamax	100 mL	Thermo Fisher Scientific	N/A
Opti-MEM	500 mL	Thermo Fisher	N/A
RPMI-1640 with glutamax	500 mL	Thermo Fisher	P/S 1% v/v
Streptomycin/Penicillin	10 000 U*µg/mL	Thermo Fisher Scientific	N/A
TrypLE™ Express	100 mL	Thermo Fisher Scientific	N/A

Table 4: list of Antibodies

Product Name	Provider	Preparation/Stock
Actin	Santa Cruz Biotechnology	1:1 000 in BSA 5% in TBS-T with NaN_3 0.02% w/v (WB)
Cas9	Cell Signaling	1:1 000 in BSA 5% in TBS-T with NaN_3 0.02% w/v (WB)
CRBN	Thermo Fisher Scientific	1:1 000 in BSA 5% in TBS-T with NaN_3 0.02% w/v (WB)
FLAG	Cell Signalling	1:1 000 in BSA 5% in TBS-T with NaN_3 0.02% w/v (WB)
SF3B1	Cell Signaling	1:1 000 in BSA 5% in TBS-T with NaN_3 0.02% w/v (WB)
Ubiquitin	Cell Signaling	1:1 000 in BSA 5% in TBS-T with NaN_3 0.02% w/v (WB)

Table 5: list of Oligonucleotides

Target Gene Name	Forward Sequence	Reverse Sequence
DNAJB1	GAACCAAAATCACTTTCCCCAAGGAAGG	AATGAGGTCCCCACGTTTCTCGGGTGT
AAVS1 on target	TGGCTACTGGCCTTATCTCACAGG	CTCTCTAGTCTGTGCTAGCTCTTCCAG
AAVS1 off target	ACTCTTCTACCTTGCACGCCTTTGC	CCTGCCTCCCATGCAAACAGTGTC
	siRNA	
MDM2 (122296)	GCCAUUGCUUUUGAAGUUAtt	UAACUUCAAAAGCAAUGGCtt
VHL (138745)	GGAGCGCAUUGCACAUCAAtt	UUGAUGUGCAAUGCGCUCCtg
CUL4A (139184)	GCGAGUACAUCAAGACUUUtt	AAAGUCUUGAUGUACUCGCtc
DDB1 (10596)	GGUUGGUCUCUCAAGAACCtt	GGUUCUUGAGAGACCAACCtc

NOTE: Primers were purchased from Eurofins Genetics, and siRNA from Thermo Fisher Scientific

AAVS1 on target sequence: GGGAGGGAGAGCTTGGCAGG**GGG** (PAM sequence is in bold)
AAVS1 off target sequence: GGGAAGGGGAGCTTGGCAGG**TGG** (PAM sequence is in bold and expected mutations in red)

Table 6: list of Recombinant DNA

Cell line	Provider
CRISPR-Cas9 CRBN double nickase knockout plasmid	Santa Cruz Biotechnology
pC014 - LwCas13a-msfGFP (91902)	Addgene
pcDNA-dCas9-HA (61355)	Addgene
pCDNA3.1-FLAG-SF3B1-WT	Addgene
pCDNA3.1-FLAG-hSF3B1-K700E	Addgene
plenti-px330-CRBN-T1-pGK-Pur (107382)	Addgene
plenti-px330-CRBN-T2-pGK-Pur (107383)	Addgene
Plenti-px330-CRBN-T1-pGK-Pur	Addgene
Plenti-px330-CRBN-T2-pGK-Pur	Addgene
pY018 (pcDNA3.1-hPdCpf1) (69990)	Addgene

Table 7: list of sgRNA

Cell line	Provider
Anti-CRISPR Protein ACRIIA4 (113037)	Addgene
AAVS1 (128119)	Addgene
CMV-SpyCas9 (113037)	Addgene

Table 8: list of Cell Lines

Cell line	Provider
K562	ATCC, USA
HeLa	ATCC, USA
HepG2	ATCC, USA
Human Fibroblasts	ATCC, USA
Hek293T	ATCC, USA

Table 9: list of Kits

Name of the Kit	Provider
Annexin V Apoptosis Detection kit	Thermo Fisher Scientific
Beetle Juice Kit Kit	PJK, Germany
EZClike global RNA Synthesis assay kit	BioVision
EnGen Mutation Detection Kit	New England BioLabs
ENLITEN® ATP Assay System	Promega
FastGene Scriptase Basic cDNA-Kit	Nippon Genetics
FLAG Immunoprecipitation kit	Sigma Aldrich
Immunoprecipitation kit DYKDDDK (FLAG) Tag immunomagnetic bead	Biozym
ProtoScript First Strand cDNA synthesis Kit	NEB

Table 10: list of Buffers and Solutions

Buffer Name	Components	Concentration
Annexin V Binding Buffer pH 7.4	HEPES NaCl KCl $MgCl_2$ $CaCl_2$	10 mM 150 mM 5 mM 1 mM 1.8 mM
Anode Buffer	Methanol Tris Distilled water to final volume	10% (v/v) 0.3 M
Blocking Buffer for ICC	Goat Serum BSA Triton X-100 DPBS to final volume	5% (v/v) 1% (w/v) 0.3% (v/v)
Cathode Buffer	Methanol Tris 6-Aminohexanoic acid Distilled water to final volume	10% (v/v) 0.25 M 40 mM
FACS Buffer	BSA EDTA In PBS	1% w/v 2 mM
Gel Loading Buffer 5x	Tris SDS Glycerol β-mercaptoethanol Bromophenol blue Distilled water to final volume	10 mM 4% (w/v) 20% (v/v) 200 mM 0.2% (w/v)
Immunoprecipitation Buffer (pH 7.5)	Tris HCl NaCl Na_2EDTA EGTA Triton X-100 $Na_4P_2O_7$ β-glyceropohosphate Na_3VO_4 Leupeptin PMSF	20 mM 150 mM 1 mM 1 mM 1% 2.5 mM 1 mM 1 mM 1 µg/mL 1 mM
Immunoprecipitation Elution Buffer pH 7.4	Glycine HCl NaCl	0.1 M 1.15 M
Immunoprecipitation Lysis Buffer	Tris HCl NaCl Nonidet P-40 EDTA NaF Na_3VO_4 Pepstatin PMSF Aprotinin	20 mM 150 mM 1% (w/v) 2 mM 5 mM 1 mM 10 µg/mL 10 µM 3 µg/mL
Immunoprecipitation Wash Buffer pH 7.4	Tris HCl NaCl	50 mM 150 mM

Luciferase Lysis Buffer	Tris phosphate EGTA Triton X-100 Glycerol (Filter through 0.45 µm sterile filter) DTT (freshly added prior use)	25 mM 4 mM 1% (w/v) 10% (w/v) 2 mM
Lysis Buffer for Protein Extraction	Aprotonin PMSF Pepstatin $Na_4P_2O_7$ $10H_2O$ Na_3VO_4	3 µg/mL 0.1 mM 1 µg/mL 100 µM 0.1 mM
PBS 10x	NaCl KCl KH_2PO_4 Na_2HPO_4 $2H_2O$ Distilled water to final volume	1.37 M 26.8 mM 14.7 mM 65.2 mM
Ponceau S	Ponceau powder Methanol Acetic acid (glacial) Distilled water to final volume	0.25% (w/v) 40% (v/v) 15% (v/v)
SDS PAGE Resolving Gel (10%)	Tris 1.5 M (pH 8.8) Acrylamide mix 30% SDS 10% TEMED APS 10% (w/v) Distilled water	25% (v/v) 33% (v/v) 1% (v/v) 0.04% (v/v) 1% (v/v) 40% (v/v)
SDS PAGE Running Buffer	Tris Glycine SDS Distilled water to final volume	25 mM 250 mM 1% (w/v)
SDS PAGE Stacking Gel	Tris 1 M (pH 6.8) Acrylamide mix 30% SDS (10%) TEMED APS 10% (w/v) Distilled water	12.5% (v/v) 17.5% (v/v) 1% (v/v) 0.1% (v/v) 1% (v/v) 68% (v/v)
TBS-T	NaCl KCl Tris powder Tween 20 Distilled water to final volume	0.14 M 1.57 mM 24.7 mM 0.1% (v/v)
Urea 6M Buffer	Urea powder Sodium fluoride Triton X-100 EDTA Na_2 H_2O Distilled water to final volume	6 M 5 mM 0.5% (v/v) 1 mM

Table 11: list of Machines and Devices

Name of device or machine	Provider
AccuBlock Tm Digital Dry Bath	Labnet International Inc., USA
Analytical Balance 440-33N	Kem und Sohn, Germany
Analytical Balance	Sartorius, Germany
BD FACSCalibur	BD, Germany
Biorevo Fluorescence Microscope BZ9000	Keyence, USA
Centrifuge 5415R	Eppendorf, Germany
Centrifuge 5702	Eppendorf, Germany
Centrifuge 5804	Eppendorf, Germany
Guava easyCyte HT sampling flow cytometer	Guava Technologies, USA
HERA cell 150i Cell Incubator	Thermofisher Scientific, Germany
Micropipettes (0.2-2, 0.5-10, 2-20, 10-100, 20-200, and 100-1000 µL)	Eppendorf, Germany
Microscope CKX41	Olympus Life Science, Germany
NanoDrop 2000 Spectrophotometer	Thermofisher Scientific, Germany
Pipetteboys	Integra Biosciences, Germany
Real Time Thermal Cycler qTower	Analytik Jena AG, Germany
TECAN Infinite F200 Pro	Tecan, Germany
TECAN Ultra Plate Reader	Tecan, Germany
Thermomixer Comfort	Eppendorf, Germany
Trans-Blot Turbo Transfer System	Bio-Rad
VIAFLO ASSIST automated multi-channel pipettes (12.5 and 1250 µL)	Integra Biosciences, Germany
Vortex-Genie®2	Scientific Industries Inc., USA
Water Bath	GFL, Germany

Table 12: list of Softwares

Name of the Software	Provider
Adobe Acrobat Reader DC	Adobe and Microsoft, USA
Aida Image	
CellQuest Pro analysis software	BD, Germany
EndNote X9	Adept Scientific PLC
GraphPAD PRISM 8	GraphPad Software Inc., USA
FIJI (Image J)	National Institutes of Health, USA
Image Lab	Bio-Rad, Germany
Microsoft Office	Microsoft, USA
NanoDrop 2000 Software	Thermofisher Scientific
qPCRsoft 3.1	Analytik Jena, Germany
Graph Prism 6	GraphPad

6.2. Cell culture

6.2.1. Cell lines maintenance

Thawing

a. Cells ere thawed by pipetting up and down, mixing with warm culture medium. Once completely thawed the cell suspension was immediately transferred to a conical 15 mL centrifuging tube that contains 8 mL of pre-warmed culture medium,
b. The cell suspension was centrifuged for 5 minutes at 300 G and at room temperature,
c. A glass Pasteur Pipette was attached to the tubing of a vacuum pump, and the supernatant in the conical tube was removed with it,
d. Using a serological 10 mL pipette, this volume of pre-warmed cell culture medium was added to a new 75 cm^2 cell culture flask
e. Then the cell pellet was re-suspended with 5 mL of pre-warmed cell culture medium and the entire suspension was transferred to a culture flask,
f. Last, the cell culture flask was place in the cell incubator at 37 ˚C, under a humified atmosphere with CO_2 5%.

The cells were kept in culture until the confluence reached 75%. At that point, cell passages took place as follows:

Passaging:

a. The culture flask was tilted to remove old culture medium with a Pasteur pipette and a vacuum pump, being careful not to scratch the flask's surfaces,
b. The cells were washed with 5 mL of pre-warmed DPBS, tilting the flask and letting the DPBS slide from the surfaces. The flask was moved gently to wash the cells, and DPBS removed using a glass Pasteur pipette and a vacuum pump,
c. To detach the cells, 3mL of trypsin were added slowly and trying to cover all the flask's bottom. The flask was incubated for 5 mins at 37 °C and CO_2 5%,
d. The culture flask was shaken until all surfaces were clear (without cells attached),
e. Pre-warmed medium (5 mL) were added to the trypsin to inactivate it,
f. The mix was then transferred to a conical 15 mL centrifuging tube, and the suspension centrifuged for 5 mins at (300G) at room temperature,
g. The supernatant was discarded with a Pasteur pipette and a vacuum pump,
h. Roughly 15 mL of pre-warmed cell culture medium were added into the culture flask,
i. The cell pellet was re-suspended with 5 mL of DMEM medium, pipetting gently in and out several times,
j. An approximate volume of 200 µL of the suspension were transferred into the cell culture flask,
k. The cells were incubated at 37 °C and CO_2 5% for 3 days (until confluent again).

6.2.2. Cell seeding for assays

Steps a. to e. from last procedure were repeated,

f. A volume of 10 µL were taken from the cell suspension and pipetted between a Neubauer Chamber and a glass cover slide, and the total cell count was determined, while the rest of the cell suspension was being centrifuged in the conditions previously mentioned,
g. The supernatant was removed as mentioned before, and the cell pellet was re-suspended in a volume such, that the cell density would be 1 000 cell/µL,
h. The volume for 100 000 cells was used to re-start the main culture, while the rest of the suspension was used to seed cells for the needed experiments.

The cell densities used for the assays were as follows:

- Wells of a 6 well plate: 300 000 cells per well (transfection, samples for WB, FACS, etc.)
- Wells of a 12 well plate: 150 000 cells per well
- Wells of a 24 well plate: 75 000 cell per well

6.2.3. Transfection

The reagent used for this work was Lipofectamine 3000 by Thermo Fisher Scientific. The procedure has no significant modifications to those recommended by the manufacturer. Briefly,

a. Old cell culture was removed from the wells with the cells to be transfected,
b. The recommended volume of DMEM FCS 10% and P/S 0% was added into the wells,
c. In a microreaction tube, the recommended volume of Opti-MEM was pipetted and mixed reagent P3000 and the maximum amount of recombinant DNA suggested by the company for the size of the well in use,
d. The mix was let to settle down for 5 min, during which the second mix was prepared. The same amount of Opti-MEM was pipetted in a separate microreaction tube and mixed with the recommended volume of Lipofectamine 3000 reagent. After 5 minutes, both mixed were combined and mixed thoroughly yet, very gently. And the new mix was let to settle down for another 10 minutes,
e. After the incubation time, the recommended volume was pipetted into the medium in the wells, and the well plate was place back in the incubator at the same conditions previously described overnight,
f. First thing the day after, the cell culture medium was exchanged for fresh medium with P/S, and the cells let recover for 24 h before any further step, regardless the type of assay.

For overexpression with plasmids or knockdown with siRNA, the cell density used was 300 000 cells per well of a 6 well plate. In this format, the volume of both transfected reagents was 6 µL each per preparation and 2 500 ng siRNA or 2 000 ng of plasmid.

6.3. Techniques and Assays

6.3.1. MTT Cell Viability Assay

The steps a. to d. from Section 6.2.1 Cell lines maintenance. "Passaging" were repeated.

e. The cell pellet was resuspended in a volume appropriate to have a concentration of 66.66 cells/µL (10 000 cells in 150 µL),
f. Using this cell suspension and a multichannel pipette 10 000 cells were seeded per well of a 96 well plate,
g. Cells were incubated for 24 hours at 37 °C and a partial CO_2 pressure of 5%,
h. The medium was removed and replaced by 100 µL of fresh medium mixed with the intended treatment,
i. The well plate was placed back in the incubator at the same conditions for the intended duration of the treatment,
j. A solution of MTT 50 mg/mL was prepared in fresh DMEM FCS 1% and P/S 1%. Due to the poor solubility of the reagent, the solution must have been sonicated for a couple of minutes,
k. The old medium with the treatment solution was removed from each well and substituted with 100 µL of MTT solution in each well,
l. The plate was placed back in the Incubator for 20 minutes at 37 °C and at a partial CO_2 pressure of 5%, and checked every 5 min until visible purple formazan precipitates appeared at the bottom of some wells,
m. The MTT solution was removed from each well very carefully, to avoid removal of formazan precipitates,
n. Using a multichannel pipette 100 µL of DMSO were pipetted into each well,
o. The plate was shaken for 1 min at 3.5mm amplitude in the Tecan plate reader,
p. The TECAN reader was set to absorbance at 595 nm with the flashes, reading from the top.

6.3.2. FITC-FCPF Staining

a. HeLa cells were transfected according to the procedure described earlier in this work (6.2.3 Transfection) with $Cas9^{FCPF}$, and $Cas9^{GFP}$ (separately) for 24 hours,
b. The old cell culture medium was removed and replaced with fresh DMEM FCS 10% and P/S 1%, to let the cells recover for another 24 hours,
c. The transfected cells were treated with FITC-FCPF 10 µM, by adding the chemical directly into the cell culture medium,
d. After 2 hours the treatment was removed using a glass Pasteur pipette and a vacuum pump. Immediately, the cells were washed by adding pre-warmed DPBS, moving the well plate gently in all directions. DPBS was removed using a glass Pasteur pipette and a vacuum pump,
e. Step d. was repeated twice more,
f. The cells were last kept in DPBS with FSC 1% for observation under the fluorescence microscope.

This procedure was repeated for WB and FACS analysis. The procedures of these assays are later described in this section.

6.3.3. *In vitro* Ubiquitination Assay (for Cas proteins)

a. Overexpression and Purification of FLAG-CRBN^{WT} and FLAG-CRBN^{FCPF}

- HeLa cells were transfected with either FLAG-CRBN^{WT} or FLAG-CRBN^{m} following the procedure mentioned before (See 6.2.3. Transfection),
- FLAG-tagged proteins were isolated and purified from the transfected HeLa cells using the FLAGIPT1 kit, following the manufacturer's instructions as briefly follows,
- A volume of 200 µL of Anti-FLAG M2 affinity gel (from the mentioned kit) was added and mixed with 500 µL of the cell lysate, and the mix was incubated overnight at 4 ˚C,
- The preparation was washed three times with Immunoprecipitation Wash buffer (see Table 10: list of Buffers and Solutions),
- The FLAG-tagged proteins were eluted using 100 µL of the Immunoprecipitation Elution Buffer (see Table 10: list of Buffers and Solutions),
- Last 900 µL of Immunoprecipitation Wash buffer were added.

b. Overexpression of Cas9^{WT} and Cas9^{FCPF} and Ubiquitination Assay

- HeLa^{CRBN} KO cells were transfected with either Cas9^{WT} or Cas9^{FCPF} plasmids as previously described in section 6.2.3. Transfection,
- Immunoprecipitation Buffer was prepared right before use (See Table 10: list of Buffers and Solutions),
- Transfected HeLa^{CRBN} KO cells were lysed with Immunoprecipitation Buffer, half of each lysate was pipetted out and transferred to separate micro reaction tubes,
- Lenalidomide was added to one set of lysates to a concentration of 100 µM as a pre-treatment. This was let incubate for 30 min,
- Either purified FLAG-CRBN^{WT} or FLAG-CRBN^{m} was added separately to HeLa^{CRBN} KO Cas9^{WT}, HeLa^{CRBN} KO Cas9^{FCPF}, HeLa^{CRBN} KO Cas9^{WT} lenalidomide-pretreated and HeLa^{CRBN} KO Cas9^{FCPF} lenalidomide pre-treated,
- The ubiquitination rates were indirectly measured the luciferase-based ENLITEN ATP Assay System kit, following the manufacturer's instructions.

NOTE: FLAG-CRBN^{WT} and FLAG-CRBN^{m} were expressed and purified from in K562^{WT} cells for the experiments of PROTAC-O4I2.

6.3.4. T7 Endonuclease I Assay

a. HeLa cells were transfected as described before (6.2.3. Transfection) to overexpress either Cas9^{WT} or Cas9^{FCPF}, together with ACRIIA4 and sgRNA against AAVS1. The transfection took place overnight, with 24 hours of recovery after,
b. Upon transfection, PROTAC-FCPF was added directly into the culture medium to a concentration on 1 µM, moving the well plate gently but thoroughly to distribute the compound,

c. After 24 hours, the culture medium with PROTAC-FCPF was removed and the cells washed with pre-warmed DPBS, removing the supernatant with a glass Pasteur pipette and a vacuum pump after,
d. Cells were trypsinized with 300 µL of TrypLE™ Express for 5 min in the cell culture incubator,
e. Trypsin was inactivated by the addition of 1.7 mL of DMEM FCS 10% and P/S 1%. The cell suspension was centrifuged at 300 G for 5 min at room temperature. Once finished, the supernatant was aspirated with a vacuum pump,
f. The cell pellet was lysed with 500 µL of Lucigen QuickExtract DNA Extraction Solution, to extract the DNA, then vortexed for 15 s,
g. The lysate was then heated up to 65 ˚C for 6 min, followed by a vortexing step of 15 s,
h. Last, the preparation was heated up to 98 ˚C for 2 min, after which the material can be stored at -70 ˚C or used immediately.
i. The AAVS1 sequences were amplified with the following PCR mix:

-Q5 Hot Start high-Fidelity 2x Master mix (12.5 µL)
-Forward and reverse primers (10 µL each)
-Genomic DNA (100 ng)
-Nuclease-free water (to a total of 25 µL)

j. Amplification took place with the following cycle:

-98 ˚C for 30 min
40 cycles of
    -98 ˚C 5 min
    -70 ˚C for 10 min
    -72 ˚C for 20 min
-72 ˚C for 2 min

k. The following procedure corresponds to heteroduplexes between the PCR products what have and do not have mutations:

-PCR product 5 µL
-10x NEBuffer2 2 µL
-Nuclease-free water 12 µL

l. This mixture underwent the following denaturation program: 95 ˚C for 5 min, and then the temperature was decreased to 85 ˚C in a rate of 2 ˚C/sec. Then the mixture was cooled down to 25 ˚C in a rate of 0.1 ˚C/sec,
m. To the resulting product 1 µL of EnGen T7 Endonuclease I was pipetted into the annealed product. This new mixture was incubated at 37 ˚C for 15 min,
n. Protein K was added (1 µL) to the preparation, followed by an incubation step of 5 min.

The final product was run in an agarose/TEA gel 2% at 90 mV for about an hour in TEA buffer.

6.3.5. Luciferase Assay

a. Hek293 OCT4 were seeded with a density of 20 000 cells per well in a white 96 well plate as previously descried in this work in 6.2.2. Seeding for assays,
b. After 24 hours, cells were treated with a concentration gradient of either O4I2 or biotinylated O4I2. The gradient was achieved by applying most concentrated solution in DMEM FCS 10% and P/S 1%, in a row of wells within the plate, and then a dilution series was made leaving the last row as non-treated,
c. After 48 hours of treatment, the cell culture medium with the treatment was aspirated using a glass Pasteur pipette,
d. The washing step was repeated twice more,
e. The cells were lysed with 50 µL per well of Luciferase Lysis buffer. It is important that in this step air bubbles are avoided as much as possible, and that this step is done as quickly as possible,
f. Beetle juice (luciferin and ATP was pipetted into each well in a volume of 100 µL per well, using a multichannel pipette,
g. After 5 minutes of incubation, the plate was placed in the TECAN reader for measurement.

6.3.6. Detection of Newly Synthesized RNA

a. Fibroblasts were seeded in 5 wells of a 24 well-plate with a count of 100 000 cells per well, as previously described in 6.2.2. Seeding for assays,
b. The day after, O4I2 was added directly into the cell culture media to final concentrations of 5, 10 and 20 µM. The same volume of DMSO required for the well with O4I2 20 µM was pipetted into one of the wells to be the non-treated. Last, the remaining well was purposed as positive control by treating the cells with Actinomycin D provided in the kit as a 100x concentrate. The plate was placed back into the cell culture incubator, and treatments held for 4 hours,
c. After that, the cells in all wells were incubated with EZClick RNA label 100x, provided in the kit (5-ethynyl uridine), following the manufacturer's instructions of the EZCLick RNA label Kit, followed by a 1-hour incubation step in the cell culture incubator,
d. The cells were washed with 100 µM of pre-warmed DPBS, then fixed with 100 µL of fixative solution for 15 minutes at room temperature,
e. After removal of the fixative solution, the cells were washed once with 200 µL of the Washing Buffer provided in the kit,
f. The Washing Buffer was removed and replaced with 100 µL of Permeabilization Buffer for 10 minutes at room temperature,
g. The Reaction cocktail that consists of a copper reagent, fluorescent azide, a reducing reagent (all included in the kit), and hoechst33342 (5 µg/mL) was added (100 µL per well) as instructed by the manufacturer, followed by an incubation step, at room, temperature, of 30 minutes and covered from light,
h. Finally, the cells were washed with 200 µL of the Washing Buffer provided in the kit.

At this point, the preparations can be observed and imaged under the fluorescence microscope.

In the case of FACS, the cells were trypsinized before the fixation step (step d. of this protocol). The fixed and permeabilized cells were resuspended at the end in DPBS for sample take up by the FACS machine.

6.3.7. FLAG-tagged Protein Purification and Determination of Denaturation Temperature

a. Hek293T were seeded to a total count of 300 000 cells per well in a 6 well plate as described in 6.2.2. Seeding for assays,
b. The day after the cells were transfected with either FLAG-SF3B1^{WT} or FLAG SFB3B1^{K700E} as previously described in 6.2.3 Transfection,
c. After 24 hours or recovery from transfection, the cells were lysed with 200 µL of Immunoprecipitation Lysis Buffer (See Table 10: list of Solutions and Buffers),
d. From the Immunoprecipitation Kit -DYKDDDDK（Flag®）Tag Immunomagnetic Beads 20 µL of the beads were added to the lysate. This was incubated overnight at 4 ˚C ,
e. The microreaction tube with the preparation was placed, next to the holder with the magnet to group the beads, and the supernatant was discarded,
f. The beads were washed with 300 µL of lysis buffer, and the previous step repeated,
g. The FLAG-tagged proteins were eluded with Elution Buffer (E6150 Sigma Aldrich) with glycine 0.1 M (pH 3.5),
h. pH was neutralized, then an aliquot of the purified proteins was taken. After determination of total protein concentration (See step g of 6.3.12. SDS PAGE and Western Blot), the protein solutions were diluted to 10 µg/mL,
i. Several 25 µL aliquots of the diluted solutions were taken and treated with O4I2 to a final concentration of 20 µM for 30 min,
j. After the incubation, the samples were placed in an Eppendorf Master cycler,
k. The samples underwent exposure to different temperatures for 20 min, after which the solutions were centrifuged for 20 min at 4 ˚C and 16 000 rpm. The supernatant was collected and used for Western Blot.

6.3.8. Fluorescence-Based Thermal Shift Assay

a. Purified FLAG-SF3B1 proteins were pipetted into well of a qTower^3 Thermocycler's plate to a final concentration of 25 µg/mL,
b. O4I2 was added to the protein solution, to a final concentration of 20 µM, and last 10x Sypro Orange in a final volume of 20 µL per well. To complete the volume a HEPES buffer pH 8 was used,
c. The cycler was set to 45 ˚C for 30 min, followed by a ramp from 45 to 75 ˚C at a rate of 0.01 ˚C/sec.

6.3.9. Alternative Splicing Assay

a. Cell treatment and sample Acquisition

- K562 suspension cells were collected with a serological pipette and transferred to a 50 mL conical centrifuging Falcon tube, then centrifuged for 5 minutes at room temperature and 300 G,
- The supernatant was aspirated with a glass Pasteur pipette and a vacuum pump,
- Cells were resuspended in 5 mL of pre-warmed DPBS, and step a. of this procedure was repeated,
- Step b was repeated,
- Cells were resuspended in 5 mL of pre-warmed RPMI 1640 FCS 10% and P/S 1%. The total cell count of this suspension was determined taking 10 µL of it and pipetting them between a Neubauer Chamber and a glass slide,
- Out this cell suspension, the volume equivalent to 300 000 cells was pipetted out and transferred into wells of a 6 well plate, which already contained 2 mL of pre-warmed RPMI 1640. The plate was then placed back into the cell culture incubator at the conditions previously mentioned, overnight,
- Out of the 6 wells, 1 was left unchanged ad negative control, as positive control pladienolide B was added to a final concentration of 1 µM; the cells in the rest of the wells were treated with O4I2 10 µM, PROTAC O4I2 0.01, 0,05, 0,1 and 0.5 µM. The treatments run for 18 hours,
- The cells were resuspended within the wells by pipetting thoroughly and gently up and down with a micro pipette, then transferred into 2 mL microreaction tubes, where they were spun down at 300 G for 5 min at room temperature,
- The supernatant was aspirated using a vacuum pump, and the cells resuspended in 1 mL of pre-warmed DPBS. Then spun down again as described in the previous step,
- The supernatant was once more aspirated, and the cell pellet was lysed in 200 µL of QIAzol.

  At his point, the cell lysates can either be stored at -80 ˚C or processed immediately.

b. Total RNA extraction

- The micro reaction tubes with the lysates were placed in ice and 40 µL of chloroform were pipetted into each tube,
- The mix was vortex for 15 seconds, then the micro reaction tubes were placed in ice and left unmoved for 15 min. During this time, a centrifuge was cooled down to 4 ˚C,
- The lysates were centrifuged at 12 000 G for 15 min at 4 ˚C,
- Being careful not to shake or rock the micro reaction tubes, the colorless phase of the three formed was pipette out (roughly 100 µL) and transferred into a new micro reaction tube,
- To precipitate the tRNA 100 µL of i-PrOH were pipetted into the micro reaction tubes, and the solution was mixed by inverting the tubes a few times. Then, the tubes were left unmoved in ice for 5 min,
- Precipitated tRNA was spun down at 4 ˚C for 15 min at 12 000 G,

- The supernatant was decanted by inverting the micro reaction tubes in one single, fluid movement. It is important not to rock the tube, otherwise the tRNA pellet will detach and most probably be lost. Alternatively, the supernatant can be pipetted out with extreme care,
- Then the tRNA pellet was washed with 500 µL of EtOH 70%, then spun down for 5 min at 4 ˚C and 7 000 G,
- The supernatant was decanted as previously described or aspirated carefully with a micro pipette,
- The washing step with EtOH was repeated exactly as described above,
- Upon decantation of the supernatant, the micro reaction tube was left open for the pellet to air-dry,
- Once all the EtOH evaporated, the pellet was dissolved in 15 µL of RNAse-free water, and the tRNA concentration measured in a Nanodrop 2000.

If not used immediately for cDNA synthesis, the tRNA solution can be stored at -80 ˚C.

c. cDNA synthesis

- The amount of tRNA of all samples were normalized to (or as close as possible to) 100 ng, using RNAse-free water to complete the volumes.

  ProtoScript First Strand cDNA synthesis kit was used, and the protocol followed exactly as recommended by the manufacturer.

d. Amplification and analysis

To amplify the target gene, the Q5 High-Fidelity 2x Master Mix was used. The Thermocycler was set up as follows:

98 ˚C for 30 seconds
40 cycles of
    98 ˚C for 10 seconds
    71 ˚C for 30 sec
    72 ˚C for 30 min
    72 ˚C 2 min

The products were analyzed in an agarose/TEA gel 2% with ethidium bromide.
The sequences of DNABJ1 can be found in Table 5.

6.3.10. Apoptosis Assay

a. K562 suspension cells were collected with a serological pipette and transferred to a 50 mL conical centrifuging Falcon tube, then centrifuged for 5 minutes at room temperature and 300 G,
b. The supernatant was aspirated with a glass Pasteur pipette and a vacuum pump,

c. Cells were resuspended in 5 mL of pre-warmed DPBS, and step a. of this procedure was repeated,
d. Step b was repeated,
e. Cells were resuspended in 5 mL of pre-warmed RPMI 1640 FCS 10% and P/S 1%. The total cell count of this suspension was determined taking 10 µL of it and pipetting them between a Neubauer Chamber and a glass slide,
f. Out this cell suspension, the volume equivalent to 200 000 cells was pipetted out and transferred into wells of a 12 well plate, which already contained 1 mL of pre-warmed RPMI 1640. The plate was then placed back into the cell culture incubator at the conditions previously mentioned, overnight,
g. The following treatments were applied: Pladienolide B 1 µM, PROTAC-O4I2 1 µM, and DMSO in the same concentration v/v as required for the drug treatments as mock. The well plate was placed back in the cell culture incubator for 48 hours,
h. The cells were pipetted up and down a few times to resuspend them thoroughly, and then transferred to a 1.5 mL microreaction tube to be centrifuged at 300 G for 5 min at room temperature,
i. After removing the supernatant with a vacuum pump, the cells were resuspended in 500 µL of pre-warmed DPBS, and centrifuged again under the same conditions,
j. DPBS supernatant was aspirated, and cells were resuspended in 50 µL of Annexin V binding buffer. Then 5 µL of FITC-conjugated Annexin V were added,
k. The cells were incubated for 15 minutes protected from the light,
l. After 1 minute, 1 µL of PI 1 mg/mL was added, incubating for 10 minutes more at room temperature,
m. Last, FACS buffer was added (450 µL) and the samples analyzed immediately in the FACSCallibur.

6.3.11. Immunoprecipitation and Ubiquitination (for SF3B1)

a. $K562^{CRBN\ KO}$ suspension cells were collected with a serological pipette and transferred to a 50 mL conical centrifuging Falcon tube, then centrifuged for 5 minutes at room temperature and 300 G,
b. The supernatant was aspirated with a glass Pasteur pipette and a vacuum pump,
c. Cells were resuspended in 5 mL of pre-warmed DPBS, and step a. of this procedure was repeated,
d. Step b was repeated,
e. Cells were resuspended in 5 mL of pre-warmed RPMI 1640 FCS 10% and P/S 1%. The total cell count of this suspension was determined taking 10 µL of it and pipetting them between a Neubauer Chamber and a glass slide,
f. Out this cell suspension, the volume equivalent to 500 000 cells was pipetted out and transferred into wells of a 6 well plate, which already contained 2 mL of pre-warmed RPMI 1640. The plate was then placed back into the cell culture incubator at the conditions previously mentioned, overnight,
g. The next day the cells were transfected with $SF3B1^{WT}$ and $SF3B1^{K700E}$ as described in 6.2.3. Transfection, using RPMI 1640 FCS 10% without P/S, instead of DMEM FCS 10%,
h. After pelleting the cells for transfection medium removal, the cells were resuspended in 2 mL of RPMI 1640 FCS 10% and P/S 1% for 24 hours of recovery,

i. Cells were pipetted up and down a few times to resuspend, and then transferred to a 2 mL microreaction tube to be centrifuged at 300 G for 5 min at room temperature,
j. After removal of the supernatant, the cells were lysed in 200 µL Immunoprecipitation Buffer,
k. Purified FLAG-CRBN^{WT} and FLAG-CRBN^{m} (See 6.3.3. In vitro Ubiquitination Assay for Cas proteins) in a volume of 20 µL each were added into aliquots of the lysate. At the same time the following treatments were added: O4I2 10 µM, PROTAC-O4I2 1 µM and DMSO as mock, pure lysis buffer was used as negative control. All treatments lasted 90 minutes,
l. The consumption of ATP was followed up with the Luciferase Assay as previously described in 6.3.3. In vitro Ubiquitination Assay for Cas proteins.

6.3.12. FRET assay

a. K562 cells were seeded in wells if a 24-well plate with a total count of 100 000 cells per well in RPMI 1640,
b. The day after they were double-transfected with CRBN-GFP and SF3B1-OFP as previously described on 2.3.3. Transfection,
c. After removal of the transfection cell culture by pelleting the cells, the cells resuspended in RPMI FCS 10% and P/S 1% with the following treatments: O4I2 10 µM, PROTAC-O4I2 0.1, 0.5, 1, 5 and 10 µM for 6 hours, in co-treatment with MLN4924 5 µM,
d. Upon treatment, cells were pelleted as previously described to remove the supernatant, and then resuspended in pre-warmed DPBS with FCS 1%,
e. The plate was introduced into the TECAN reader with the following set up: Em/Ex 485/510 for GFP and Em/Ex 548/573 for OFP. Wild type cells were used as blank.

The relative intensity was calculated as follows:

$$\text{Relative intensity} = \frac{\text{Signal}_{\text{treatment}} - \text{signal}_{\text{nlank}}}{\text{signal}_{\text{non treated}} - \text{signal}_{\text{blank}}}$$

6.3.13. SDS PAGE and Western Blot

a. Cell lysis

a. To maximize the cell recovery, and thus the sample collection, the adherent cells were trypsinized for 5 min with 300 µL of pre-warmed up, unsterile TrypLE^{TM} Express (Thermofisher Scientific), after a washing once with unsterile DPBS,
b. After the incubation time with trypsin, the cells were fully resuspended with 700 µL of unsterile DPBS, recovering all the cells possible with the micro pipette,
c. The suspension was transferred to a 1.5 mL micro reaction tube and spun down for 3 min at room temperature and 300 G,
d. Using a glass Pasteur pipette and a vacuum pump, the supernatant was carefully aspirated, and the cell pellets were thoroughly lysed in 80 µL of Lysis Buffer for Protein Extraction (See table 8),

e. If not further processed immediately, the lysates could be stored at -20 ˚C. Otherwise the samples were centrifuged at 4 ˚C for 30 min at 17 000 G,
f. Using a micro pipette, the DNA pellet was removed of the protein solution by slightly piercing it with the pipette tip and then lightly aspirating it and pulling out of the micro reaction tube,
g. The protein concentration was determined by the Bradford Assay, measuring technical triplicates per sample, by pipetting 2 µL of protein solution into the well, followed by 200 µL of Bradford Reagent (Sigma Aldrich). A calibration curve was made for every measurement, using a seven-point curve from 2 mg/mL in a 1:2 dilution series,
h. The protein amounts were normalized to the least concentrated protein solution, completing the volumes with Urea Buffer 6 M, and adding the corresponding volume of GLB 5x,
i. Last, the protein samples were heated up to 95 ˚C for 3 min, and immediately placed in ice for SDS PAGE.

b. SDS PAGE

a. All gels were prepared to a polyacrylamide concentration of 10% (See table 8), using a 15-solt comb,
b. Given that some antibodies come from the same host and target proteins of similar molecular weights, the membranes had to be doubled for every biological triplicate. For such purpose every set of 5 samples (Day 0, 1, 3, 5, and 7) were pipetted twice per gel,
c. The electrophoresis was run at 80 mV until the samples reached with resolving gel, then the voltage was increased to 100 mV.

c. Western Blot

a. The WB sandwich was prepared by stacking three layers of filter paper soaked in Anode Buffer, followed by a PVDF membrane, that was previously activated with MeOH for a few minutes before being soaked in Anode Buffer. On top, the gel soaked in cathode buffer was placed, followed by three layers of filter paper soaked in cathode buffer, placing them one by one, and removing air bubbles in every step,
b. The protein transfer was done using the pre-defined Standard program of the Bio-rad Trans-Blot Turbo Transfer System,
c. The transferred membranes were retrieved from their respective sandwiches and incubated immediately in Ponceau solution for 5 min, after which, the membranes were washed in TBS-T very shortly to remove the excess of the reagent, and an image was taken using the colorimetric blotting setting of the CHEMIDoc (Bio-rad),
d. Then, the membranes were washed three times for 10 mins with TBS-T with gently rocking, until most of the Ponceau reagent was washed away,
e. Blocking took place using a suspension of Blotting-grade Milk 5% in TBS-T at 4 ˚C overnight,
f. The membranes were then washed three times for 5 minutes with enough TBS-T to cover them fully, with gently rocking,

g. The membranes were cut vertically to produce the two membranes for every biological triplicate (6 membranes in total), taking care of cutting at the empty space between the sample sets,
h. Incubation with primary took place overnight at 4 ˚C, in solutions of concentrations recommended by the manufacturer, in BSA 5%, with NaN_3 0.02%,
i. Three washing steps in TBS-T for 5 mins in gently rocking motion followed the incubation,
j. Incubation in peroxidase-coupled secondary antibodies took place for 1 h, at room temperature. The secondary antibody was diluted to the recommended concentration by the manufacturer, in Blotting-grade Milk 5% in TBS-T,
k. The membranes were washed three times with TBS-T for 5 min with gently rocking motion,
l. The ELC reagents (SuperSignal West Pico Plus Chemiluminiscent Substrate, Thermo Fisher Scientific) were mixed and immediately used, flushing thoroughly and evenly the membranes, one at a time. The images were taken with CHEMIDoc and Image Lab systems (Bio-rad).

6.3.14. FACS

a. Cell Acquisition

a. Cell culture supernatant was removed using a glass Pasteur pipette and a vacuum pump,
b. The transfected cells were treated with 300 µL of TrypLE^{TM} Express for 5 min in the cell incubator at the conditions previously described,
c. Trypsin was inactivated by addition of 1.7 mL of DMEM FCS 10% and P/S 1%. The cell suspension was pipetted up and down several times to mix, and to harvest as many cells as possible,
d. The cell suspension was then centrifuged at room temperature at 200 G for 5 min,
e. The supernatant was removed with the vacuum pump, and a washing step with 1 mL of DPBS took place,
f. Step e. (washing step), was repeated twice more,
g. Last, the cell pellet was resuspended in DPBS with BSA 1% and EDTA 2 mM for measurement and data acquisition.

b. FACS set up and data acquisition

HeLa WT cells were used as negative control and HeLa^{GFP} were used as positive control. The acquisition was gated in accordance with these controls, in a Guava easyCyte machine.

Each cell suspension (HeLa WT, HeLa^{GFP,} and HeLa^{FCPF}) was pipetted into a U bottom transparent 96-well plate with a volume of 200 µL, pipetting up and down the suspension to mix thoroughly.

After treatment, K562$^{CRBN\ KD}$ were resuspended in 50 µL of Annexin V Binding Buffer (See Table 10: Buffers and solutions) to which 5 µL of FITC-conjugated Annexin V were added.

Cells were incubated for 15 minutes in the dark at room temperature. Then, 1 µL of PI 1 mg/mL was added to the cell suspension, followed by an incubation time of 10 minutes. Cells were pelleted and resuspended in 450 µL of FACS buffer, then, immediately measured.

7. REFERENCES

An, S., & Fu, L. (2018). Small-molecule PROTACs: An emerging and promising approach for the development of targeted therapy drugs. *EBioMedicine, 36*, 553-562. doi:10.1016/j.ebiom.2018.09.005

Aschenbrenner, S., Kallenberger, S. M., Hoffmann, M. D., Huck, A., Eils, R., & Niopek, D. (2020). Coupling Cas9 to artificial inhibitory domains enhances CRISPR-Cas9 target specificity. *Sci Adv, 6*(6), eaay0187. doi:10.1126/sciadv.aay0187

Bargagna-Mohan, P., Baek, S. H., Lee, H., Kim, K., & Mohan, R. (2005). Use of PROTACS as molecular probes of angiogenesis. *Bioorg Med Chem Lett, 15*(11), 2724-2727. doi:10.1016/j.bmcl.2005.04.008

Bishop, A. E., Buttery, L. D., & Polak, J. M. (2002). Embryonic stem cells. *J Pathol, 197*(4), 424-429. doi:10.1002/path.1154

Bondeson, D. P., & Crews, C. M. (2017). Targeted Protein Degradation by Small Molecules. *Annu Rev Pharmacol Toxicol, 57*, 107-123. doi:10.1146/annurev-pharmtox-010715-103507

Bondeson, D. P., Mares, A., Smith, I. E., Ko, E., Campos, S., Miah, A. H., . . . Crews, C. M. (2015). Catalytic in vivo protein knockdown by small-molecule PROTACs. *Nat Chem Biol, 11*(8), 611-617. doi:10.1038/nchembio.1858

Bradbury, R. H., Hales, N. J., Rabow, A. A., Walker, G. E., Acton, D. G., Andrews, D. M., . . . Mortlock, A. A. (2011). Small-molecule androgen receptor downregulators as an approach to treatment of advanced prostate cancer. *Bioorg Med Chem Lett, 21*(18), 5442-5445. doi:10.1016/j.bmcl.2011.06.122

Bubeck, F., Hoffmann, M. D., Harteveld, Z., Aschenbrenner, S., Bietz, A., Waldhauer, M. C., . . . Niopek, D. (2018). Engineered anti-CRISPR proteins for optogenetic control of CRISPR-Cas9. *Nat Methods, 15*(11), 924-927. doi:10.1038/s41592-018-0178-9

Buckley, D. L., & Crews, C. M. (2014). Small-molecule control of intracellular protein levels through modulation of the ubiquitin proteasome system. *Angew Chem Int Ed Engl, 53*(9), 2312-2330. doi:10.1002/anie.201307761

Buckley, D. L., Raina, K., Darricarrere, N., Hines, J., Gustafson, J. L., Smith, I. E., . . . Crews, C. M. (2015). HaloPROTACS: Use of Small Molecule PROTACs to Induce Degradation of HaloTag Fusion Proteins. *ACS Chem Biol, 10*(8), 1831-1837. doi:10.1021/acschembio.5b00442

Burslem, G. M., Schultz, A. R., Bondeson, D. P., Eide, C. A., Savage Stevens, S. L., Druker, B. J., & Crews, C. M. (2019). Targeting BCR-ABL1 in Chronic Myeloid Leukemia by PROTAC-Mediated Targeted Protein Degradation. *Cancer Res, 79*(18), 4744-4753. doi:10.1158/0008-5472.CAN-19-1236

Burslem, G. M., Smith, B. E., Lai, A. C., Jaime-Figueroa, S., McQuaid, D. C., Bondeson, D. P., . . . Crews, C. M. (2018). The Advantages of Targeted Protein Degradation Over Inhibition: An RTK Case Study. *Cell Chem Biol, 25*(1), 67-77 e63. doi:10.1016/j.chembiol.2017.09.009

Cao, F., de Weerd, S., Chen, D., Zwinderman, M. R. H., van der Wouden, P. E., & Dekker, F. J. (2020). Induced protein degradation of histone deacetylases 3 (HDAC3) by proteolysis targeting chimera (PROTAC). *Eur J Med Chem, 208*, 112800. doi:10.1016/j.ejmech.2020.112800

Cao, J., Hou, P., Chen, J., Wang, P., Wang, W., Liu, W., . . . He, X. (2017). The overexpression and prognostic role of DCAF13 in hepatocellular carcinoma. *Tumour Biol, 39*(6), 1010428317705753. doi:10.1177/1010428317705753

Cecchini, C., Pannilunghi, S., Tardy, S., & Scapozza, L. (2021). From Conception to Development: Investigating PROTACs Features for Improved Cell Permeability and Successful Protein Degradation. *Front Chem, 9*, 672267. doi:10.3389/fchem.2021.672267

Chen, X., Shen, H., Shao, Y., Ma, Q., Niu, Y., & Shang, Z. (2021). A narrative review of proteolytic targeting chimeras (PROTACs): future perspective for prostate cancer therapy. *Transl Androl Urol, 10*(2), 954-962. doi:10.21037/tau-20-1357

Cheng, B., Ren, Y., Cao, H., & Chen, J. (2020). Discovery of novel resorcinol diphenyl ether-based PROTAC-like molecules as dual inhibitors and degraders of PD-L1. *Eur J Med Chem, 199*, 112377. doi:10.1016/j.ejmech.2020.112377

Cheng, X., Dimou, E., Alborzinia, H., Wenke, F., Gohring, A., Reuter, S., . . . Wolfl, S. (2015). Identification of 2-[4-[(4-Methoxyphenyl)methoxy]-phenyl]acetonitrile and Derivatives as Potent Oct3/4 Inducers. *Journal of Medicinal Chemistry, 58*(12), 4976-4983. doi:10.1021/acs.jmedchem.5b00144

Cheng, X., Kim, J. Y., Ghafoory, S., Duvaci, T., Rafiee, R., Theobald, J., . . . Wolfl, S. (2016). Methylisoindigo preferentially kills cancer stem cells by interfering cell metabolism via inhibition of LKB1 and activation of AMPK in PDACs. *Mol Oncol, 10*(6), 806-824. doi:10.1016/j.molonc.2016.01.008

Cheng, X., Yoshida, H., Raoofi, D., Saleh, S., Alborzinia, H., Wenke, F., . . . Wolfl, S. (2015). Ethyl 2-((4-Chlorophenyl)amino)thiazole-4-carboxylate and Derivatives Are Potent Inducers of Oct3/4. *Journal of Medicinal Chemistry, 58*(15), 5742-5750. doi:10.1021/acs.jmedchem.5b00226

Chu, T. T., Gao, N., Li, Q. Q., Chen, P. G., Yang, X. F., Chen, Y. X., . . . Li, Y. M. (2016). Specific Knockdown of Endogenous Tau Protein by Peptide-Directed Ubiquitin-Proteasome Degradation. *Cell Chem Biol, 23*(4), 453-461. doi:10.1016/j.chembiol.2016.02.016

Churcher, I. (2018). Protac-Induced Protein Degradation in Drug Discovery: Breaking the Rules or Just Making New Ones? *J Med Chem, 61*(2), 444-452. doi:10.1021/acs.jmedchem.7b01272

Cox, D. B. T., Gootenberg, J. S., Abudayyeh, O. O., Franklin, B., Kellner, M. J., Joung, J., & Zhang, F. (2017). RNA editing with CRISPR-Cas13. *Science, 358*(6366), 1019-1027. doi:10.1126/science.aaq0180

Cretu, C., Agrawal, A. A., Cook, A., Will, C. L., Fekkes, P., Smith, P. G., . . . Pena, V. (2018). Structural Basis of Splicing Modulation by Antitumor Macrolide Compounds. *Mol Cell, 70*(2), 265-273 e268. doi:10.1016/j.molcel.2018.03.011

Crew, A. P., Raina, K., Dong, H., Qian, Y., Wang, J., Vigil, D., . . . Crews, C. M. (2018). Identification and Characterization of Von Hippel-Lindau-Recruiting Proteolysis Targeting Chimeras (PROTACs) of TANK-Binding Kinase 1. *J Med Chem, 61*(2), 583-598. doi:10.1021/acs.jmedchem.7b00635

Cui, X., Shen, W., Wang, G., Huang, Z., Wen, D., Yang, Y., . . . Cui, L. (2018). Ring finger protein 152 inhibits colorectal cancer cell growth and is a novel prognostic biomarker. *Am J Transl Res, 10*(11), 3701-3712.

Dabiri, Y., Gama-Brambila, R. A., Taskova, K., Herold, K., Reuter, S., Adjaye, J., . . . Cheng, X. (2019). Imidazopyridines as Potent KDM5 Demethylase Inhibitors Promoting Reprogramming Efficiency of Human iPSCs. *iScience, 12*, 168-181. doi:10.1016/j.isci.2019.01.012

Demizu, Y., Okuhira, K., Motoi, H., Ohno, A., Shoda, T., Fukuhara, K., . . . Kurihara, M. (2012). Design and synthesis of estrogen receptor degradation inducer based on a protein knockdown strategy. *Bioorg Med Chem Lett, 22*(4), 1793-1796. doi:10.1016/j.bmcl.2011.11.086

Donoghue, C., Cubillos-Rojas, M., Gutierrez-Prat, N., Sanchez-Zarzalejo, C., Verdaguer, X., Riera, A., & Nebreda, A. R. (2020). Optimal linker length for small molecule PROTACs that selectively target p38alpha and p38beta for degradation. *Eur J Med Chem, 201*, 112451. doi:10.1016/j.ejmech.2020.112451

Doudna, J. A., & Charpentier, E. (2014). Genome editing. The new frontier of genome engineering with CRISPR-Cas9. *Science, 346*(6213), 1258096. doi:10.1126/science.1258096

Douglass, E. F., Jr., Miller, C. J., Sparer, G., Shapiro, H., & Spiegel, D. A. (2013). A comprehensive mathematical model for three-body binding equilibria. *J Am Chem Soc, 135*(16), 6092-6099. doi:10.1021/ja311795d

Duan, J., Wu, Y., Liu, J., Zhang, J., Fu, Z., Feng, T., . . . Chen, S. (2019). Genetic Biomarkers For Hepatocellular Carcinoma In The Era Of Precision Medicine. *J Hepatocell Carcinoma, 6*, 151-166. doi:10.2147/JHC.S224849

Dvinge, H., Kim, E., Abdel-Wahab, O., & Bradley, R. K. (2016). RNA splicing factors as oncoproteins and tumour suppressors. *Nat Rev Cancer, 16*(7), 413-430. doi:10.1038/nrc.2016.51

Effenberger, K. A., Urabe, V. K., & Jurica, M. S. (2017). Modulating splicing with small molecular inhibitors of the spliceosome. *Wiley Interdiscip Rev RNA, 8*(2). doi:10.1002/wrna.1381

Eskens, F. A., Ramos, F. J., Burger, H., O'Brien, J. P., Piera, A., de Jonge, M. J., . . . Tabernero, J. (2013). Phase I pharmacokinetic and pharmacodynamic study of the first-in-class spliceosome inhibitor E7107 in patients with advanced solid tumors. *Clin Cancer Res, 19*(22), 6296-6304. doi:10.1158/1078-0432.CCR-13-0485

Esvelt, K. M., Mali, P., Braff, J. L., Moosburner, M., Yaung, S. J., & Church, G. M. (2013). Orthogonal Cas9 proteins for RNA-guided gene regulation and editing. *Nat Methods, 10*(11), 1116-1121. doi:10.1038/nmeth.2681

Fan, X., Jin, W. Y., Lu, J., Wang, J., & Wang, Y. T. (2014). Rapid and reversible knockdown of endogenous proteins by peptide-directed lysosomal degradation. *Nat Neurosci, 17*(3), 471-480. doi:10.1038/nn.3637

Feng, Y., Su, H., Li, Y., Luo, C., Xu, H., Wang, Y., . . . Bu, X. (2020). Degradation of intracellular TGF-beta1 by PROTACs efficiently reverses M2 macrophage induced malignant pathological events. *Chem Commun (Camb), 56*(19), 2881-2884. doi:10.1039/c9cc08391j

Fu, Y., Foden, J. A., Khayter, C., Maeder, M. L., Reyon, D., Joung, J. K., & Sander, J. D. (2013). High-frequency off-target mutagenesis induced by CRISPR-Cas nucleases in human cells. *Nat Biotechnol, 31*(9), 822-826. doi:10.1038/nbt.2623

Gabizon, R., Shraga, A., Gehrtz, P., Livnah, E., Shorer, Y., Gurwicz, N., . . . London, N. (2020). Efficient Targeted Degradation via Reversible and Irreversible Covalent PROTACs. *J Am Chem Soc, 142*(27), 11734-11742. doi:10.1021/jacs.9b13907

Gadd, M. S., Testa, A., Lucas, X., Chan, K. H., Chen, W., Lamont, D. J., . . . Ciulli, A. (2017). Structural basis of PROTAC cooperative recognition for selective protein degradation. *Nat Chem Biol, 13*(5), 514-521. doi:10.1038/nchembio.2329

Gama-Brambila, R. A., Chen, J., Dabiri, Y., Tascher, G., Nemec, V., Munch, C., . . . Cheng, X. (2021). A Chemical Toolbox for Labeling and Degrading Engineered Cas Proteins. *JACS Au, 1*(6), 777-785. doi:10.1021/jacsau.1c00007

Gama-Brambila, R. A., Chen, J., Zhou, J., Tascher, G., Munch, C., & Cheng, X. (2021). A PROTAC targets splicing factor 3B1. *Cell Chem Biol*. doi:10.1016/j.chembiol.2021.04.018

Garcia-Doval, C., & Jinek, M. (2017). Molecular architectures and mechanisms of Class 2 CRISPR-associated nucleases. *Curr Opin Struct Biol, 47*, 157-166. doi:10.1016/j.sbi.2017.10.015

Gechijian, L. N., Buckley, D. L., Lawlor, M. A., Reyes, J. M., Paulk, J., Ott, C. J., . . . Bradner, J. E. (2018). Functional TRIM24 degrader via conjugation of ineffectual bromodomain and VHL ligands. *Nat Chem Biol, 14*(4), 405-412. doi:10.1038/s41589-018-0010-y

Ghidini, A., Clery, A., Halloy, F., Allain, F. H. T., & Hall, J. (2021). RNA-PROTACs: Degraders of RNA-Binding Proteins. *Angew Chem Int Ed Engl, 60*(6), 3163-3169. doi:10.1002/anie.202012330

Goettel, J. A., Liang, D., Hilliard, V. C., Edelblum, K. L., Broadus, M. R., Gould, K. L., . . . Polk, D. B. (2011). KSR1 is a functional protein kinase capable of serine autophosphorylation and direct phosphorylation of MEK1. *Exp Cell Res, 317*(4), 452-463. doi:10.1016/j.yexcr.2010.11.018

Golas, M. M., Sander, B., Will, C. L., Luhrmann, R., & Stark, H. (2003). Molecular architecture of the multiprotein splicing factor SF3b. *Science, 300*(5621), 980-984. doi:10.1126/science.1084155

Hanafi, M., Chen, X., & Neamati, N. (2021). Discovery of a Napabucasin PROTAC as an Effective Degrader of the E3 Ligase ZFP91. *J Med Chem, 64*(3), 1626-1648. doi:10.1021/acs.jmedchem.0c01897

He, Y., Khan, S., Huo, Z., Lv, D., Zhang, X., Liu, X., . . . Zhou, D. (2020). Proteolysis targeting chimeras (PROTACs) are emerging therapeutics for hematologic malignancies. *J Hematol Oncol, 13*(1), 103. doi:10.1186/s13045-020-00924-z

He, Y., Koch, R., Budamagunta, V., Zhang, P., Zhang, X., Khan, S., . . . Zhou, D. (2020). DT2216-a Bcl-xL-specific degrader is highly active against Bcl-xL-dependent T cell lymphomas. *J Hematol Oncol, 13*(1), 95. doi:10.1186/s13045-020-00928-9

Henning, R. K., Varghese, J. O., Das, S., Nag, A., Tang, G., Tang, K., . . . Heath, J. R. (2016). Degradation of Akt using protein-catalyzed capture agents. *J Pept Sci, 22*(4), 196-200. doi:10.1002/psc.2858

Hetz, C., & Papa, F. R. (2018). The Unfolded Protein Response and Cell Fate Control. *Mol Cell, 69*(2), 169-181. doi:10.1016/j.molcel.2017.06.017

Hines, J., Lartigue, S., Dong, H., Qian, Y., & Crews, C. M. (2019). MDM2-Recruiting PROTAC Offers Superior, Synergistic Antiproliferative Activity via Simultaneous Degradation of BRD4 and Stabilization of p53. *Cancer Res, 79*(1), 251-262. doi:10.1158/0008-5472.CAN-18-2918

Hsu, J. H., Rasmusson, T., Robinson, J., Pachl, F., Read, J., Kawatkar, S., . . . Bloecher, A. (2020). EED-Targeted PROTACs Degrade EED, EZH2, and SUZ12 in the PRC2 Complex. *Cell Chem Biol, 27*(1), 41-46 e17. doi:10.1016/j.chembiol.2019.11.004

Hu, J. H., Miller, S. M., Geurts, M. H., Tang, W., Chen, L., Sun, N., . . . Liu, D. R. (2018). Evolved Cas9 variants with broad PAM compatibility and high DNA specificity. *Nature, 556*(7699), 57-63. doi:10.1038/nature26155

Itoh, Y., Ishikawa, M., Naito, M., & Hashimoto, Y. (2010). Protein knockdown using methyl bestatin-ligand hybrid molecules: design and synthesis of inducers of ubiquitination-mediated degradation of cellular retinoic acid-binding proteins. *J Am Chem Soc, 132*(16), 5820-5826. doi:10.1021/ja100691p

Itoh, Y., Kitaguchi, R., Ishikawa, M., Naito, M., & Hashimoto, Y. (2011). Design, synthesis and biological evaluation of nuclear receptor-degradation inducers. *Bioorg Med Chem, 19*(22), 6768-6778. doi:10.1016/j.bmc.2011.09.041

Jao, C. Y., & Salic, A. (2008). Exploring RNA transcription and turnover in vivo by using click chemistry. *Proc Natl Acad Sci U S A, 105*(41), 15779-15784. doi:10.1073/pnas.0808480105

Jiang, X., Zhou, J., Wang, Y., Liu, X., Xu, K., Xu, J., . . . Sun, H. (2021). PROTACs suppression of GSK-3beta, a crucial kinase in neurodegenerative diseases. *Eur J Med Chem, 210*, 112949. doi:10.1016/j.ejmech.2020.112949

Jimenez-Vacas, J. M., Herrero-Aguayo, V., Gomez-Gomez, E., Leon-Gonzalez, A. J., Saez-Martinez, P., Alors-Perez, E., . . . Luque, R. M. (2019). Spliceosome component SF3B1 as novel prognostic biomarker and therapeutic target for prostate cancer. *Transl Res, 212*, 89-103. doi:10.1016/j.trsl.2019.07.001

Jin, Y. H., Lu, M. C., Wang, Y., Shan, W. X., Wang, X. Y., You, Q. D., & Jiang, Z. Y. (2020). Azo-PROTAC: Novel Light-Controlled Small-Molecule Tool for Protein Knockdown. *J Med Chem, 63*(9), 4644-4654. doi:10.1021/acs.jmedchem.9b02058

Kaida, D., Motoyoshi, H., Tashiro, E., Nojima, T., Hagiwara, M., Ishigami, K., . . . Yoshida, M. (2007). Spliceostatin A targets SF3b and inhibits both splicing and nuclear retention of pre-mRNA. *Nat Chem Biol, 3*(9), 576-583. doi:10.1038/nchembio.2007.18

Kakeya, H., Kaida, D., Sekiya, H., Nagai, K., Yoshida, M., & Osada, H. (2016). RQN-18690A (18-deoxyherboxidiene) targets SF3b, a spliceosome component, and inhibits angiogenesis. *J Antibiot (Tokyo), 69*(2), 121-123. doi:10.1038/ja.2015.94

Khan, S., Zhang, X., Lv, D., Zhang, Q., He, Y., Zhang, P., . . . Zhou, D. (2019). A selective BCL-XL PROTAC degrader achieves safe and potent antitumor activity. *Nat Med, 25*(12), 1938-1947. doi:10.1038/s41591-019-0668-z

Kim, S., Kim, D., Cho, S. W., Kim, J., & Kim, J. S. (2014). Highly efficient RNA-guided genome editing in human cells via delivery of purified Cas9 ribonucleoproteins. *Genome Res, 24*(6), 1012-1019. doi:10.1101/gr.171322.113

Kleinstiver, B. P., Prew, M. S., Tsai, S. Q., Topkar, V. V., Nguyen, N. T., Zheng, Z., . . . Joung, J. K. (2015). Engineered CRISPR-Cas9 nucleases with altered PAM specificities. *Nature, 523*(7561), 481-485. doi:10.1038/nature14592

Kotake, Y., Sagane, K., Owa, T., Mimori-Kiyosue, Y., Shimizu, H., Uesugi, M., . . . Mizui, Y. (2007). Splicing factor SF3b as a target of the antitumor natural product pladienolide. *Nat Chem Biol, 3*(9), 570-575. doi:10.1038/nchembio.2007.16

Krall, N., da Cruz, F. P., Boutureira, O., & Bernardes, G. J. (2016). Site-selective protein-modification chemistry for basic biology and drug development. *Nat Chem, 8*(2), 103-113. doi:10.1038/nchem.2393

Lai, A. C., & Crews, C. M. (2017). Induced protein degradation: an emerging drug discovery paradigm. *Nat Rev Drug Discov, 16*(2), 101-114. doi:10.1038/nrd.2016.211

Lai, A. C., Toure, M., Hellerschmied, D., Salami, J., Jaime-Figueroa, S., Ko, E., . . . Crews, C. M. (2016). Modular PROTAC Design for the Degradation of Oncogenic BCR-ABL. *Angew Chem Int Ed Engl, 55*(2), 807-810. doi:10.1002/anie.201507634

Lebraud, H., Wright, D. J., Johnson, C. N., & Heightman, T. D. (2016). Protein Degradation by In-Cell Self-Assembly of Proteolysis Targeting Chimeras. *ACS Cent Sci, 2*(12), 927-934. doi:10.1021/acscentsci.6b00280

Lecker, S. H., Goldberg, A. L., & Mitch, W. E. (2006). Protein degradation by the ubiquitin-proteasome pathway in normal and disease states. *J Am Soc Nephrol, 17*(7), 1807-1819. doi:10.1681/ASN.2006010083

Lee, G. T., Nagaya, N., Desantis, J., Madura, K., Sabaawy, H. E., Kim, W. J., . . . Kim, I. Y. (2021). Effects of MTX-23, a Novel PROTAC of Androgen Receptor Splice Variant-7 and Androgen Receptor, on CRPC Resistant to Second-Line Antiandrogen Therapy. *Mol Cancer Ther, 20*(3), 490-499. doi:10.1158/1535-7163.MCT-20-0417

Lee, H., Puppala, D., Choi, E. Y., Swanson, H., & Kim, K. B. (2007). Targeted degradation of the aryl hydrocarbon receptor by the PROTAC approach: a useful chemical genetic tool. *Chembiochem, 8*(17), 2058-2062. doi:10.1002/cbic.200700438

Li, Y., Li, S., Wang, J., & Liu, G. (2019). CRISPR/Cas Systems towards Next-Generation Biosensing. *Trends Biotechnol, 37*(7), 730-743. doi:10.1016/j.tibtech.2018.12.005

Li, Y., Yang, J., Aguilar, A., McEachern, D., Przybranowski, S., Liu, L., . . . Wang, S. (2019). Discovery of MD-224 as a First-in-Class, Highly Potent, and Efficacious Proteolysis Targeting Chimera Murine Double Minute 2 Degrader Capable of Achieving Complete and Durable Tumor Regression. *J Med Chem, 62*(2), 448-466. doi:10.1021/acs.jmedchem.8b00909

Li, Z., Lin, Y., Song, H., Qin, X., Yu, Z., Zhang, Z., . . . Li, M. (2020). First small-molecule PROTACs for G protein-coupled receptors: inducing alpha 1A-adrenergic receptor degradation. *Acta Pharm Sin B, 10*(9), 1669-1679. doi:10.1016/j.apsb.2020.01.014

Lian, Y. F., Huang, Y. L., Zhang, Y. J., Chen, D. M., Wang, J. L., Wei, H., . . . Huang, Y. H. (2019). CACYBP Enhances Cytoplasmic Retention of P27(Kip1) to Promote Hepatocellular Carcinoma Progression in the Absence of RNF41 Mediated Degradation. *Theranostics, 9*(26), 8392-8408. doi:10.7150/thno.36838

Liu, X., Zhang, X., Lv, D., Yuan, Y., Zheng, G., & Zhou, D. (2020). Assays and technologies for developing proteolysis targeting chimera degraders. *Future Med Chem, 12*(12), 1155-1179. doi:10.4155/fmc-2020-0073

Lu, G., Middleton, R. E., Sun, H., Naniong, M., Ott, C. J., Mitsiades, C. S., . . . Kaelin, W. G., Jr. (2014). The myeloma drug lenalidomide promotes the cereblon-dependent destruction of Ikaros proteins. *Science, 343*(6168), 305-309. doi:10.1126/science.1244917

Lu, J., Qian, Y., Altieri, M., Dong, H., Wang, J., Raina, K., . . . Crews, C. M. (2015). Hijacking the E3 Ubiquitin Ligase Cereblon to Efficiently Target BRD4. *Chem Biol, 22*(6), 755-763. doi:10.1016/j.chembiol.2015.05.009

Lu, M., Liu, T., Jiao, Q., Ji, J., Tao, M., Liu, Y., . . . Jiang, Z. (2018). Discovery of a Keap1-dependent peptide PROTAC to knockdown Tau by ubiquitination-proteasome degradation pathway. *Eur J Med Chem, 146*, 251-259. doi:10.1016/j.ejmech.2018.01.063

Madak, J. T., Cuthbertson, C. R., Chen, W., Showalter, H. D., & Neamati, N. (2017). Design, Synthesis, and Characterization of Brequinar Conjugates as Probes to Study DHODH Inhibition. *Chemistry, 23*(56), 13875-13878. doi:10.1002/chem.201702999

Maeda, H., & Khatami, M. (2018). Analyses of repeated failures in cancer therapy for solid tumors: poor tumor-selective drug delivery, low therapeutic efficacy and unsustainable costs. *Clin Transl Med, 7*(1), 11. doi:10.1186/s40169-018-0185-6

Maneiro, M. A., Forte, N., Shchepinova, M. M., Kounde, C. S., Chudasama, V., Baker, J. R., & Tate, E. W. (2020). Antibody-PROTAC Conjugates Enable HER2-Dependent Targeted Protein Degradation of BRD4. *ACS Chem Biol, 15*(6), 1306-1312. doi:10.1021/acschembio.0c00285

Maniaci, C., Hughes, S. J., Testa, A., Chen, W., Lamont, D. J., Rocha, S., . . . Ciulli, A. (2017). Homo-PROTACs: bivalent small-molecule dimerizers of the VHL E3 ubiquitin ligase to induce self-degradation. *Nat Commun, 8*(1), 830. doi:10.1038/s41467-017-00954-1

Montrose, K., & Krissansen, G. W. (2014). Design of a PROTAC that antagonizes and destroys the cancer-forming X-protein of the hepatitis B virus. *Biochem Biophys Res Commun, 453*(4), 735-740. doi:10.1016/j.bbrc.2014.10.006

Nabet, B., Roberts, J. M., Buckley, D. L., Paulk, J., Dastjerdi, S., Yang, A., . . . Bradner, J. E. (2018). The dTAG system for immediate and target-specific protein degradation. *Nat Chem Biol, 14*(5), 431-441. doi:10.1038/s41589-018-0021-8

Neklesa, T. K., Tae, H. S., Schneekloth, A. R., Stulberg, M. J., Corson, T. W., Sundberg, T. B., . . . Crews, C. M. (2011). Small-molecule hydrophobic tagging-induced degradation of HaloTag fusion proteins. *Nat Chem Biol, 7*(8), 538-543. doi:10.1038/nchembio.597

Neklesa, T. K., Winkler, J. D., & Crews, C. M. (2017). Targeted protein degradation by PROTACs. *Pharmacol Ther, 174*, 138-144. doi:10.1016/j.pharmthera.2017.02.027

Niinuma, T., Kitajima, H., Kai, M., Yamamoto, E., Yorozu, A., Ishiguro, K., . . . Suzuki, H. (2019). UHRF1 depletion and HDAC inhibition reactivate epigenetically silenced genes in colorectal cancer cells. *Clin Epigenetics, 11*(1), 70. doi:10.1186/s13148-019-0668-3

Nunes, J., McGonagle, G. A., Eden, J., Kiritharan, G., Touzet, M., Lewell, X., . . . Anderson, N. A. (2019). Targeting IRAK4 for Degradation with PROTACs. *ACS Med Chem Lett, 10*(7), 1081-1085. doi:10.1021/acsmedchemlett.9b00219

O'Connell, M. R. (2019). Molecular Mechanisms of RNA Targeting by Cas13-containing Type VI CRISPR-Cas Systems. *J Mol Biol, 431*(1), 66-87. doi:10.1016/j.jmb.2018.06.029

Ocana, A., & Pandiella, A. (2020). Proteolysis targeting chimeras (PROTACs) in cancer therapy. *J Exp Clin Cancer Res, 39*(1), 189. doi:10.1186/s13046-020-01672-1

Ohoka, N., Nagai, K., Hattori, T., Okuhira, K., Shibata, N., Cho, N., & Naito, M. (2014). Cancer cell death induced by novel small molecules degrading the TACC3 protein via the ubiquitin-proteasome pathway. *Cell Death Dis, 5*, e1513. doi:10.1038/cddis.2014.471

Ohoka, N., Okuhira, K., Ito, M., Nagai, K., Shibata, N., Hattori, T., . . . Naito, M. (2017). In Vivo Knockdown of Pathogenic Proteins via Specific and Nongenetic Inhibitor of Apoptosis Protein (IAP)-dependent Protein Erasers (SNIPERs). *J Biol Chem, 292*(11), 4556-4570. doi:10.1074/jbc.M116.768853

Pan, H. W., Chou, H. Y., Liu, S. H., Peng, S. Y., Liu, C. L., & Hsu, H. C. (2006). Role of L2DTL, cell cycle-regulated nuclear and centrosome protein, in aggressive hepatocellular carcinoma. *Cell Cycle, 5*(22), 2676-2687. doi:10.4161/cc.5.22.3500

Papaemmanuil, E., Cazzola, M., Boultwood, J., Malcovati, L., Vyas, P., Bowen, D., . . . Chronic Myeloid Disorders Working Group of the International Cancer Genome, C. (2011). Somatic SF3B1 mutation in myelodysplasia with ring sideroblasts. *N Engl J Med, 365*(15), 1384-1395. doi:10.1056/NEJMoa1103283

Pedersen, S. M., Chan, W., Jattani, R. P., Mackie d, S., & Pomerantz, J. L. (2015). Negative Regulation of CARD11 Signaling and Lymphoma Cell Survival by the E3 Ubiquitin Ligase RNF181. *Mol Cell Biol, 36*(5), 794-808. doi:10.1128/MCB.00876-15

Pettersson, M., & Crews, C. M. (2019). PROteolysis TArgeting Chimeras (PROTACs) - Past, present and future. *Drug Discov Today Technol, 31*, 15-27. doi:10.1016/j.ddtec.2019.01.002

Pinkas, D. M., Sanvitale, C. E., Bufton, J. C., Sorrell, F. J., Solcan, N., Chalk, R., . . . Bullock, A. N. (2017). Structural complexity in the KCTD family of Cullin3-dependent E3 ubiquitin ligases. *Biochem J, 474*(22), 3747-3761. doi:10.1042/BCJ20170527

Posternak, G., Tang, X., Maisonneuve, P., Jin, T., Lavoie, H., Daou, S., . . . Sicheri, F. (2020). Functional characterization of a PROTAC directed against BRAF mutant V600E. *Nat Chem Biol, 16*(11), 1170-1178. doi:10.1038/s41589-020-0609-7

Prozzillo, Y., Fattorini, G., Santopietro, M. V., Suglia, L., Ruggiero, A., Ferreri, D., & Messina, G. (2020). Targeted Protein Degradation Tools: Overview and Future Perspectives. *Biology (Basel), 9*(12). doi:10.3390/biology9120421

Raina, K., Lu, J., Qian, Y., Altieri, M., Gordon, D., Rossi, A. M., . . . Coleman, K. G. (2016). PROTAC-induced BET protein degradation as a therapy for castration-resistant prostate cancer. *Proc Natl Acad Sci U S A, 113*(26), 7124-7129. doi:10.1073/pnas.1521738113

Remillard, D., Buckley, D. L., Paulk, J., Brien, G. L., Sonnett, M., Seo, H. S., . . . Bradner, J. E. (2017). Degradation of the BAF Complex Factor BRD9 by Heterobifunctional Ligands. *Angew Chem Int Ed Engl, 56*(21), 5738-5743. doi:10.1002/anie.201611281

Reynders, M., Matsuura, B. S., Berouti, M., Simoneschi, D., Marzio, A., Pagano, M., & Trauner, D. (2020). PHOTACs enable optical control of protein degradation. *Sci Adv, 6*(8), eaay5064. doi:10.1126/sciadv.aay5064

Robb, C. M., Contreras, J. I., Kour, S., Taylor, M. A., Abid, M., Sonawane, Y. A., . . . Rana, S. (2017). Chemically induced degradation of CDK9 by a proteolysis targeting chimera (PROTAC). *Chem Commun (Camb), 53*(54), 7577-7580. doi:10.1039/c7cc03879h

Rodriguez-Gonzalez, A., Cyrus, K., Salcius, M., Kim, K., Crews, C. M., Deshaies, R. J., & Sakamoto, K. M. (2008). Targeting steroid hormone receptors for ubiquitination and degradation in breast and prostate cancer. *Oncogene, 27*(57), 7201-7211. doi:10.1038/onc.2008.320

Roth, S., Fulcher, L. J., & Sapkota, G. P. (2019). Advances in targeted degradation of endogenous proteins. *Cell Mol Life Sci, 76*(14), 2761-2777. doi:10.1007/s00018-019-03112-6

Sakamoto, K. M., Kim, K. B., Kumagai, A., Mercurio, F., Crews, C. M., & Deshaies, R. J. (2001). Protacs: chimeric molecules that target proteins to the Skp1-Cullin-F box complex for ubiquitination and degradation. *Proc Natl Acad Sci U S A, 98*(15), 8554-8559. doi:10.1073/pnas.141230798

Sakamoto, K. M., Kim, K. B., Verma, R., Ransick, A., Stein, B., Crews, C. M., & Deshaies, R. J. (2003). Development of Protacs to target cancer-promoting proteins for ubiquitination and degradation. *Mol Cell Proteomics, 2*(12), 1350-1358. doi:10.1074/mcp.T300009-MCP200

Schiedel, M., Herp, D., Hammelmann, S., Swyter, S., Lehotzky, A., Robaa, D., . . . Jung, M. (2018). Chemically Induced Degradation of Sirtuin 2 (Sirt2) by a Proteolysis Targeting Chimera (PROTAC) Based on Sirtuin Rearranging Ligands (SirReals). *J Med Chem, 61*(2), 482-491. doi:10.1021/acs.jmedchem.6b01872

Schneekloth, A. R., Pucheault, M., Tae, H. S., & Crews, C. M. (2008). Targeted intracellular protein degradation induced by a small molecule: En route to chemical proteomics. *Bioorg Med Chem Lett, 18*(22), 5904-5908. doi:10.1016/j.bmcl.2008.07.114

Schneekloth, J. S., Jr., Fonseca, F. N., Koldobskiy, M., Mandal, A., Deshaies, R., Sakamoto, K., & Crews, C. M. (2004). Chemical genetic control of protein levels: selective in vivo targeted degradation. *J Am Chem Soc, 126*(12), 3748-3754. doi:10.1021/ja039025z

Seiler, M., Yoshimi, A., Darman, R., Chan, B., Keaney, G., Thomas, M., . . . Buonamici, S. (2018). H3B-8800, an orally available small-molecule splicing modulator, induces lethality in spliceosome-mutant cancers. *Nat Med, 24*(4), 497-504. doi:10.1038/nm.4493

Shan, Y., Si, R., Wang, J., Zhang, Q., Li, J., Ma, Y., & Zhang, J. (2020). Discovery of novel anti-angiogenesis agents. Part 11: Development of PROTACs based on active molecules with potency of promoting vascular normalization. *Eur J Med Chem, 205*, 112654. doi:10.1016/j.ejmech.2020.112654

Si, J., Shi, X., Sun, S., Zou, B., Li, Y., An, D., . . . Liao, X. (2020). Hematopoietic Progenitor Kinase1 (HPK1) Mediates T Cell Dysfunction and Is a Druggable Target for T Cell-Based Immunotherapies. *Cancer Cell, 38*(4), 551-566 e511. doi:10.1016/j.ccell.2020.08.001

Slaymaker, I. M., Gao, L., Zetsche, B., Scott, D. A., Yan, W. X., & Zhang, F. (2016). Rationally engineered Cas9 nucleases with improved specificity. *Science, 351*(6268), 84-88. doi:10.1126/science.aad5227

Soucy, T. A., Smith, P. G., Milhollen, M. A., Berger, A. J., Gavin, J. M., Adhikari, S., . . . Langston, S. P. (2009). An inhibitor of NEDD8-activating enzyme as a new approach to treat cancer. *Nature, 458*(7239), 732-736. doi:10.1038/nature07884

Sreekanth, V., Zhou, Q., Kokkonda, P., Bermudez-Cabrera, H. C., Lim, D., Law, B. K., . . . Choudhary, A. (2020). Chemogenetic System Demonstrates That Cas9 Longevity Impacts Genome Editing Outcomes. *ACS Cent Sci, 6*(12), 2228-2237. doi:10.1021/acscentsci.0c00129

Stein, C. A., & Castanotto, D. (2017). FDA-Approved Oligonucleotide Therapies in 2017. *Mol Ther, 25*(5), 1069-1075. doi:10.1016/j.ymthe.2017.03.023

Su, S., Yang, Z., Gao, H., Yang, H., Zhu, S., An, Z., . . . Rao, Y. (2019). Potent and Preferential Degradation of CDK6 via Proteolysis Targeting Chimera Degraders. *J Med Chem, 62*(16), 7575-7582. doi:10.1021/acs.jmedchem.9b00871

Theunissen, T. W., & Jaenisch, R. (2014). Molecular control of induced pluripotency. *Cell Stem Cell, 14*(6), 720-734. doi:10.1016/j.stem.2014.05.002

Veldhoen, M., & Duarte, J. H. (2010). The aryl hydrocarbon receptor: fine-tuning the immune-response. *Curr Opin Immunol, 22*(6), 747-752. doi:10.1016/j.coi.2010.09.001

Wang, L., Lawrence, M. S., Wan, Y., Stojanov, P., Sougnez, C., Stevenson, K., . . . Wu, C. J. (2011). SF3B1 and other novel cancer genes in chronic lymphocytic leukemia. *N Engl J Med, 365*(26), 2497-2506. doi:10.1056/NEJMoa1109016

Wang, S., Huang, X., Li, Y., Lao, H., Zhang, Y., Dong, H., . . . Li, M. (2011). RN181 suppresses hepatocellular carcinoma growth by inhibition of the ERK/MAPK pathway. *Hepatology, 53*(6), 1932-1942. doi:10.1002/hep.24291

Wang, S., Wang, X., Gao, Y., Peng, Y., Dong, N., Xie, Q., . . . Li, J. L. (2019). RN181 is a tumour suppressor in gastric cancer by regulation of the ERK/MAPK-cyclin D1/CDK4 pathway. *J Pathol, 248*(2), 204-216. doi:10.1002/path.5246

Wang, X., Feng, S., Fan, J., Li, X., Wen, Q., & Luo, N. (2016). New strategy for renal fibrosis: Targeting Smad3 proteins for ubiquitination and degradation. *Biochem Pharmacol, 116*, 200-209. doi:10.1016/j.bcp.2016.07.017

Wang, Z., He, N., Guo, Z., Niu, C., Song, T., Guo, Y., . . . Zhang, Z. (2019). Proteolysis Targeting Chimeras for the Selective Degradation of Mcl-1/Bcl-2 Derived from Nonselective Target Binding Ligands. *J Med Chem, 62*(17), 8152-8163. doi:10.1021/acs.jmedchem.9b00919

Watters, K. E., Fellmann, C., Bai, H. B., Ren, S. M., & Doudna, J. A. (2018). Systematic discovery of natural CRISPR-Cas12a inhibitors. *Science, 362*(6411), 236-239. doi:10.1126/science.aau5138

Wei, M., Zhao, R., Cao, Y., Wei, Y., Li, M., Dong, Z., . . . Yang, C. (2021). First orally bioavailable prodrug of proteolysis targeting chimera (PROTAC) degrades cyclin-dependent kinases 2/4/6 in vivo. *Eur J Med Chem, 209*, 112903. doi:10.1016/j.ejmech.2020.112903

Winter, G. E., Buckley, D. L., Paulk, J., Roberts, J. M., Souza, A., Dhe-Paganon, S., & Bradner, J. E. (2015). DRUG DEVELOPMENT. Phthalimide conjugation as a strategy for in vivo target protein degradation. *Science, 348*(6241), 1376-1381. doi:10.1126/science.aab1433

Wolter, F., & Puchta, H. (2018). The CRISPR/Cas revolution reaches the RNA world: Cas13, a new Swiss Army knife for plant biologists. *Plant J, 94*(5), 767-775. doi:10.1111/tpj.13899

Xu, A., & Sun, S. (2015). Genomic profiling screens small molecules of metastatic prostate carcinoma. *Oncol Lett, 10*(3), 1402-1408. doi:10.3892/ol.2015.3472

Yamakawa, K., Nakano-Narusawa, Y., Hashimoto, N., Yokohira, M., & Matsuda, Y. (2019). Development and Clinical Trials of Nucleic Acid Medicines for Pancreatic Cancer Treatment. *Int J Mol Sci, 20*(17). doi:10.3390/ijms20174224

Yang, K., Song, Y., Xie, H., Wu, H., Wu, Y. T., Leisten, E. D., & Tang, W. (2018). Development of the first small molecule histone deacetylase 6 (HDAC6) degraders. *Bioorg Med Chem Lett, 28*(14), 2493-2497. doi:10.1016/j.bmcl.2018.05.057

Yang, Y., Kitagaki, J., Dai, R. M., Tsai, Y. C., Lorick, K. L., Ludwig, R. L., . . . Weissman, A. M. (2007). Inhibitors of ubiquitin-activating enzyme (E1), a new class of potential cancer therapeutics. *Cancer Res, 67*(19), 9472-9481. doi:10.1158/0008-5472.CAN-07-0568

Yokoo, H., Shibata, N., Naganuma, M., Murakami, Y., Fujii, K., Ito, T., . . . Demizu, Y. (2021). Development of a Hematopoietic Prostaglandin D Synthase-Degradation Inducer. *ACS Med Chem Lett, 12*(2), 236-241. doi:10.1021/acsmedchemlett.0c00605

Zengerle, M., Chan, K. H., & Ciulli, A. (2015). Selective Small Molecule Induced Degradation of the BET Bromodomain Protein BRD4. *ACS Chem Biol, 10*(8), 1770-1777. doi:10.1021/acschembio.5b00216

Zhang, C., Han, X. R., Yang, X., Jiang, B., Liu, J., Xiong, Y., & Jin, J. (2018). Proteolysis Targeting Chimeras (PROTACs) of Anaplastic Lymphoma Kinase (ALK). *Eur J Med Chem, 151*, 304-314. doi:10.1016/j.ejmech.2018.03.071

Zhang, C., Welborn, M., Zhu, T., Yang, N. J., Santos, M. S., Van Voorhis, T., & Pentelute, B. L. (2016). Pi-Clamp-mediated cysteine conjugation. *Nat Chem, 8*(2), 120-128. doi:10.1038/nchem.2413

Zhang, D., Baek, S. H., Ho, A., & Kim, K. (2004). Degradation of target protein in living cells by small-molecule proteolysis inducer. *Bioorg Med Chem Lett, 14*(3), 645-648. doi:10.1016/j.bmcl.2003.11.042

Zhang, H., Song, Y., Yang, C., & Wu, X. (2018). UHRF1 mediates cell migration and invasion of gastric cancer. *Biosci Rep, 38*(6). doi:10.1042/BSR20181065

Zhou, B., Hu, J., Xu, F., Chen, Z., Bai, L., Fernandez-Salas, E., . . . Wang, S. (2018). Discovery of a Small-Molecule Degrader of Bromodomain and Extra-Terminal (BET) Proteins with Picomolar Cellular Potencies and Capable of Achieving Tumor Regression. *J Med Chem, 61*(2), 462-481. doi:10.1021/acs.jmedchem.6b01816

Zhou, H., Bai, L., Xu, R., Zhao, Y., Chen, J., McEachern, D., . . . Wang, S. (2019). Structure-Based Discovery of SD-36 as a Potent, Selective, and Efficacious PROTAC Degrader of STAT3 Protein. *J Med Chem, 62*(24), 11280-11300. doi:10.1021/acs.jmedchem.9b01530

Zoppi, V., Hughes, S. J., Maniaci, C., Testa, A., Gmaschitz, T., Wieshofer, C., . . . Ciulli, A. (2019). Iterative Design and Optimization of Initially Inactive Proteolysis Targeting Chimeras (PROTACs) Identify VZ185 as a Potent, Fast, and Selective von Hippel-Lindau (VHL) Based Dual Degrader Probe of BRD9 and BRD7. *J Med Chem, 62*(2), 699-726. doi:10.1021/acs.jmedchem.8b01413